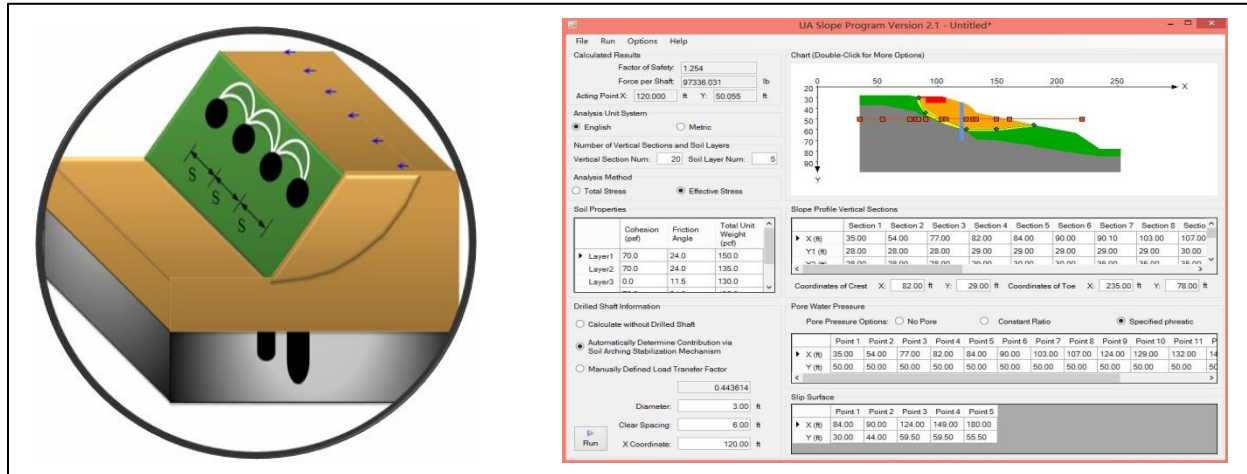


Probabilistic Analysis Algorithm for *UA Slope* Software Program



Prepared by:
Robert Y. Liang and Lin Li

Prepared for:
The Ohio Department of Transportation,
Office of Statewide Planning & Research

State Job Number 134710

December 2013

Final Report



Technical Report Documentation Page

1. Report No. FHWA/OH-2013/14	2. Government Accession No.	3. Recipient's Catalog No.	
4. Title and Subtitle Probabilistic Analysis Algorithm for <i>UA Slope</i> Software Program		5. Report Date December 2013	
7. Author(s) Robert Y. Liang and Lin Li		6. Performing Organization Code	
9. Performing Organization Name and Address University of Akron Department of Civil Engineering Akron, OH, 44325		8. Performing Organization Report No. N/A	
12. Sponsoring Agency Name and Address Ohio Department of Transportation 1980 West Broad Street Columbus, Ohio 43223		10. Work Unit No. (TRAVIS)	
		11. Contract or Grant No. SJN 134710	
		13. Type of Report and Period Covered Final Report	
15. Supplementary Notes		14. Sponsoring Agency Code	
16. Abstract A reliability-based computational algorithm for using a single row and equally spaced drilled shafts to stabilize an unstable slope has been developed in this research. The Monte-Carlo simulation (MCS) technique was used in the previously developed deterministic computational program, in which the limiting equilibrium method of slices was modified to incorporate the arching effects of the drilled shafts in a slope. Uncertainties of soil parameters in the slope were considered by statistical descriptors, including mean, coefficient of variance (c.o.v.), and distribution function. Model errors of the semi-empirical predictive equation for the load transfer factor for characterizing the soil arching effects were considered by statistics of bias. A PC-based research grade program, <i>UA Slope 3.0</i>, was coded to allow for analysis of probability of failure and reliability index of a shaft/slope system. The illustrative example demonstrated that a single value of factor of safety chosen in the deterministic approach may not yield the desired level of reliability as uncertainties of soil parameters and model errors cannot be accounted for systematically. As an extension of this research, importance sampling technique (IST) on drilled shaft/slope system has been proposed to demonstrate its high efficiency, in which the importance function and design point are determined for the ordinary method of slices (OMS) with the accompanying load transfer factor. In addition, the design method of using multiple rows of drilled shaft was developed to stabilize a large slope, in which the design and optimization criteria were proposed to reach the target safety and the constructability while meeting the service limit requirement.			
17. Keywords Drilled Shafts, Slope, Reliability, Software, Monte-Carlo.		18. Distribution Statement No restrictions. This document is available to the public through the National Technical Information Service, Springfield, Virginia 22161	
19. Security Classification (of this report) Unclassified	20. Security Classification (of this page) Unclassified	21. No. of Pages 120	22. Price

Form DOT F 1700.7(8-72)

Reproduction of completed pages authorized

Probabilistic Analysis Algorithm for *UA Slope* Software Program

Prepared by:
Robert Y. Liang and Lin Li

December 2013

Prepared in cooperation with the Ohio Department of Transportation
and the U.S. Department of Transportation, Federal Highway Administration

The contents of this report reflect the views of the author(s) who is (are) responsible for the facts and the accuracy of the data presented herein. The contents do not necessarily reflect the official views or policies of the Ohio Department of Transportation or the Federal Highway Administration. This report does not constitute a standard, specification, or regulation.

Acknowledgments

The authors would like to acknowledge the support and guidance provided by the ODOT Technical Panel: Chris Merklin and Alexander Dettloff, both of Office of Geotechnical Engineering.

Table of Contents

1. Introduction.....	1
1.1. Overview	1
1.2. Statement of the Problem	2
1.3. Objectives.....	5
1.4. Scope of Work.....	7
1.5. Report Outline	10
2. Literature Review	12
2.1. State-of-the-Art Review for Drilled Shaft/Slope System.....	12
2.2. Previous Work by the University of Akron Group	14
2.2.1. Arching Theory in Slope Stabilization	15
2.2.2. Research by Zeng and Liang (2002).....	17
2.2.3. Research by Yamin (2007)	19
2.2.4. Research by Al Bodour (2010)	22
2.2.5. Research by Joorabchi (2011).....	25
2.3. Multiple Rows of Drilled Shafts Stabilizing Slope.....	28
2.4. Probabilistic Study	29

2.4.1.	Importance Sampling Technique	30
3.	Probabilistic Version of <i>UA Slope</i> Computing Algorithm	31
3.1.	Introduction	31
3.2.	Deterministic Limiting Equilibrium Method of Slices in Drilled Shaft/Slope System..	32
3.2.1.	Latest Study of Load Transfer Factor by Joorabchi (2011).....	36
3.3.	Probabilistic Version of <i>UA Slope</i>	42
3.3.1.	Uncertain Parameters in a Drilled Shaft/Slope System	42
3.3.2.	Bias of Load Transfer Factor	42
3.3.3.	Monte-Carlo Simulation	43
3.4.	Monte-Carlo Coding Strategy for <i>UA Slope</i> Program	44
3.5.	Design Method	46
3.5.1.	Step-by-Step Design Procedure	46
3.5.2.	Illustrative Example 1	47
3.5.3.	Illustrative Example 2	54
3.6.	Summary and Conclusions.....	60
4.	Advanced Probabilistic Technique in a Drilled Shaft/Slope System	63
4.1.	Introduction	63

4.2.	Basic Concept of Importance Sampling Technique	65
4.3.	Importance Sampling Technique for the Drilled Shaft/Slope System	66
4.3.1.	Design point of importance function	66
4.3.2.	The ratio between $f(x)$ and $IS(x)$	69
4.4.	Procedure of Importance Sampling Calculation using the Design Point	72
4.5.	Illustrative Example of Application	74
4.6.	Summary and Conclusions.....	79
5.	Limit Equilibrium Based Design Approach for Slope Stabilization Using Multiple Rows of Drilled Shafts	80
5.1.	Introduction	81
5.2.	Using Multiple Rows of Drilled Shafts for Stabilizing a Slope.....	83
5.2.1.	Method of Slices for a Two-Row Drilled Shaft/Slope System.....	83
5.2.2.	Optimization Strategy and Criteria	88
5.3.	Illustrative Design Example	89
5.3.1.	Step-by-Step Design Procedure	90
5.4.	Summary and Conclusion	98
6.	Summary and Conclusions	100

6.1. Summary of Work Accomplished.....	100
6.2. Conclusions	102
6.3. Recommendations for Implementation	103
6.4. Recommendations for Future Research	105
7. Bibliography	107

List of Tables

Table 2-1: The Ranges of the Parameters Used in the Parametric Study (Al Bodour, 2010)	27
Table 2-2: The importance of each parameter in affecting load transfer factor	27
Table 3-1: Soil Properties of the Two-Layer Slope	49
Table 3-2: Soil properties at the slope of ATH-124 project	56
Table 3-3: Comparison between Reliability Index and Factor of Safety ($D = 0.6$ m).....	60
Table 4-1: Convergence analysis between IST and MCS	78
Table 4-2: Accuracy analysis between IST and MCS	78
Table 5-1: Soil Properties of Illustrative Example	90
Table 5-2: Design Results using Two Rows of Drilled Shafts	94
Table 5-3: Design Results using Three Rows of Drilled Shafts	96
Table 5-4: Design Results of the Two Combinations Shown in Table 5-3	97
Table 5-5: Total Volume per Unit Width for the Four Combinations	98

List of Figures

Figure 1-1: Flowchart depicting the scope of work	10
Figure 2-1: Finite element model for slope/shaft system (after Liang and Zeng, 2002)	18
Figure 2-2: 3D Finite Element Model Developed by Yamin (2007).....	20
Figure 2-3: 3D Finite Element Model Developed by Al Bodour (2010).....	23
Figure 2-4: Illustration of the Terms Related to the Slope Geometry (Al Bodour, 2010).....	24
Figure 3-1a: A typical slice showing all force components.....	33
Figure 3-2a: Definition of the soil arching	35
Figure 3-3a: Geometry and dimensions of the 3D model a) Cross-section b) Top view	38
Figure 3-4: Soil arching as observed from the horizontal soil stresses in the direction of the soil movement (after Al Bodour, 2010).....	39
Figure 3-5: Illustration of the Terms Related to the Slope Geometry	40
Figure 3-6: Comparison of load transfer factor computed by semi-empirical equation and FEM (after Joorabchi, 2011).....	41
Figure 3-7: Preliminary research version of Monte Carlo coding strategy for <i>UA Slope</i> program	45
Figure 3-8: Flowchart of MCS method for the drilled shaft/slope system	47

Figure 3-9: Slope geometry for two-layer slope	48
Figure 3-10: Reliability index of the shaft-slope system versus shaft location for different (S, D) combinations	51
Figure 3-11: Shaft force versus shaft location for different (S, D) combinations.....	51
Figure 3-12: Relationship between P_f and mean of bias of η for different standard deviation	54
Figure 3-13: Slope geometry for ATH-124 slope (shaft location 26 m)	55
Figure 3-14: Reliability index of the shaft-slope system versus shaft location for different (S, D) combinations	57
Figure 3-15: Shaft force versus shaft location for different (S, D) combinations.....	58
Figure 4-1: Sketch of PDF Comparison between MCS and IST (1D)	64
Figure 4-2: Flowchart of importance sampling technique in a drilled shaft/slope system	73
Figure 4-3: Comparison of P_f between MCS and IST ($P_f = 2.8\%$ after 40,000 MCS).....	76
Figure 4-4: c.o.v. of P_f for MCS and IST with different standard deviations.....	76
Figure 4-5: Number of failure events for MCS and IST with different standard deviations	77
Figure 5-1: A typical slice showing all force components	85
Figure 5-2: A typical cross-section divided into slices for a slope reinforced with two rows of drilled shafts.....	86

Figure 5-3: Method of slices using two rows of drilled shafts 86

Figure 5-4: Geometry of illustrative example (Unit: meter)..... 90

Figure 5-5: Global FS versus shaft location for different (S , D) combinations using one row of drilled shafts..... 92

Figure 5-6: Shaft force versus shaft location for different (S , D) combinations using one row of drilled shafts..... 93

1. INTRODUCTION

1.1. Overview

Deterministic analysis of a drilled shaft/slope system has been a research topic since the 1960s (Chelapati, 1960; Getzler et al., 1968; Fukumoto, 1972 and 1973; Wang and Yen, 1974, Sommer, 1977). In general, the analysis methods for considering the effects of reinforcing drilled shafts could be categorized into two approaches: a) increase in the resistance due to the added shear strength of the reinforced concrete drilled shafts (e.g., Ito, et al., 1981; Hassiotis, et al., 1997; Reese, et al., 1992; Poulos, 1995 and 1999), b) decrease in the driving force due to the soil arching as a result of the inclusion of rigid structural elements on the slope (e.g., Liang and Zeng, 2002; Yamin, 2007; Al Bodour, 2010; Joorabchi, 2011). Despite the increased use of drilled shafts for slope stabilization in recent years, there still is a lack of coherent and widely accepted reliability based design methodology to ensure both safe and economical design outcomes.

Probability-based approaches for assessing probability of failure of a slope have been the focus of research since the 1970s (e.g., Tang et al., 1976; Wu et al., 1989; Oka and Wu, 1990). The methodologies in probabilistic analysis of a slope usually employ first-order-second-moment (FOSM), first-order-reliability-method (FORM), and Monte-Carlo simulation (MCS) (e.g., Low et al., 1998; Liang et al., 1999; Malkawi et al., 2000; Cheung and Tang, 2005; Griffiths and Fenton, 2004; Zhang and Tang, 2011). Of these, MCS is commonly considered as the most robust methodology dealing with reliability analysis (Robert and Casella, 2004); however, it requires a large number of random samples in order to calculate the probability of failure.

A more advanced technique, the importance sampling technique (IST), is a probabilistic approach that is more efficient than MCS in reducing the sample calculations and increasing the accuracy in predictions for the probability of failure (Robert and Casella, 2004; Au et. al, 1999; Au and Beck, 2003; Ching et al., 2009 and 2010). Ching et al. (2009, 2010) have presented analytical techniques for determining the probability of failure (reliability index) of a slope using IST in connection with the ordinary method of slices (OMS). The literature on IST contains very few studies on slope stability analysis using drilled shafts. As a result, additional investigations that apply IST for slope stabilization are needed.

An additional consideration in the design process for slope stabilization is the configuration of the drilled shafts. A single row of drilled shafts may not be adequate for stabilizing a slope, if the failed slope length is large and the force thrusting onto the drilled shaft is high. Multiple rows of drilled shafts are needed to arrest slope movement and enhance the safety margin of the failing slope. To date, there is no available literature on design and analysis methods for a drilled shaft/slope system using multiple rows of drilled shafts to stabilize an unstable slope.

1.2. Statement of the Problem

Landslides and slope failures occur frequently every year, which have a major impact on the operational safety of roadways and add financial burdens to the highway agencies responsible for performing slope repairs and maintenance. Although many slope improvement methods are available, the use of drilled shafts has been a commonly adopted method with several advantages: this method offers a permanent structural fix, it normally does not require additional right of way, it can be constructed in most soil and rock conditions, and it can be constructed rather rapidly. In

the design of slope stabilization, much of the challenge involved in evaluating alternative maintenance and repair actions lies in the fact that the future performance of a slope is uncertain. Because of this uncertainty, future costs for maintenance and repair are also uncertain. We simply cannot achieve—or cannot afford to achieve—absolute safety for any slope. There will always be underlying geotechnical variability, a potential for unforeseen loading conditions from extreme events, or the possibility that an unknown behavior will occur because of an incomplete understanding of slope performance.

A deterministic computer program known as *UA Slope* was originally developed by a research team at the University of Akron (Liang, 2010) with funding from the Ohio Department of Transportation (ODOT). The *UA Slope* program has been used by ODOT and its consultants to design drilled shafts for the stabilization of unstable slopes. The program uses the concept of soil arching to account for the stabilization effects of drilled shafts on the slope. The basic idea is that with properly spaced drilled shafts on a slope, the movement of soils on the slope will cause the transfer of the downslope earth thrust to the more rigid inclusions (i.e., drilled shafts), thus reducing the driving stresses on the slope. Consequently, the factor of the safety of the drilled shaft stabilized slope would be increased when compared to that of the original unstable slope. The load transfer due to the presence of drilled shafts was found to be influenced by several major factors, such as soil strength parameters (i.e., cohesion c , friction angle ϕ), slope geometry (i.e., slope angle β), drilled shaft center-to-center spacing (S_0), shaft diameter (D), and shaft location (ξ_x). A semi-empirical equation was developed for calculating the load transfer factor (η) based on a regression analysis of approximately 41 finite element (FE) numerical simulation results using the strength reduction method. Although the *UA Slope* program has been used by

ODOT's Office of Geotechnical Engineering and by consultants, there are several features of the program that could be improved:

- 1) The equation for the load transfer factor is critical for the accuracy of the computational algorithm in *UA Slope* program. Due to the semi-empirical nature of an equation that is based on a limited number of FE simulation/modeling results, uncertainties and errors associated with this semi-empirical equation need to be systematically accounted for in a probability framework. A method based on probabilistic description of the bias of the semi-empirical equation can be developed so that the uncertainties of the load transfer factor could be incorporated systematically in the computational algorithm of the *UA Slope* program.
- 2) The *UA Slope* program utilizes the conventional method of slices within the principle of limiting equilibrium. The computational algorithm, however, is deterministic as far as the soil properties are concerned. The determination of soil properties for a slope can be uncertain due to the nature of the soil boring information and the necessary engineering judgment in selecting the representative parameters. Therefore, a probabilistic computational algorithm needs to be developed to systematically take into account the uncertainties of soil parameters.

Using current approaches, the uncertainties are typically addressed collectively by imposing a required factor of safety, such as a factor of safety equals to 1.3 for both temporary and permanent slopes and a factor of safety equals to 1.5 for slopes supporting or containing a structure or structure foundation elements. Nevertheless, the prescribed factor of safety does not change, regardless of the degree of uncertainties and variability in soil parameters. Furthermore,

more conservative design having a higher FS with the consequent high construction costs cannot guarantee that it can reasonably increase the degree of safety of a slope, because the variability in soil parameters and model errors were not systematically taken into account. Therefore, a truly reliability-based design method for using drilled shafts to stabilize a slope is highly desirable.

Mathematically speaking, traditional MCS uses samples that “randomly” fall into the failure region to calculate the probability of failure (P_f), which means that if the P_f is quite small, it must require a large number of sample calculations. Obviously, plenty of calculation time has been wasted unless the samples can undergo “parallel translation” and/or “shrink” into the failure zone. IST is based on the above theory, and it can generate the more “important” samples falling into the failure region to achieve a fast calculation while attaining the required accuracy.

In practical cases, to prevent a large-scale landslide, multiple rows of drilled shafts may often be used. The two major reasons for employing multiple rows instead of one row of drilled shafts are: (1) the global factor of safety of the slope will never satisfy the target factor of safety (FS_{Target}) if only one row of drilled shafts is used to stabilize the slope; and (2) although the global factor of safety of the slope can reach the target, the net force on the drilled shafts is tremendous, in which case the slope does not satisfy the service limitation (for example, when the lateral deflection of the drilled shafts exceeds the target).

1.3. Objectives

- 1) The main objective of this research is to refine a previously developed deterministic design and analysis method and the accompanied computer program (*UA Slope*) into a reliability

based computational algorithm, as well as to develop a research-grade probabilistic computer program for a drilled shaft/slope system. The uncertainties of three soil properties (cohesion c , friction angle ϕ and unit weight γ) will be considered in the developed reliability based method. In addition, the bias (δ) of the load transfer factor (η) will be considered and assumed to follow the lognormal distribution with the mean (μ_δ) and variance (σ_δ), which will be determined by comparing the results of 41 FE models with those of the semi-empirical equation. By employing Monte-Carlo simulation (MCS), the probability of failure (P_f) for the drilled shafts/slope system will be determined. Specific objectives of this research are enumerated as follows:

- a) Formulate the deterministic limit equilibrium equation into a probabilistic Monte-Carlo algorithm for the *UA Slope* soil-arching based theory;
 - b) Develop a research-grade computer program to calculate probability of failure and the reliability index in a drilled shaft/slope system, using the existing *UA Slope* program as the basis.
 - c) Develop a step-by-step design procedure for reliability based optimization design for using a row of drilled shafts to stabilize a slope, and compare the relationship between the reliability index and the factor of safety.
- 2) As an extension of this research study, further objectives will be achieved as follows:
- a) Adopt IST in reliability assessment of a drilled shaft/slope system for improved computational efficiency. A combination of ordinary method of slices (OMS) and arching theory will be proposed to determine the performance function, $g(x)$, and the

design point will be pinpointed using this function. The importance function $IS(x)$ will be formed based on the design point. Meanwhile, a range in the standard deviation (SD) from 0.92 to 1.00 for the importance function $IS(x)$ will be selected to analyze the accuracy and convergence rate of the estimator.

- b) Develop a computer program for handling multiple rows of drilled shafts to stabilize a slope. Specific objectives are enumerated as follows: i) Write a PC-based program to deal with multiple rows of drilled shafts for slope stabilization; ii) Develop an optimization strategy and criteria for the selection of the shaft diameter, clear spacing, the total number of rows, and the position of each row; iii) Develop a step-by-step design procedure for multiple rows of drilled shafts in stabilizing slopes.

1.4. Scope of Work

The goal of this study is to develop a new reliability-based optimization design for drilled shafts used in stabilizing slopes. The specific scope of work is enumerated as follows:

- 1) Reliability-based optimization design for drilled shafts to stabilize a slope using MCS. Uncertainties involved in the deterministic method are identified as: 1) soil properties as input data (i.e. cohesion, friction angle, and unit weight) caused by soil boring selections, soil variability, and measurement error; and 2) the model error of the semi-empirical equation of the load transfer factor caused by 41 finite element regressions. To take into account the uncertainties of these two sources, a probabilistic framework will be developed. A Monte Carlo random number generator algorithm will be developed and applied to the

soil properties, including the Mohr-Coulomb strength parameters and the unit weight of the soil. The statistical description of these input soil parameters as well as the bias of the semi-empirical equation will include the mean, standard deviation, and lognormal distribution. Once the statistical characteristics of these variables are developed, then the MCS will be performed to assess the probability of failure and reliability index of the drilled shaft-slope system. Thereafter, the computer program, *LPILE* (developed by Ensoft, Inc.), will be utilized to perform the structural analysis. After that, a step-by-step design procedure will be developed. The final design result will be optimized by changing drilled shaft parameters in order to achieve the minimum total concrete volume based on satisfying the target reliability index and structural performance.

- 2) Computationally efficient reliability analysis of the drilled shaft/slope system using IST. Uncertainties of soil parameters in the slope will be considered by statistical descriptors, including mean, coefficient of variance (c.o.v.), and lognormal distribution. Model errors of the semi-empirical predictive equation for computing the load transfer factor for characterizing the drilled shaft-induced soil arching effects will be considered by the statistics of bias. The importance function and the design point will be determined by the OMS with the accompanying load transfer factor. Once the importance sampling design point is obtained, it can be employed in constructing a new probability density function (PDF) of importance function. And finally, the probability of failure for the drilled shaft/slope system will be calculated based on the importance function.
- 3) The deterministic optimization design method on multiple rows of drilled shafts in stabilizing slope will be developed. The global factor of safety and the net force on each row of drilled shafts will be calculated by modifying the *UA Slope* program. The

optimization strategy and criteria will be developed, and a step-by-step design procedure will be provided to deal with multiple rows of drilled shafts in stabilizing slopes. During calculation, the assumptions of this analysis are enumerated as follows:

- a) FS was considered to be identical for all slices;
- b) Normal force on the base of the slice was applied at the midpoint of the slice base;
- c) The location of the thrust line of the interslice forces was placed at one-third of the average interslice height above the failure surface, as in Janbu (1973);
- d) In the method of slices calculation, the right-interslice force was assumed to be parallel to the inclination of the preceding slice base. The left-interslice force was assumed to be parallel to the current slice base;
- e) There is no group pile effect between the two adjacent rows of drilled shafts; and
- f) There is no soil arching influence between the two adjacent rows of drilled shafts.

Figure 1-1 illustrates the scope of work to achieve the stated objectives of this research.

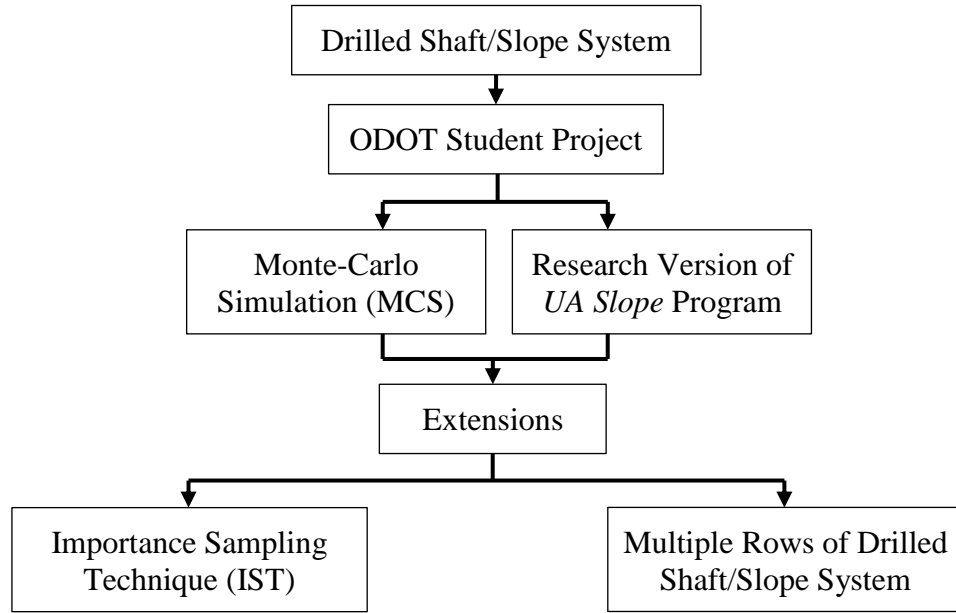


Figure 0-1: Flowchart depicting the scope of work

1.5. Report Outline

Chapter 2 presents a brief summary of state-of-the-art studies on the design methods for using the drilled shafts to stabilize an unstable slope.

Chapter 3 presents the development of the *UA Slope* computing algorithm from deterministic version to probabilistic version using MCS, and it also introduces the developed reliability-based optimization design methodology of a single row of rock-socketed drilled shafts for stabilizing an unstable slope, based on two illustrative examples.

Chapter 4 presents a more advanced probabilistic technique (importance sampling technique) in a drilled shaft/slope system.

Chapter 5 presents a deterministic design approach of multiple rows of drilled shafts in stabilizing a large failed slope, and it provides the optimization strategy and criteria used in the design process.

Chapter 6 provides a summary of work completed as a part of this study, as well as conclusions and recommendations for implementation.

2. LITERATURE REVIEW

2.1. State-of-the-Art Review for Drilled Shaft/Slope System

To effectively carry out a design for drilled shafts that are capable of mitigating landslides, it is necessary to correctly understand the stabilizing mechanism of drilled shafts. The use of drilled shafts to stabilize a failed slope has been widely adopted over the past several decades (Bulley, 1965; Morgenstern and Price, 1965; Taniguchi, 1967; De Beer et al., 1972; Fukumoto, 1972; Esu and D'Elia, 1974; Ito and Matsui, 1975; Sommer, 1977; Fukuoka, 1977; Offenberger, 1981; Ito et al., 1981 and 1982; Morgenstern, 1982; Nethero, 1982; Gudehus and Schwarz, 1985; Norris, 1986; Hada et al., 1988; Reese et al., 1992; Rollins and Rollins, 1992; Poulos, 1995 and 1999; Ashour et al., 1997 and 2002; Firat, 1998; Bicocchi, 2001; Zeng and Liang, 2002; Smethurst, 2003; Merklin et al., 2007; Yamin, 2007; Ngwenya, 2007; Reid, 2008; Wei, 2008; Yoon, 2008, Durrani et al., 2008; Ghee, 2009; Kourkoulis, 2009; Qin, 2010; Al Bodour, 2010; Kanagashabai, 2010; Jiang, 2011; Kanagasabai et al., 2011; Zacharopoulos, 2012; Joorabchi et al., 2013; Zacharopoulos, 2013), where more than 30 doctoral theses have been identified globally on various elements of this specific foundation engineering topic. Following the publication of studies by Poulos (1973, 1995, 1999) and Viggiani (1981), which became the pillars of the practicing analyses of this particular complex problem in foundation engineering, a worldwide surge in research has focused on the design of the piles under complex soil movements. Research has increased significantly during the last decade, as the increasingly catastrophic effects of climate change on the built environment have become more apparent. The last decades' active research groups in this area have attempted to demystify the complex behaviour of the drilled shaft/slope system. These research teams include Hong-Song's group in Seoul Korea, Powrie's

group (Smethurst, Kanagasabai, Biccocchi, Pan, Zacharopoulos) in University of Southampton in the U.K.; Loehr's group (Ang, Bozok) at the University of Missouri; Gazetas's group (Kourkoulis, Athanasopoulos, Gerolymos) at the National Technical University of Athens in Greece; Anagnostopoulos-Georgiadis group at Aristotle University of Thessaloniki in Greece; Poulos and his students/colleagues (Chen L.T. Lee, Hull, Xu) in Sydney, Australia; Guo's group (Ghee, Qin) in Brisbane, Australia; Ellis group (Durrani, Yoon) in Nottingham and Portsmouth in the U.K.; Evangelista-Conte-Viggiani's (Lirer, Ausilio, Cairo, Dente, Urciuoli, Pellegrino, Fortunate, Morra) combined efforts in Italy; Cai and Ugai in Japan; Elsawaaf's group in Egypt; Ashour's group (Norris, Pilling, Ardalán) in Nevada and Alabama; and Liang's group (Zeng, Yamin, Al Bodour, Joorabchi, Li) at The University of Akron, to name but a few. The success of these documented successful cases of using drilled shafts to stabilize an unstable slope could be attributed to rather conservative design approaches and the large structural capacity offered by drilled shafts or cast-in-place piles. The practical experience of the authors has showed that, in large part, current practice often leads to the overdesign of the structures, because some of the complexities and uncertainties that influence designing factors are not truly clarified and well understood (Cornforth, 2005; Ho and Lau, 2010).

A new era in the design of stabilizing piles has emerged with certain theories (e.g. Liang et al., 2010, 2013; Kourkoulis et al., 2009, 2012; Guo, 2013, Ashour and Ardalán, 2012) able to create close predictions against known well-documented full scale load tests and site data that have been published in the literature (e.g. Carrubba et al., 1989; Kalteziotis et al., 1993; Leung et al., 2000; Cai and Ugai, 2003; Richardson, 2005; and Smethurst and Powrie, 2007). Despite the success of these field applications, it is also clear that no universally accepted reliability based optimization design method is available for assessing the probability of failure (P_f) and reliability

index (β) of a slope reinforced with a single row of spaced drilled shafts as well as for determining the earth thrusts on the drilled shafts in the process of the structural design of the shafts.

2.2. Previous Work by the University of Akron Group

During previous years, the method for incorporating the effects of drilled shafts in a failed slope within the framework of limit equilibrium approach has been accomplished in one of two ways. In the first approach, as given in Equation 2-1, the resistance to the slope sliding is increased after installation of a row of drilled shafts, thus enhancing the safety factor (Ito et al., 1981; Reese et al., 1992; Poulos, 1995). In contrast, the second approach as given in Equation 2-2, the increase of the factor of safety is due to soil arching induced reduction on the driving force (Liang and Zeng, 2002; Yamin, 2007; Al-Bodour, 2010, Joorabchi, 2011).

$$FS = \frac{F_R + (\Delta F_R)_{Shaft}}{F_D} \quad (2-1)$$

$$FS = \frac{F_R}{F_D - (\Delta F_D)_{arching}} \quad (2-2)$$

where, FS is global factor of safety of a slope/shaft system, F_R is the resistance force, $(\Delta F_R)_{shaft}$ is additional resistance due to drilled shafts, F_D is driving force, and $(\Delta F_D)_{arching}$ is drilled shaft induced arching effect on the driving force.

To address the structural issues, the force and moment distribution on the shaft need to be identified. However, this is a very complicated issue because it involves soil-structure interaction. The force that is applied to the shaft is a function of the movement of the soil mass and the

amount of stresses transferred from the upslope to the downslope. Once the force on the drilled shaft is recognized, the analysis typically uses the beam on Winkler spring type of solution algorithm, such as those employing the *LPILE* (Reese et al., 2004) computer program, to compute the internal forces due to the prearranged external loads or displacement field. The amount of stress that is reduced, as soil mass moves from upslope to downslope, can be captured by the arching concept. The arching function is a function of several parameters, including the spacing between the shafts, soil properties, and the diameter of the shaft. Three-dimensional FE analysis is necessary to quantify the arching phenomena based on these parameters.

2.2.1. Arching Theory in Slope Stabilization

The soil arching concept was first introduced by Terzaghi (1936, 1943). Some experimental research was done by Bosscher and Gray (1986) to identify the vertical stress re-distribution caused by arching, through the use of a trap door device. The objective and motive of early research in arching was to gain a better understanding of the earth pressure acting on the underground pipes or tunnel linings. Kellogg (1987) observed different shapes of soil arching (such as parabolic, hemispherical, and corbelled shapes) under different conditions. Recently, a renewed interest in soil arching has focused on applications related to pile-supported embankments on soft ground, such as the work done by Hewlett and Randolph (1988).

There is some literature available regarding soil arching in the drilled shaft/slope system. For example, Chen and Martin (2002) used the finite difference method to analyze the soil structure interaction for a slope reinforced with different types of piles. Several assumptions were involved in this research. Chen and Martin used a two-dimensional model for studying a three-

dimensional problem, and they assumed rigid piles and relatively small soil movements in the modeling. Earlier, Wang and Yen (1974) also investigated the soil arching in a slope. In his study, the slope was considered as an infinite slope while the soil was modeled as an elastic-perfectly plastic soil. Based on their numerical study, Wang and Yen concluded that soil strength parameters and the spacing between the piles played an important role in arching behavior. Adachi et al. (1989) described the arching zone as an equilateral triangular arch and characterized the arching foothold around the drilled shaft. However, they did not provide any quantitative estimation for the load transfer behavior from the soil to the pile.

Bransby and Springman (1999) studied the effect of pile spacing and the soil constitutive law on the load transfer process in a slope reinforced with a row of drilled shafts, using small-scale model tests along with FE simulation techniques. Their study showed the link between the soil stress-strain behavior, the soil deformation mechanism, and the load transfer curves. However, their work was limited to sandy soils. Jeong et al. (2003) applied FE analysis to examine the response of a row of slope-stabilizing piles to the lateral loads. They described the load transfer factor using the maximum moment produced in a pile in a row of reinforcing piles to the maximum moment built up in an isolated single pile. The Jeong study illustrated the group effect of a row of drilled shafts for stabilizing a slope.

To interpret the interaction between the drilled shaft and slope, a soil arching theory was proposed by Liang and Zeng (2002) that used a two-dimensional finite element approach to obtain a semi-empirical equation for the load transfer factor. They found that soil arching in a drilled shaft/slope system is highly dependent upon the soil movement relative to the drilled shafts, soil properties, and drilled shaft configurations (diameter and spacing). Yamin (2007) focused on a comprehensive three-dimensional FE simulation, calculating the ultimate state of

the shaft/slope system by incrementally increasing the surcharge load at the top of the slope. Al Bodour (2010) presented three-dimensional FE analysis using the strength reduction finite element simulation method to obtain regression-based, semi-empirical equations for quantifying the arching effect through the load transfer factor. Recently, Joorabchi (2011) ascertained that six parameters (soil cohesion c , soil friction angle ϕ , slope angle β , shaft diameter D , shaft center to center spacing S_0 , and shaft location ξ_x) are highly related to the load transfer factor based on the importance parameter analysis. Joorabchi further modified the semi-empirical load transfer factor equation based on 41 high-quality FE model simulation results.

2.2.2. Research by Zeng and Liang (2002)

Zeng and Liang (2002) presented a two-dimensional finite element approach, as shown in Figure 2-1, to investigate soil arching behavior. In the FE simulations, Zeng and Liang used Mohr Coulomb failure criteria in which the soil is assumed to be an elastic–perfectly plastic material, and the drilled shafts were modeled as a rigid material. Applying these assumptions, this model was very similar to a trap door experiment. To formulate the effect of soil arching, Zeng and Liang used a triangular displacement field, placed in the soil between the drilled shafts. Based on this study, it was found that soil arching is highly dependent upon the prescribed soil movement, soil properties, and drilled shaft configurations.

By applying a systematic parametric finite element simulation, the arching effect in the slope/shaft system was formed through the use of the load reduction factor and residual stresses. The load reduction factor was described as the percent of the soil stresses remaining in the soil between the adjacent drilled shafts, assuming that full arching in the drilled shaft/slope system

was developed. In addition, a limiting equilibrium based method of slices for slope stability analysis was developed to incorporate the load reduction factor. A computer program, *UA SLOPE 1.0*, was developed based on Zeng and Liang's work. This work was later revised and improved by Yamin, through the development of three-dimensional finite element simulations of the drilled shaft/slope system in order to better measure the load reduction factor.

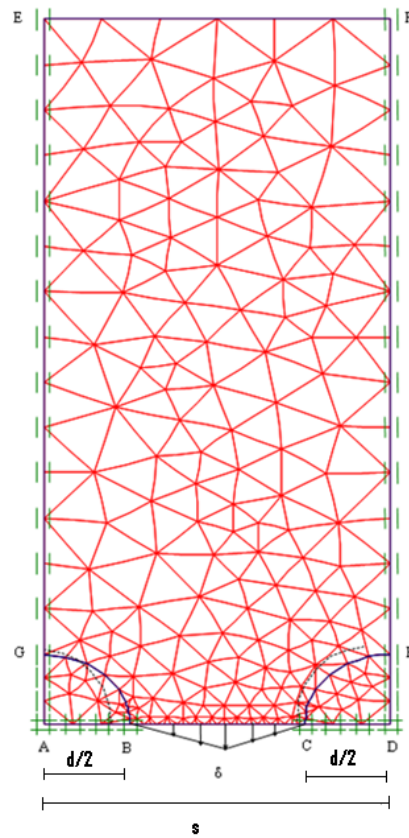


Figure 0-1: Finite element model for slope/shaft system (after Liang and Zeng, 2002)

2.2.3. Research by Yamin (2007)

Yamin (2007) focused on a comprehensive three-dimensional FE simulation in order to evaluate the effects of the drilled shafts in promoting the development of soil arching between the adjacent drilled shafts in a slope/shaft system. The representative finite element mesh used by Yamin is shown in Figure 2-2. The model includes a single drilled shaft due to the nature of symmetry. In Yamin's methodology, the slope fails by increasing the applied load at the crest. The slope movement was initiated by incrementally raising the magnitude of the surcharge load placed at the top of the slope crest. Failure criteria are defined by either the numerical convergence problem or by excessive deflection of the drilled shaft. The forces on the upslope and downslope side of the drilled shaft are obtained by integrating the stresses surrounding the drilled shaft. The load transfer factor was then defined as the ratio of force downslope to the force on the upslope side, and it was used to formulate the stability analysis equations of the drilled shaft/slope system.

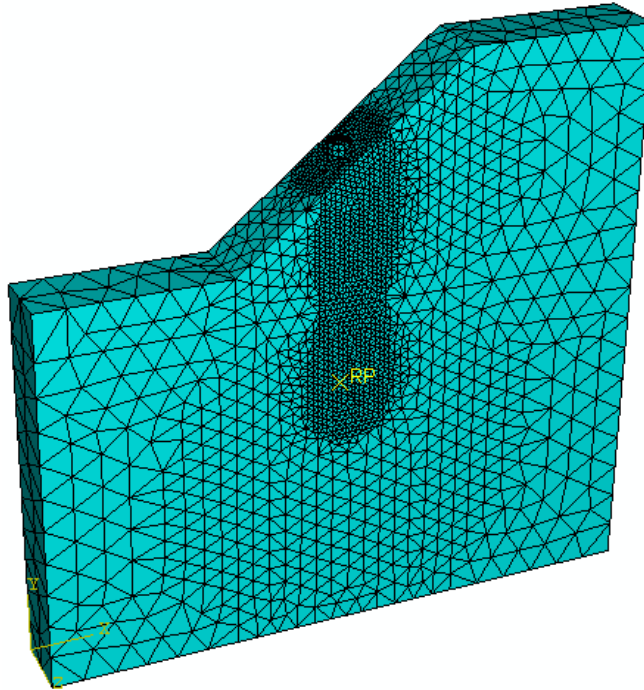


Figure 0-2: 3D Finite Element Model Developed by Yamin (2007)

Based on Yamin's study, nine parameters were found to have controlling influences on the load transfer factor. These parameters include soil cohesion, soil angle of internal friction, shaft diameter, shaft length, shaft elastic modulus, shaft location, spacing-to-diameter ratio, rock socket length of the shaft, and failure surface depth. Liang and Yamin (2010) presented a series of design charts to estimate the load transfer factor for specific conditions. Yamin and Liang (2010) presented a closed solution for calculating the factor of safety of a drilled shaft/slope system using the load transfer concept. The closed form solution is given in Equation 2-3, where FS needs to be calculated in an iterative manner to satisfy the force equilibrium requirement.

$$\eta_m = \frac{\left[L_n - A_n - \left(\sum_{i=m+2}^n A_{i-1} \prod_{j=i}^n B_j \right) \right]}{\left[\left(B_{m+1} \sum_{i=2}^{m+1} A_{i-1} \prod_{\substack{j=i; \\ j \neq m+1}}^n B_j \right) + \left(B_n B_m \prod_{\substack{i=1; \\ i \neq m}}^{n-1} B_i \right) R_1 \right]} ; 0 < \eta_m \leq 1.0 \quad (2-3)$$

$$A_i = \left[W_i \sin(\alpha_i) + Q_i \sin(\beta_i - \alpha_i) - \frac{c_i b_i \sec(\alpha_i)}{FS} \right] \frac{\tan(\phi_i)}{FS} - \left[W_i \cos(\alpha_i) + Q_i \cos(\beta_i - \alpha_i) - U_i \right] \frac{\tan(\phi_i)}{FS} \quad (2-4)$$

$$B_i = \left[\cos(\alpha_{i-1} - \alpha_i) - \sin(\alpha_{i-1} - \alpha_i) \frac{\tan(\phi_i)}{FS} \right] \quad (2-5)$$

where, η_m : is the required load transfer factor

W_i : weight of Slice i

N_i : force normal to the base of Slice i

T_i : force parallel to the base of Slice i

Q_i : external surcharge applied at Slice i

R_i : right-interslice force of Slice i

L_i : left-interslice force of Slice i

α_i : inclination of Slice i base

α_{i-1} : inclination of Slice i-1 base

β_i : inclination of the external surcharge applied at Slice i

c_i : soil cohesion at the base of Slice i

φ_i : soil friction angle at the base of Slice i

In Yamin's study, the ultimate state of the slope-shaft system was achieved by incrementally increasing the surcharge load at the top of the slope. The ultimate state was defined by the limiting shaft displacement. In the majority of instances, failure of slope/shaft system is caused by excessive soil movement at small shaft displacements. The limiting shaft displacement in Yamin's study is greater than the shaft displacement at failure. Finally, there are not any validations for the results of the method proposed in his study.

2.2.4. Research by Al Bodour (2010)

To address the deficiency of Yamin's work, Al Bodour (2010) presents the three-dimensional FE analysis to obtain the regression-based semi-empirical equations for quantifying the arching effect through the load transfer factor by incorporating the strength reduction methodology into the FE simulations. An approach combining the strength reduction method with the FE method was introduced by Zienkiewicz et al. (1975) and Duncan (1996). The strength reduction method reduced the soil strength parameters (c and φ) incrementally to cause the slope to reach failure mode. The factor of safety of the slope is equal to strength reduction factor, which is the available soil strength divided by the reduced soil strength at slope failure, as shown in Equations 2-6 and 2-7. The strength reduction method is well-matched for the soil behavior and obeys the elastic-perfectly plastic constitutive law with strength parameters of c and φ , such as Mohr-Coulomb model or Drucker-Prager model.

$$c_R = c / RF \quad (2-6)$$

$$[\tan(\varphi)]_R = \tan(\varphi) / RF \quad (2-7)$$

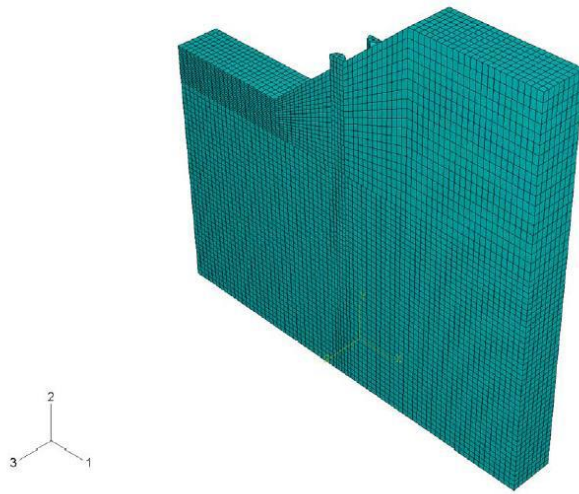


Figure 0-3: 3D Finite Element Model Developed by Al Bodour (2010)

Based on Al Bodour's study, the load transfer factor was defined as force downslope to upslope side of the shaft area, and it was formulated using the results of a parametric study of different parameters as shown in Figure 2-4. Al Bodour quantified the load transfer factor as a function of eight parameters, which are presented in Equations 2-8 through 2-13.

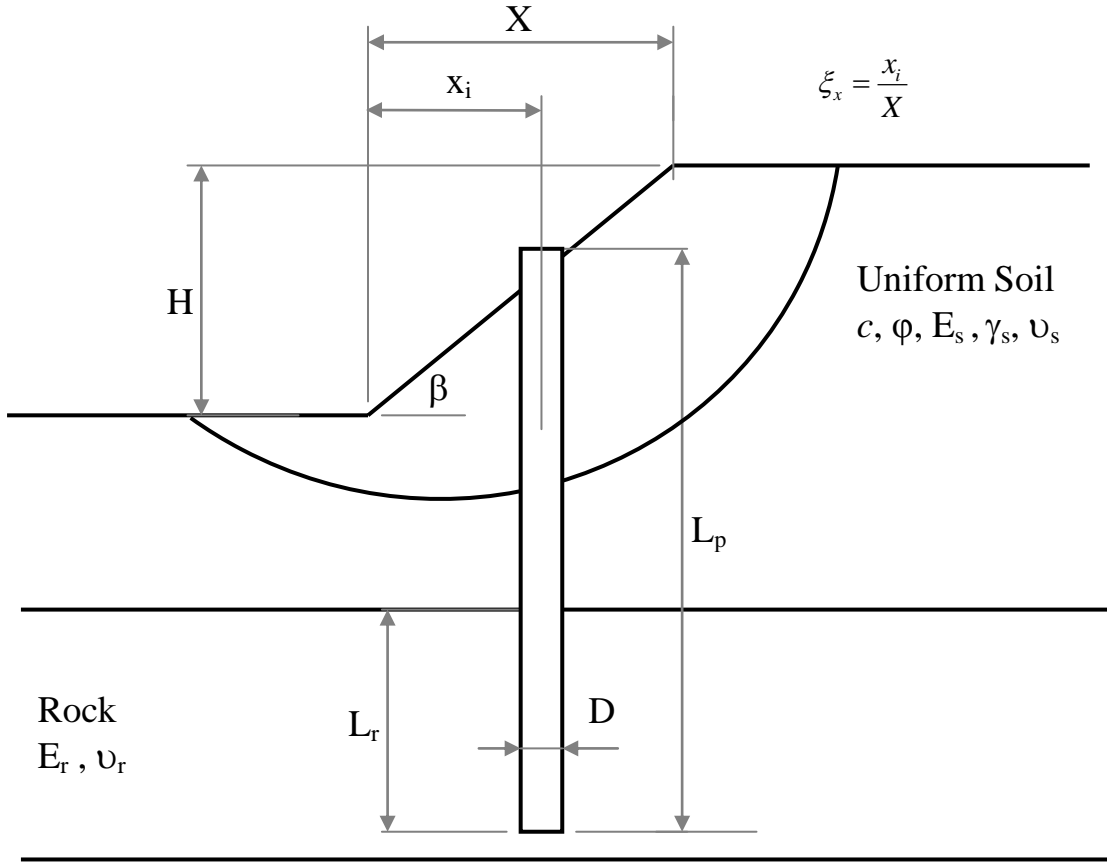


Figure 0-4: Illustration of the Terms Related to the Slope Geometry (Al Bodour, 2010)

$$\eta = \eta_1^{0.7} \eta_3^{0.76} (3.23 + 0.96 \ln \eta_2) \quad (2-8)$$

where,

$$\eta_1 = \frac{c^{0.287}}{E^{0.418}} [0.018 + 0.256 \tan \varphi] \quad (2-9)$$

$$E = \frac{E_s}{10^6} \quad (2-10)$$

$$\eta_2 = 0.24 \ln(S_0 / D) - 0.047 \xi_x^{3.95} \tan \beta \quad (2-11)$$

$$\xi_x = \frac{x_i}{X} \quad (2-12)$$

$$\eta_3 = \frac{0.004D^{11.2}}{L_p^{0.412}} (0.091)^D \quad (2-13)$$

$$0 < \eta < 1.0$$

$$L_r > 0.15L_p$$

Using the load transfer factor equation, Al Bodour was successful in adopting the arching in the limit equilibrium analysis to calculate the factor of safety. Also, a case study of a fully instrumented and monitored slope stabilization project, ATH-124, in Athens County, Ohio, is introduced. The analysis of the stabilized slope at the ATH-124 project site using finite element modeling (FEM) is presented along with the field monitoring data. However, Al Bodour could not validate the result of the proposed methodology with the FE results when using different definitions for the load transfer factor. Instead, he proposed an empirical formula based on the FE result to obtain the maximum force on the shaft.

2.2.5. Research by Joorabchi (2011)

To address the deficiency of the work done by Al Bodour (2010), the finite element analysis is reviewed and returned to quantify the arching by Joorabchi (2011). The main purpose of this study was to define the major parameters that control the load transfer process under the effect of shear strength reduction in a slope reinforced with a single row of drilled shafts. The parametric study was performed by scientifically changing the value of one parameter while keeping all of

the other parameters the same as a baseline model. The range of all the parameters is shown in Table 2-1. The parameters, which showed no significant effect on the load transfer factor, were further investigated by randomly exchanging them with other parameters to ensure that the same conclusions could be reached. The parameters that were considered to be non-significant were based on the total importance percentage of less than 5%. The importance of each parameter was calculated from the following equation:

$$I = \frac{\eta_i^{\max} - \eta_i^{\min}}{\sum(\eta_i^{\max} - \eta_i^{\min})} \quad (2-14)$$

where

I = importance of the parameter (i)

η_i^{\max} = the maximum load transfer factor obtained from the parameter (i)

η_i^{\min} = the minimum load transfer factor obtained from the parameter (i)

The parameters that were found to have a controlling effect are presented in Table 2-2.

Table 0-1: The Ranges of the Parameters Used in the Parametric Study (Al Bodour, 2010)

Group	No.	Parameter	Parameter Value	Range of Parameter
Soil Properties	1	Angle of internal friction (ϕ , degrees)	10	0,5,10,15,20,25,30,35,40,45,50
	2	Cohesion (c , psf)	400	0,250,400,500,750,1000,1250,1500,1750,2000
	3	Soil Elastic Modulus (E_s , psf)	2×10^5	1,2,5,7.5,10,12.5,15,17.5,20($\times 10^5$)
	4	Dry Soil Unit weight (γ_d , pcf)	115	100,105,110,115,120,125,130
Shaft Parameters	5	Pile Diameter (D , ft)	4.0	2,3,4,5,6,8,9,10
	6	Pile length (L_p , ft)	50	30,40,45,50,60,65,70,75,80
	7	Pile Elastic Modulus (E_p , psf)	4.2×10^8	3.5, 4.2,4.8,5.6,6.8 ($\times 10^8$)
	8	Pile Poisson's Ratio (ν_p)	0.2	0.12,0.15,0.18,0.22,0.25
	9	Rock Socket Length ratio (L_r/L_p)	0.2	0.15,0.2,0.25,0.35,0.45,0.5
Rock Properties	10	Rock Elastic Modulus (E_r)	5×10^8	0.5,1,3,5,5.5,7,8 ($\times 10^8$)
	11	Rock Poisson's Ratio (ν_r)	0.2	0.15,0.2,0.18,0.23,0.25
Geometry and Arrangement	12	Slope angle (β , degrees)	40	25,30,35,40,45,50,55,60
	13	S_0/D Ratio	3.0	1.875,2,2.75,3.25,3.5,4,4.5,5
	14	Pile location (x_i/X) = ξ_x	0.5	0.15,0.3,0.4,0.6,0.75,0.9
Interaction	15	Soil-Pile friction ($\tan\delta$)	0.3	0,0.1,0.2,0.3,0.4,0.5

Table 0-2: The importance of each parameter in affecting load transfer factor

Ranking	Parameters	Importance
1	Pile diameter (D)	28%
2	Internal friction angle (ϕ)	21%
3	Pile location (ξ_x)	18%
4	S_0/D ratio	16%
5	Cohesion (c)	12%
6	Slope angle (β)	6%

Based on the importance of parameters analysis from Joorabchi's study, the load transfer factor was related to six parameters: shaft diameter D , friction angle ϕ , shaft location ξ_x , ratio between center to center spacing and shaft diameter S_0/D , cohesion c , and slope angle β . Joorabchi's final equation for the load transfer factor is presented in Equation 2-15.

$$\eta = -0.272C^{0.153}(\tan \beta)^{-0.429}(-1.17 + 1.114 \frac{S_0}{D})(e^{-0.578 \tan \phi})(0.065 + 0.876D) \quad (2-15)$$

$$(-0.252 + 0.61 \xi_x - 0.57(\xi_x^2))$$

where all the parameters have been shown in the above expression.

2.3. Multiple Rows of Drilled Shafts Stabilizing Slope

To prevent a large-scale landslide, multiple rows of drilled shafts are frequently used. A number of studies have dealt with the analysis of multiple rows of piles to stabilize a slope. Ito et al. (1982) analyzed eight rows of piles in stabilizing a slope, considering both pile stability and slope stability. Mujah et al. (2013) analyzed the mechanism of small-diameter steel piles and investigated how multiple rows of arrangement of the piles would affect the reinforced slope failure in a landslide countermeasure. In Mujah's study, finite element analysis employing Mohr-Coulomb's elastic-perfectly plastic soil model was carried out to simulate real conditions, in which the effect of the varying ground densities ($D_r = 30\%$ and $D_r = 80\%$) and two pile cross sections were considered for landslide prevention. However, none of the studies in the literature has introduced soil arching to calculate the factor of safety and the force on the drilled shaft.

2.4. Probabilistic Study

Probability-based approaches for slope stability analysis have been a topic of research since the 1970s. Notable examples of probabilistic theory for slope stability analysis are cited in this section. Tang et al. (1976) presented a probability-based method for evaluating the short-term stability of a slope, involving consideration of uncertainties based on an extensive literature survey. Oka and Wu (1990) elucidated that the upper bound of the system failure probability could be twice as large as the failure probability of a critical slip surface. Low et al. (1998) calculated the reliability index of a slope by using generalized method of slices of the Hasofer-Lind second moment. Liang et al. (1999) developed the reliability and probability theory for assessing the reliability index and the corresponding probability of failure of multi-layered embankment dams and slopes. Malkawi et al. (2000) compared FOSM and Monte-Carlo simulation (MCS) for analyzing the reliability of a slope. Griffiths and Fenton (2004) analyzed the slope spatial variability using a two-dimensional random field. Cheung and Tang (2005) proposed a procedure to model the slope deteriorating effect on the probability of failure with time. Hong and Roh (2008) employed the first-order reliability method (FORM) for estimating the reliability index of earth slopes. Zhang and Tang (2011) proved that neglecting the past failure information of the slope may lead to unsafe or uneconomical decisions based on site-specific performance information.

It is noted that none of the existing literature deals with the probability framework for a drilled shaft stabilized slope. Nevertheless, the critical knowledge base gathered from reviewing these probability based analysis methods for slope safety evaluation should provide a fundamental basis for the proposed research work.

2.4.1. Importance Sampling Technique

MCS is commonly considered as the most robust methodology dealing with reliability analysis (Robert and Casella, 2004). Mathematically, however, traditional MCS involves samples “randomly” falling into the failure region to calculate the estimator (P_f), which means if the estimator (P_f) is quite small, it requires a large number of samples. If we intend to generate random samples more efficiently, we make an effort to distribute more “useful” samples into the failure zone, which means fewer samples should be wasted during the probabilistic calculation. Au et al. (1999) and Au and Beck (2003) proved the feasibility in high dimensional cases by employing statistical calculations, and they suggested that keeping the covariance matrices (Σ) of $IS(x)$ and $f(x)$ equal to identical matrix E is a much more accurate way to deal with high dimensional cases. Ching et al. (2009, 2010) studied landslides without drilled shafts using the importance sampling technique (IST) based on the ordinary method of slices (OMS). Although multiple soil layers have been proposed, only one soil parameter (such as cohesion c) has been considered as an uncertainty and others (e.g. friction angle ϕ and unit weight γ) have been assumed as certainties during sample calculations. However, in practice, uncertainties for all soil parameters are present at all times.

It should be noted that there are no prior studies that consider IST in dealing with a drilled shafts/slope system.

3. PROBABILISTIC VERSION OF *UA SLOPE* COMPUTING ALGORITHM

3.1. Introduction

Stabilization of unstable slopes or man-made embankments along highways has been an important geotechnical issue that needs to be addressed to ensure the operational safety of roadways. A wide variety of slope stabilization methods have been presented by numerous researchers in the past. Among these methods, the concept of using a row of drilled shafts to reinforce unstable slopes has been used successfully by state transportation agencies. Although the analysis and design of these drilled shafts has been a research topic since the 1960s, a complete reliability-based design for drilled shaft/slope systems is still a new area of study.

A deterministic analysis and design method for a slope reinforced with a row of drilled shafts using the concept of soil arching (Liang and Zeng, 2002; Yamin, 2007; Al Bodour, 2010; Joorabchi, 2011) has been developed and coded into a computer program called *UA Slope* (version 2.1). However, this program cannot systematically account for the uncertainties of soil parameters and the semi-empirical equation for quantifying the soil arching effects. Presented in this report is the mathematical formulation of the probabilistic computational algorithms for determining the probability of failure (or reliability index) of a slope reinforced with a row of equally spaced drilled shafts, considering all important sources of uncertainties of the input soil parameters and any bias introduced by the semi-empirical equations for the soil arching effects. The details of FEM techniques for quantifying characteristics of soil arching effects are presented, together with the statistical analysis for deriving the mean and variance of bias of the semi-empirical predictive equation for the arching effects. Finally, two design examples are

presented to illustrate the use of the probabilistic computing algorithm for achieving optimized design.

3.2. Deterministic Limiting Equilibrium Method of Slices in Drilled Shaft/Slope System

The formulation of the method of slices incorporating the arching effects caused by the drilled shafts is presented briefly in this section. Details regarding the development of the methodology can be found in Liang (2010). The interslice force P_i^L and P_i^R shown in Figure 3-1a can be related by considering the force equilibrium and Mohr-Coulomb strength criterion, as given in Equation 3-1. With the insertion of drilled shafts into the slope, the force on the downslope side of the drilled shaft will be reduced by multiplying the load transfer factor (η) to the previous interslice force, P_{i-1}^L , expressed by Equations 3-2 and 3-3:

$$P_i^L = w_i \sin \alpha_i - \left[\frac{c_i l_i}{FS} + (w_i \cos \alpha_i - u_i l_i) \frac{\tan \phi_i}{FS} \right] + k_i P_i^R \quad (3-1)$$

$$P_i^L = w_i \sin \alpha_i - \left[\frac{c_i l_i}{FS} + (w_i \cos \alpha_{i-1} - u_i l_i) \frac{\tan \phi_i}{FS} \right] + k_i \eta P_{i-1}^L \quad (3-2)$$

$$k_i = \cos(\alpha_{i-1} - \alpha_i) - \sin(\alpha_{i-1} - \alpha_i) \frac{\tan \phi_i}{FS} \quad (3-3)$$

The net force applied to the drilled shaft due to the difference in the interslice forces on the upslope and downslope sides of the drilled shaft can be calculated as follows:

$$F_{Shaft} = (1 - \eta) P_{i-1}^L S \quad (3-4)$$

where w_i is the weight of Slice i ; N_i is the force normal to the base of the Slice i ; T_i is the force parallel to the base of Slice i ; P_i^L is the interslice force acting on the left side of the slice; P_i^R is the interslice force acting on the right side of the slice; α_i is the inclination of Slice i base; α_{i-1} is the inclination of Slice $i-1$ base; c_i is the soil cohesion at the base of Slice i ; and ϕ_i is the soil friction angle at the base of Slice i . Based on Equations 3-1 to 3-3, the factor of safety for a drilled shaft/slope system can be calculated in an iterative computational process by satisfying boundary load conditions and equilibrium requirements, along with the Mohr-Coulomb strength criterion.

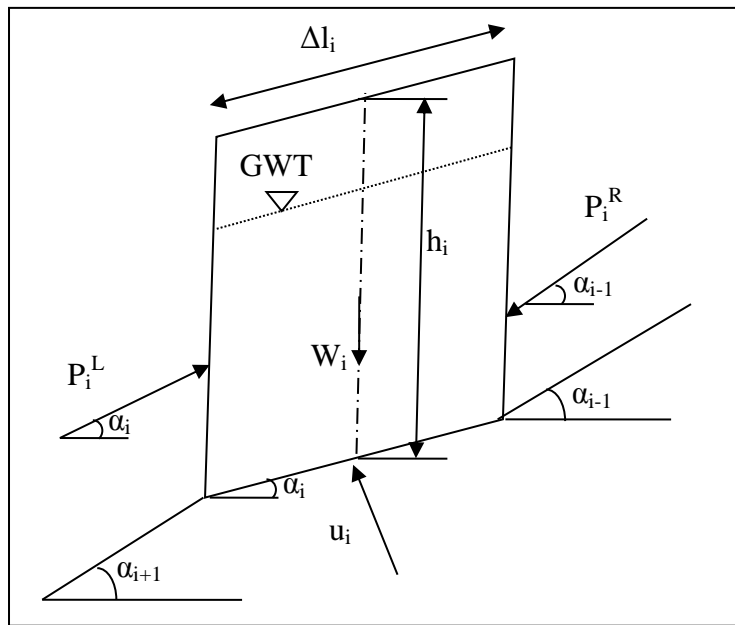


Figure 0-1a: A typical slice showing all force components

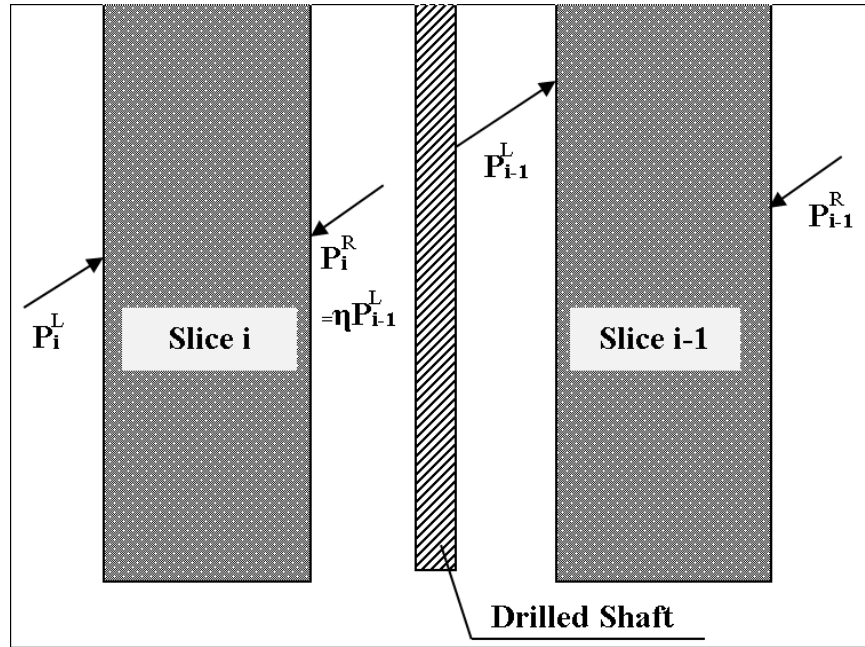


Figure 0-1b: Slice force change due to arching

To interpret the arching effects in a drilled shafts/slope system, a load transfer factor and soil stress distribution have been introduced as shown in Figures 3-2a and 3-2b, which is defined as the ratio of the horizontal force on the downslope side of the vertical plane at the interface between the drilled shaft and soil (i.e., $P_{\text{downslope}}$) to the horizontal force on the upslope side of the vertical plane at the interface between the drilled shaft and soil (i.e., P_{upslope}). Mathematically, the load transfer factor is expressed as:

$$\eta = P_{\text{downslope}}/P_{\text{upslope}} \quad (3-5)$$

The resultant force in the upslope and downslope sides of drilled shaft is calculated by integrating the horizontal soil stresses from the top of the shaft down to the failure surface, as described in Equations 3-6 and 3-7.

$$F_{up} = \int_0^{L_f} \int_0^{\pi D/2} \sigma_{xx} ds dz \quad (3-6)$$

$$F_{down} = \int_0^{L_f} \int_0^{\pi D/2} \sigma'_{xx} ds dz \quad (3-7)$$

where D is the diameter of the drilled shaft; L_f is the distance from the top of the shaft down to the failure surface; σ_{xx} is the horizontal soil stresses on the upslope side of the shaft; σ'_{xx} is the horizontal soil stresses on the downslope side of the shaft; ds is the integration increment along the periphery of the shaft; and dz is the depth increment.

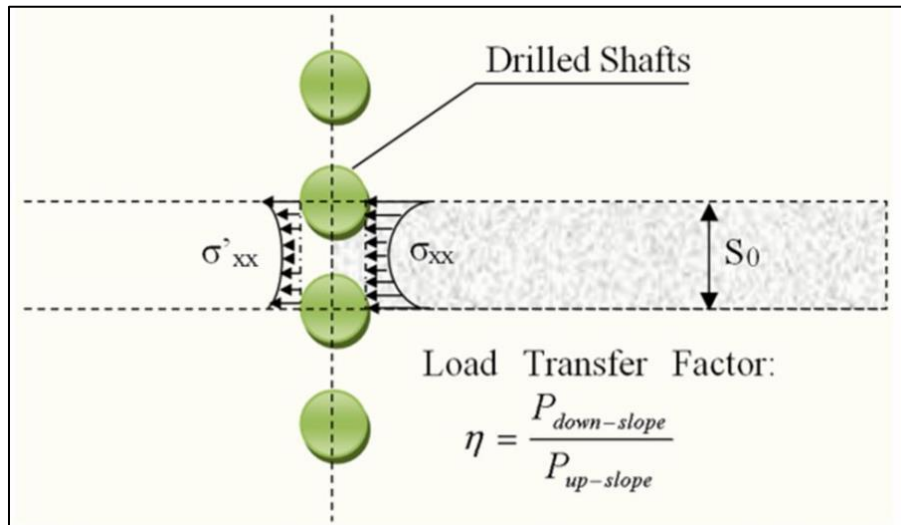


Figure 0-2a: Definition of the soil arching

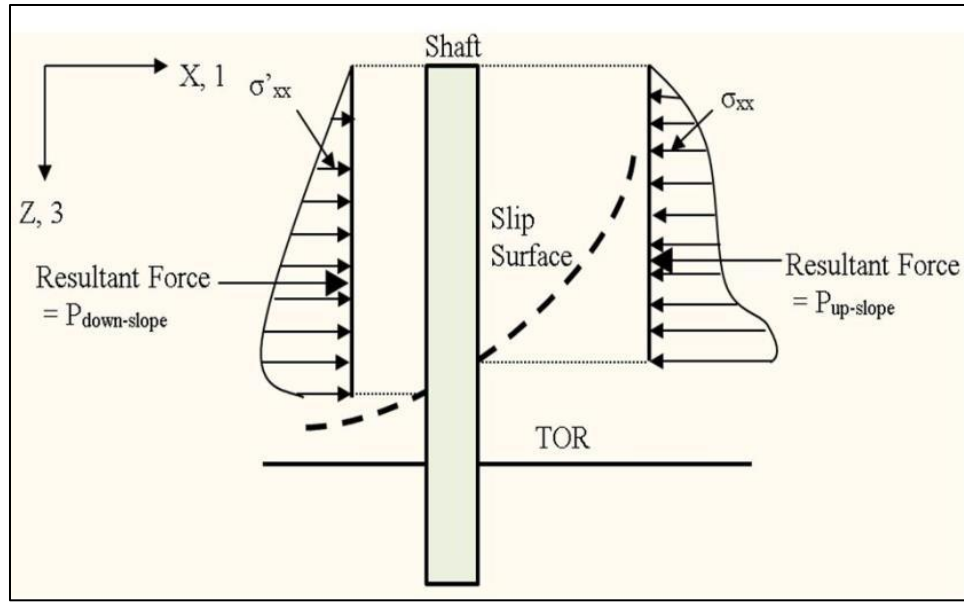


Figure 0-2b: Soil stress distribution

3.2.1. Latest Study of Load Transfer Factor by Joorabchi (2011)

To quantify the soil arching effects and the load transfer factor in a drilled shaft/slope system, Al Bodour (2010) constructed a baseline 3D finite element model using *ABAQUS v. 6.7-1* for studying the soil structure interaction behavior of the drilled shafts on a slope under the effect of shear strength reduction method (SSRM). The strength reduction method in finite element simulation was first proposed by Zienkiewicz (1975) to study the slope stability problem. The concept of the strength reduction method in the finite element method for determining FS of a slope is to gradually decrease the soil strength parameters (c and ϕ) until the condition of slope failure ($FS = 1$) is reached. The initial soil strength parameters [c and $\tan(\phi)$] are reduced incrementally by dividing them with a reduction factor (R_F). Therefore, the reduced cohesion, C_R and internal friction angle, ϕ_R are given as:

$$C_R = C/R_F \quad (3-8)$$

$$[\tan(\varphi)]_R = \tan(\varphi)/RF \quad (3-9)$$

In the 3D finite element model in Al Bodour (2010), soil is modeled as a linear elastic–perfectly plastic material characterized by the angle of internal friction, cohesion, elastic modulus, and Poisson’s ratio. The geometry and finite element mesh of the 3D model are depicted in Figures 3-3a and 3-3b, respectively, which consists of 7,696 hexahedral elements for soil body, 23,600 similar elements for rock, and 420 similar elements for drilled shafts. The mesh of the drilled shaft and the adjacent area was finer than that of the other zones. The mesh was refined on the basis of the convergence of the numerically computed FS. The baseline model geometry and the parameters for this study were selected such that the non-reinforced slope has FS = 1. A series of parametric finite element studies were conducted, in which each parameter was investigated by changing its value over a reasonable range. For each different value of each parameter, the model was analyzed using both FEM and the shear strength reduction method. At failure, the FS, the upslope and downslope horizontal soil stresses around the shaft perimeter, and the depth of the failure surface at the drilled shaft location were obtained. The soil arching effect can be observed in the computed horizontal stresses on the upslope and downslope sides of the drilled shafts, shown in Figure 3-4 as a stress contour plot of a horizontal plane.

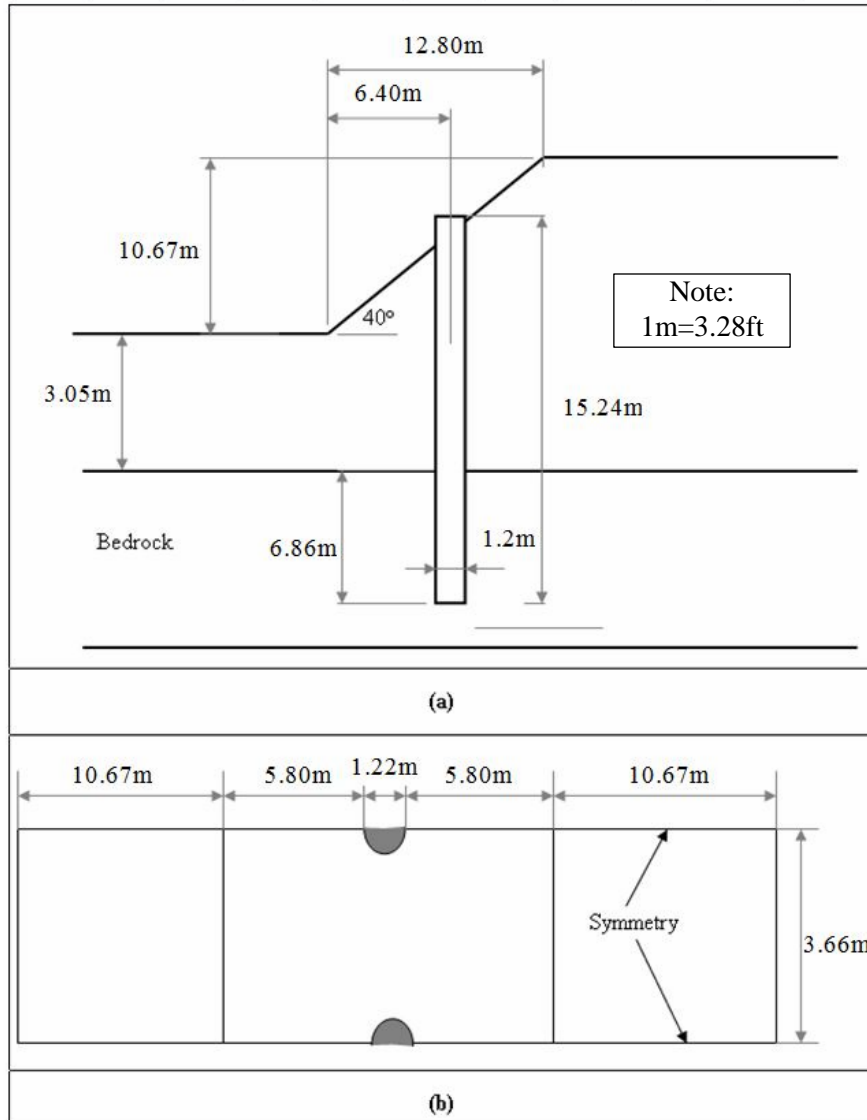


Figure 0-3a: Geometry and dimensions of the 3D model a) Cross-section b) Top view

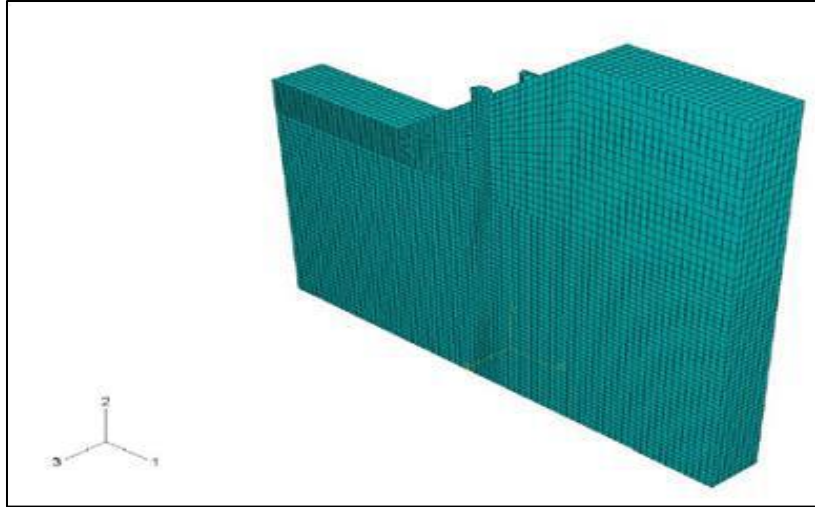


Figure 0-3b: 3D finite element model developed by Al Bodour (2010)

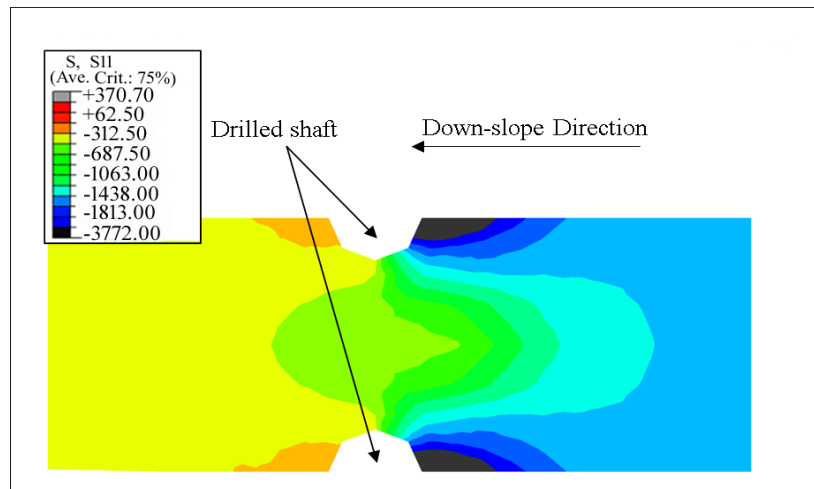


Figure 0-4: Soil arching as observed from the horizontal soil stresses in the direction of the soil movement (after Al Bodour, 2010)

The parameters affecting soil arching effects can be divided into five groups: 1) Soil parameters (cohesion c , internal friction ϕ , elastic modulus E_s , and unit weight γ); 2) Rock properties (Elastic modulus E_r , and Poisson's ratio ν_r); 3) Shaft properties (total shaft length L_p , rock socket length L_r , diameter D , elastic modulus E_p , and Poisson's ratio ν_p); 4) Geometry (spacing to

diameter ratio S/D , slope angle β , dimensionless shaft location $\xi = x_i/X$; and finally 5) The soil-shaft friction at interface δ . The geometry of the slope is shown in Figure 3-5 with all the related terms defined. A detailed importance analysis of these influencing parameters on the arching effect was presented in Joorabchi (2011). Based on FE simulation results and the regression analysis, Joorabchi (2011) proposed a semi-empirical equation as shown in Equation 3-10 below, which includes the important influencing parameters: soil cohesion c , friction angle ϕ , drilled shafts diameter D , center to center shaft spacing S_0 , shaft location on slope ξ_x , and slope angle β .

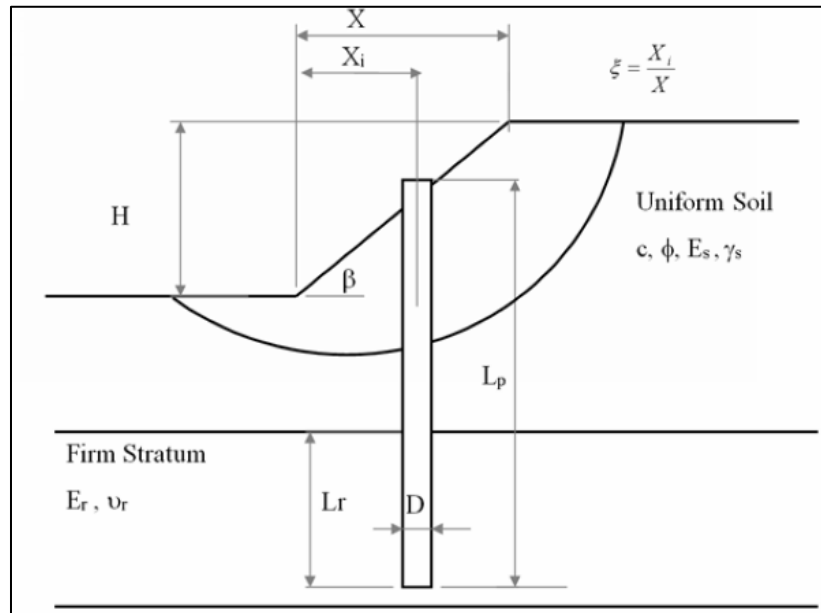


Figure 0-5: Illustration of the Terms Related to the Slope Geometry

$$\eta = -0.272c^{0.153}(\tan \beta)^{-0.429}(-1.17 + 1.114 \frac{S_0}{D})(e^{-0.578 \tan \phi})(0.065 + 0.876D) \\ (-0.252 + 0.61 \xi_x - 0.57(\xi_x^2)) \quad (3-10)$$

$$0 < \eta < 1.0; L_r > 0.15L_p$$

The load transfer factor should always be greater than zero and less than one. The value of zero indicates that drilled shafts take all of the earth thrust. Also, the load transfer factor equal to 1.0 indicates that drilled shafts exert no effect on arching. For the purpose of checking the validity of the developed semi-empirical equations, the load transfer factor was calculated using Equation 3-10 for all the FE models. The results obtained from Equation 3-10 are compared against the FE results shown in Figure 3-6. It can be seen that there is a good agreement between the FE results and the results obtained from Equation 3-10. A PC-based deterministic computer program, *UA Slope 2.1*, has been developed by Liang (2010) based on the above computational algorithm to calculate the factor of safety of a slope reinforced with a row of equally spaced drilled shafts and the net force on the drilled shaft.

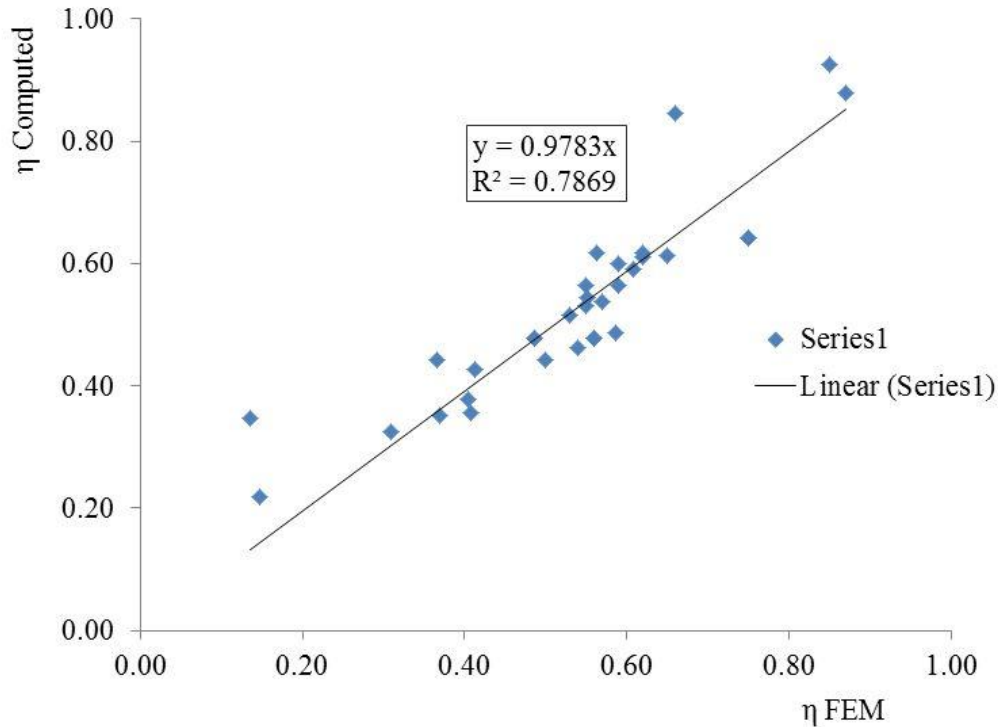


Figure 0-6: Comparison of load transfer factor computed by semi-empirical equation and FEM (after Joorabchi, 2011)

3.3. Probabilistic Version of *UA Slope*

The goal of this study is to develop of a new computational algorithm that is probabilistic in nature to take into account the uncertainties of the soil parameters (i.e., cohesion c , friction angle ϕ and unit weight γ) and the load transfer factors (η) in the current *UA Slope* computational algorithm, which is deterministic in nature.

3.3.1. Uncertain Parameters in a Drilled Shaft/Slope System

The influencing parameters in a drilled shaft reinforced slope system can be divided into two major categories: soil properties (cohesion c , friction angle ϕ , and unit weight γ) and drilled shaft related parameters (shaft diameter D , clear spacing S between the adjacent drilled shafts, the location of the shaft on the slope ξ_x). In this report, the drilled shaft related parameters are treated as certain, while the soil properties are considered as uncertain in the developed reliability based analysis method for a drilled shafts/reinforced slope system.

3.3.2. Bias of Load Transfer Factor

The semi-empirical load transfer factor (η) function given in Equation 3-10 contains bias as compared to the “true” value from the results of the 41 cases of 3D finite element simulations. The load transfer factor bias (δ) is considered as a random variable with the mean and variance statistically analyzed by comparing the finite element simulation results and the predictions of the semi-empirical equation. The mean and c.o.v. are 1.01 and 0.15, respectively. As indicated in Equation 3-11, the load transfer factor is randomly generated through the randomly generated bias:

$$\eta = \delta \eta(\hat{c}, \varphi, \beta, D, \xi_x, S_0) \quad (3-11)$$

where, η is the randomly generated load transfer factor; δ is the randomly generated bias of load transfer factor; \hat{c} and φ are the randomly generated soil cohesion and friction angle, respectively; β , D , ξ_x and S_0 are considered as deterministic parameters.

3.3.3. Monte-Carlo Simulation

The probability of failure for the drilled shafts/slope system is computed by means of Monte Carlo simulation (MCS) method, as expressed by Equations 3-12 to 3-13. In this report, a probabilistic version of the *UA Slope* computer program, *UA Slope 3.0*, was coded for reliability analysis of a drilled shaft stabilized slope. The *UA Slope 3.0* is a newly developed computer code based on the previous deterministic program *UA Slope 2.1*. Instead of inputting the deterministic soil parameters (c , φ , γ), the randomly generated parameters can be inputted into the *UA Slope 3.0* program for Monte Carlo simulations of the selected simulation sample sizes to obtain the corresponding probability of failure. In addition, the bias of load transfer factor δ will be considered using Equation 3-11. The probability of failure and the associated coefficient of variance (c.o.v.) are given in Equations 3-12 and 3-13.

$$P_f = E(I[x]) \cong \frac{1}{N} \sum_{i=1}^N I[FS < 1] = \frac{1}{N} \sum_{i=1}^N I_i \left[\frac{F_R - F_D + (\Delta F_D)_{arching}}{F_D - (\Delta F_D)_{arching}} < 0 \right] \quad (3-12)$$

$$\delta(P_f) = \sigma_{P_f} / \mu_{P_f} \cong \sqrt{\frac{1}{N} \sum_{i=1}^N \left(I_i \left(\frac{F_R - F_D + (\Delta F_D)_{arching}}{F_D - (\Delta F_D)_{arching}} < 0 \right) - P_f \right)^2} / P_f \quad (3-13)$$

$$\beta = 1 - \Phi(P_f) \quad (3-14)$$

where P_f is the computed probability of failure for the drilled shafts/slope system, $\delta(P_f)$ is the coefficient of variance (c.o.v.) of P_f , $I[FS < 1]$ is the indicator function, N is the sample numbers, and β is the reliability index. The value for β can be negative when the P_f is larger than 0.5.

The advantages of using Monte Carlo simulation are numerous: 1) it can address the various sources of uncertainties mentioned; 2) the consideration of uncertainties is more transparent to the designers; 3) the user is able to define statistical descriptions of the uncertainties of the input parameters in the *UA Slope* program; and 4) it can accommodate different site conditions.

3.4. Monte-Carlo Coding Strategy for *UA Slope* Program

A research version computer program for *UA Slope* has been developed during this study by using *MATLAB* and *C++*. *MATLAB* will be used to generate the Monte Carlo random variables (c , ϕ , γ , δ) by using the ziggurat algorithm, and *C++* will be used to perform the reliability analysis by Monte Carlo simulation. Figure 3-7 presents a preliminary version of the coding strategy of Monte Carlo simulation within *UA Slope* program. Essentially, the work involves the following steps:

- Step 1: Specify the input slope and drilled shaft geometry.
- Step 2: Read three data fields from three text files (c.txt, Fai.txt, Gamma.txt).
- Step 3: Read one data field from a bias of load transfer factor file (Bias.txt).
- Step 4: Calculate the factor of safety of the shafts/slope system one time.

- Step 5: Perform Monte Carlo simulation for N times.
- Step 6: Calculate the probability of failure and reliability index for the drilled shaft/slope system.

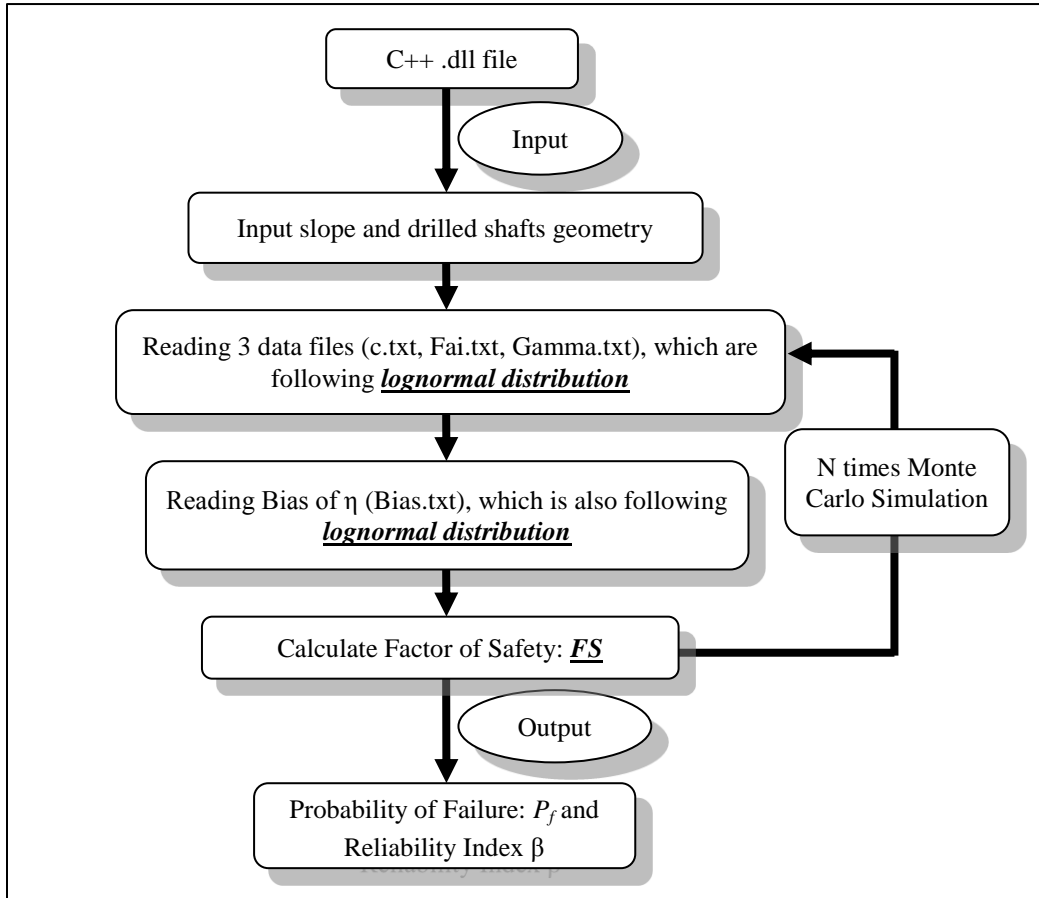


Figure 0-7: Preliminary research version of Monte Carlo coding strategy for *UA Slope* program

3.5. Design Method

3.5.1. Step-by-Step Design Procedure

The computational algorithms of the *UA Slope 3.0* program include the following features and steps.

- Step 1: Specify the slope and drilled shaft geometry.
- Step 2: Specify the probability distribution for soil properties, (i.e. cohesion c , friction angle ϕ and unit weight γ); currently, it is assumed that these variables follow a lognormal function with the specified mean and variance values.
- Step 3: Perform statistical analysis of the bias of the load transfer factor, expressed in the previous section.
- Step 4: Perform Monte-Carlo simulations using the deterministic computing algorithm for the drilled shafts/slope system; the ziggurat algorithm is used as a pseudo-random number generator.
- Step 5: Obtain the reliability index for a drilled shaft/slope system.

The flowchart of the *UA Slope 3.0* program is depicted in Figure 3-8.

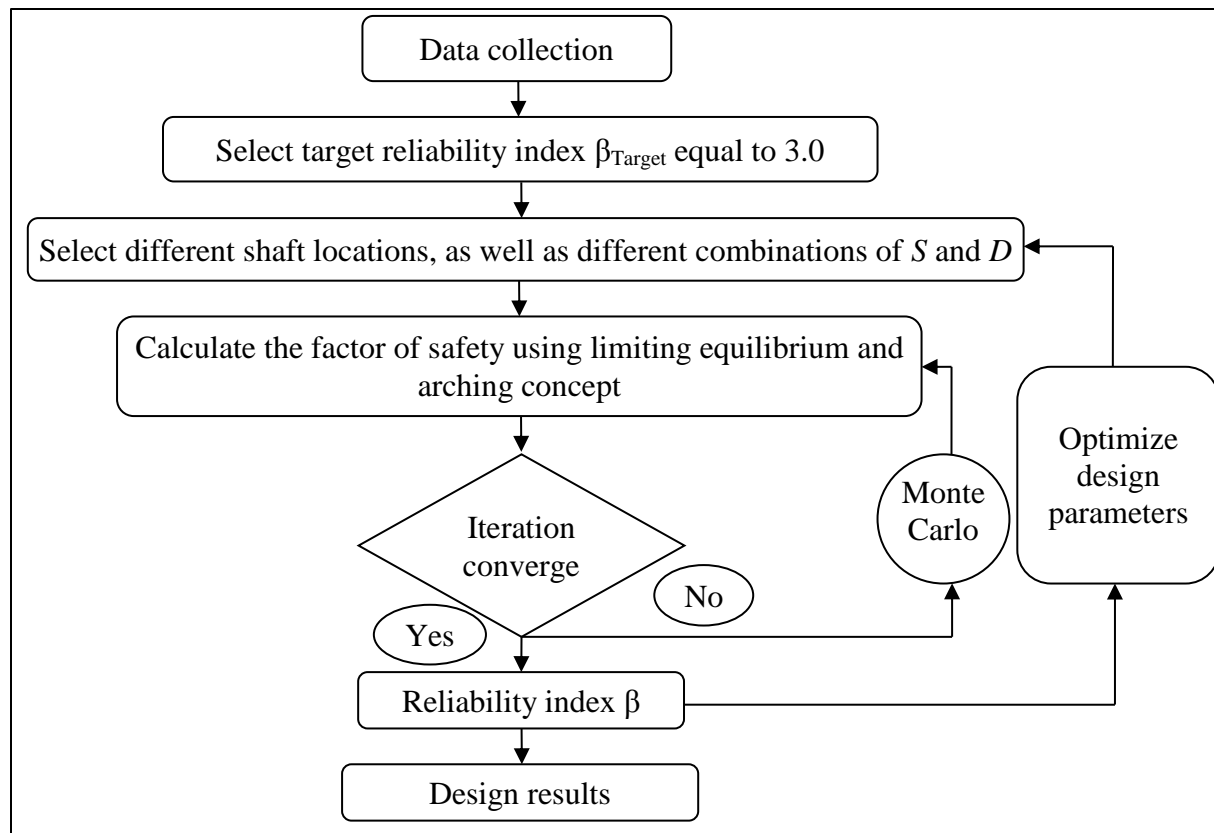


Figure 0-8: Flowchart of MCS method for the drilled shaft/slope system

3.5.2. Illustrative Example 1

The slope shown in Figure 3-9 consists of two soil layers with soil properties for each layer summarized in Table 3-1, in which the range of coefficient of variance for each soil parameter is taken from Phoon and Kulhawy (1999) and the soil parameters for the two soil layers follow an independent identical distribution. The critical slip surface for the slope without the drilled shafts was determined by a conventional slope stability analysis program, such as *STABL* (developed by Purdue University), with the computed FS equal to 0.78. The identified critical slip surface is represented by connecting 14 points. In most design problems that involve reinforcing an

unstable slope, the slip surface can be obtained through field monitoring or other means. Therefore, in the present study, the slip surface is treated as a pre-existing failure surface and is fixed in the probability analysis. The groundwater table is assumed to be at an elevation of -7.93 m. It is noted that effective stress approach is used in the analysis.

The relationship between probability of failure (P_f) and the corresponding coefficient of variation (c.o.v.) can be expressed as follows:

$$c.o.v.(P_f) = \sqrt{(1 - P_f) / (N \cdot P_f)} \cong \sqrt{1 / (N \cdot P_f)} \tag{3-15}$$

In the present design example, we generate 100,000 samples for each variable: cohesion (c), friction angle (ϕ) and unit weight (γ), as well as the bias (δ) of load transfer factor.

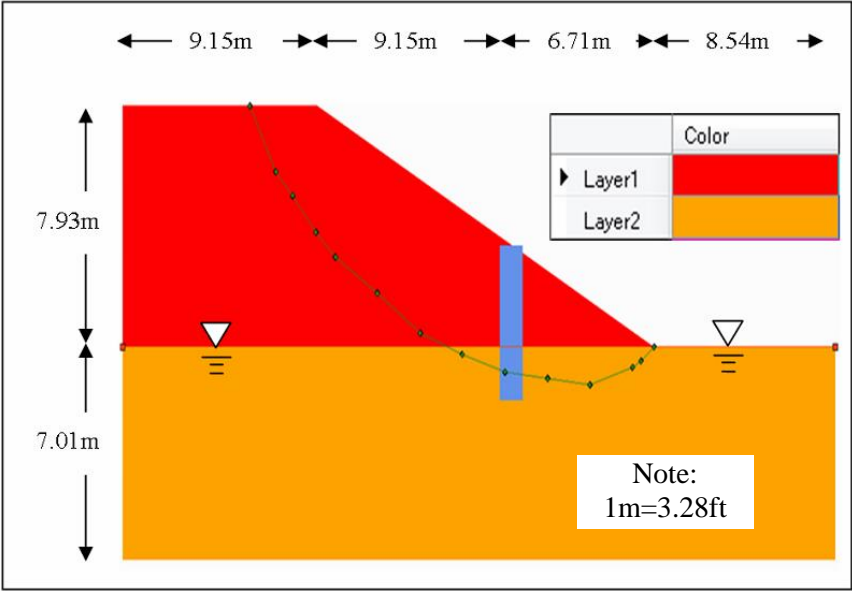


Figure 0-9: Slope geometry for two-layer slope

Table 0-1: Soil Properties of the Two-Layer Slope

Layer No.	Mean		c.o.v.
	Layer 1	Layer 2	
c (kN/m ²)	0.958	2.394	0.2
	(20psf)	(50psf)	
φ (degree)	11	18	0.1
γ (kN/m ³)	21.21	22.78	0.01
	(135pcf)	(145pcf)	

3.5.2.1. Step-by-Step Design Procedure for Drilled Shaft/Slope Design for Example 1

The step-by-step procedure for designing a drilled shaft/slope system for the slope in Example 1 is as follows:

- Step 1: Collect data concerning the geometry of the slope, soil parameters, groundwater table, critical slip surface, etc. (the collected data are presented in Figure 3-9 and Table 3-1). Again, the slip surface is considered deterministic and fixed in the present approach.
- Step 2: Choose a target reliability index. As recommended by Abramson et al. (2002), the target reliability index β_{Target} can be selected as 3.0.
- Step 3: Select different drilled shaft locations. Feasible locations for drilled shafts are between 12.3 m (40 ft) and 21.8 m (70ft) ($\xi_x = 0.2\sim 0.8$) horizontally from the crest of the slope to the toe of the slope (as shown in Figure 8). In the current design, we analyze the

location starting from $X = 12.3$ m (40 ft) and ending at $X = 21.8$ m (70ft), with an increment equal to 1.9 m (6ft).

- Step 4: Select different pairs of clear spacing S and shaft diameter D combinations within the permissible range. This usually depends on site accessibility and local availability of construction equipment. In this example, the range for D is selected to be between 0.6 m and 2.4 m (2 ft~8 ft), and the range of the S/D ratio is selected to be between 1.0 and 3.0. The following combinations for (S, D) are selected: (0.6m (2.0ft), 0.6m (2.0ft)), (1.2m (4.0ft), 0.6m (2.0ft)), (1.8m (6.0ft), 0.6m (2.0ft)), (1.2m (4.0ft), 1.2m (4.0ft)), (2.4m (8.0ft), 1.2m (4.0ft)), (1.8m (6.0ft), 1.8m (6.0ft)), and (2.4m (8.0ft), 2.4m (8.0ft)).
- Step 5: For each (S, D) combination, plot the relationship between the computed reliability index and shaft location, as shown in Figure 3-10.
- Step 6: For each (S, D) combination, plot the relationship between the computed net force on the drilled shaft and shaft location, as shown in Figure 3-11.

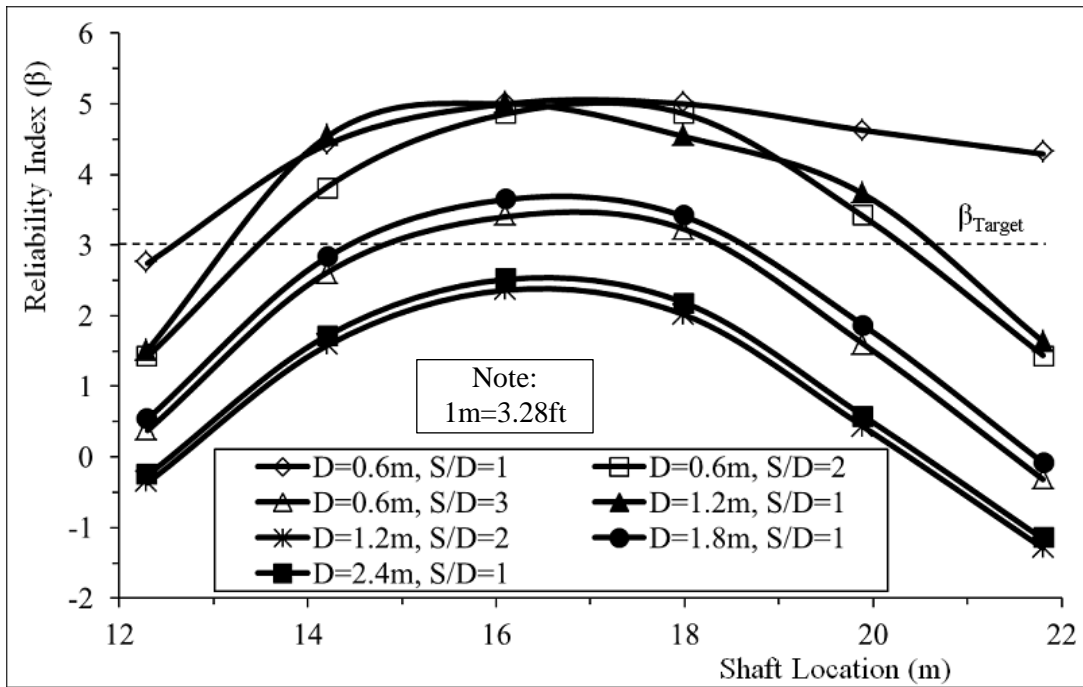


Figure 0-10: Reliability index of the shaft-slope system versus shaft location for different (S, D) combinations

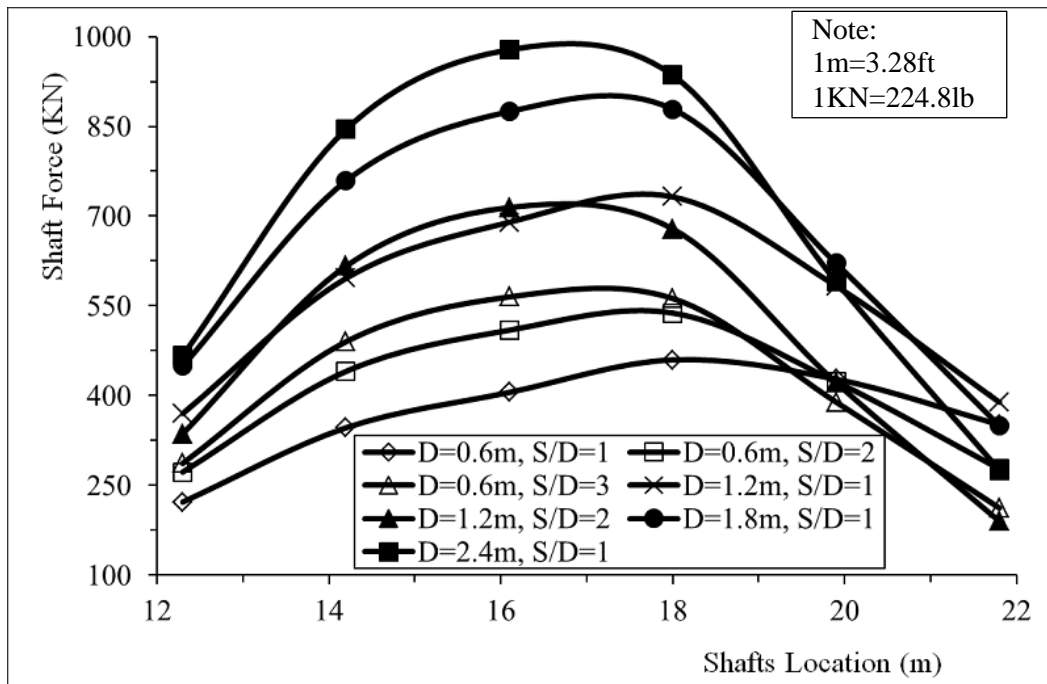


Figure 0-11: Shaft force versus shaft location for different (S, D) combinations

- Step 7: Optimize the design for achieving the target reliability index, while requiring the least amount of drilled shaft volume for the project. As can be seen in Figure 3-10, the reliability index (β) tends to increase with shaft location (measured by the distance from the crest of slope) and then decreases after reaching the middle location of the slope. The location of 16 m provides the highest reliability index for the given shaft diameter and spacing. However, as shown in Figure 3-11, the drilled shafts at the location equal to 16 m are also subject to the largest net forces, which would have resulted in higher internal moments and shears in the shaft and higher required reinforcement ratios as well. It appears that the force on the shafts would decrease after the location 18 m, and the computed reliability index (β) would still satisfy the target reliability index. Furthermore, the required length of drilled shafts could be reduced if the location of the drilled shaft is moved further downslope. From these considerations, three combinations are selected: (a) location $X = 21.8$ m (70ft), $D = 0.6$ m (2.0ft), $S/D = 1.0$; (b) $X = 19.9$ m (65ft), $D = 0.6$ m (2.0ft), $S/D = 2.0$; and (c) $X = 19.9$ m (65ft), $D = 1.2$ m (4.0ft), $S/D = 1.0$.
- Step 8: The software *LPILE* (developed by Reese et al., 2004), which is based on a p-y method of analysis for laterally loaded piles, was used for the analysis of the structural response of the shaft. The three combinations obtained from Step 7 (i.e., (a) $D = 0.6$ m (2.0ft), $S/D = 1.0$, $F = 351$ kN (78.9 kips), $X = 21.8$ m (70 ft); (b) $D = 0.6$ m (2.0 ft), $S/D = 2.0$, $F = 423$ kN (95.1 kips), $X = 19.9$ m (65 ft); (c) $D = 1.2$ m (4.0 ft), $S/D = 1.0$, $F = 583$ kN (131 kips), $X = 19.9$ m (65 ft)) with the corresponding net forces can be used as inputs to the *LPILE* program to calculate the lateral deflections and the internal forces and moments in the drilled shaft. After calculation with *LPILE*, the lateral deflections on the top of the shaft are 0.0035 m (0.14 inch), 0.0052 m (0.20 inch), and 0.0081 m (0.32

inch), respectively, for the three design combinations (a, b and c), and the total shaft lengths for the three combinations are 2.5 m (8.5ft) , 3.5 m (11.5ft), and 3.5 m (11.5ft), respectively. All the lateral deflections on the top of the shaft can be considered to be within the allowable deflection (say, half an inch, or approximately 12.7 mm). If we perform the quantitative analysis of the required drilled shaft volume, the drilled shaft volumes per unit width of a slope for the three combinations are 0.588 m³, 0.550 m³, and 1.649 m³, respectively. Thus, Combination (b) ($D = 0.6$ m (2.0ft), $S/D = 2.0$, $F = 423$ kN (95 kips), $X = 19.9$ m (65ft)) can be chosen as the most economical design with the least amount of drilled shaft volume required to meet the required target reliability index. The computed reliability index is 3.4 for Combination (b).

3.5.2.2. Sensitivity Analysis of Soil Arching Model Errors

This section presents a sensitivity analysis on the influence of model errors associated with the empirical equation for the load transfer factor. This analysis is performed because the statistics of bias for the predictive equation for the load transfer factor could be different from current values, if additional finite element simulation results or if high-quality field monitoring data becomes available. Combination (b) ($D = 0.6$ m (2.0ft), $S/D = 2.0$, $F = 423$ kN (95 kips), $X = 19.9$ m (65 ft)) in the previous section is chosen as a case in the sensitivity analysis to demonstrate how the model errors will affect the design results. Figure 3-12 presents the relationship between the computed probability of failure and the mean value of bias of the load transfer factor; the other values remain the same as in the example. The notation SD in Figure 3-12 is standard deviation of bias of the predictive equation for the load transfer factor. It can be seen that the computed

probability of failure is sensitive to the statistics of the bias of η . Therefore, a more refined predictive equation for the load transfer factor with a smaller value of standard deviation of bias would be desirable.

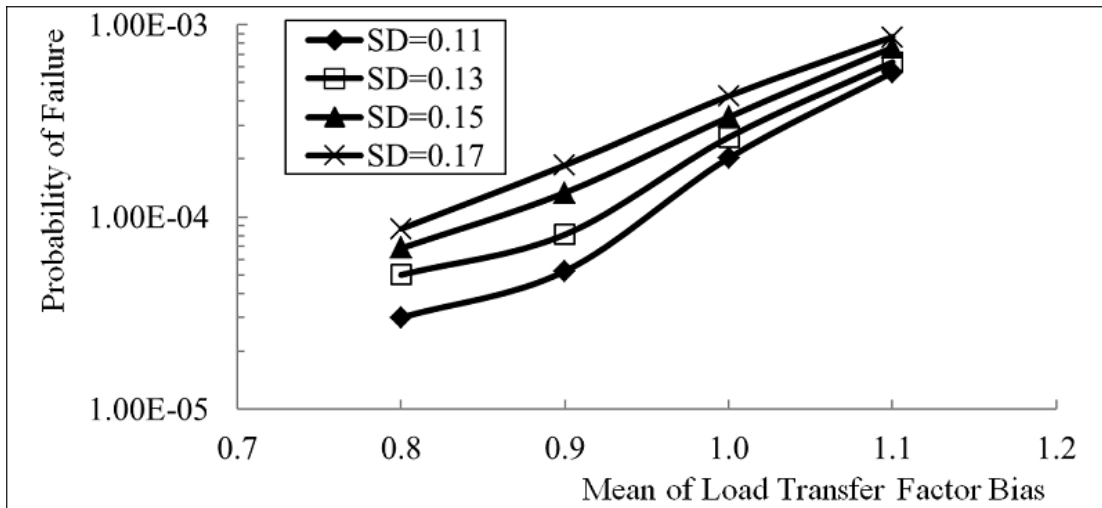


Figure 0-12: Relationship between P_f and mean of bias of η for different standard deviation

3.5.3. Illustrative Example 2

The slope failure at the ATH-124 project site in Ohio was previously analyzed by Liang (2010, 2011) using the deterministic computer program *UA Slope*. The failed slope at Ohio State Route 124 from Station 107 + 40 to Station 108 + 60 was part of a test site sponsored by ODOT. The laboratory tests of soil samples retrieved from the field included the determination of specific gravity and natural water content, as well as direct shear test, the isotropically consolidated-undrained test, and the unconfined compression test. In addition, the rock-quality designation and unconfined compression strength of rock cores were obtained. The critical factor of safety for the failed slope was calculated as 0.909. The simplified soil profile of the failed slope and the

soil properties based on the two site investigation reports are presented in Figure 3-13. The slip surface of the failed slope was determined from inclinometer readings during the two years of monitoring after the occurrence of the first slippage (in 2004), and this data is shown in Figure 3-13 as well. The pertinent soil and rock properties including strength parameters (c , ϕ and γ) are summarized as mean values in Table 3-2, while the coefficient of variation (c.o.v.) of these soil parameters are taken from Phoon and Kulhawy (1999).

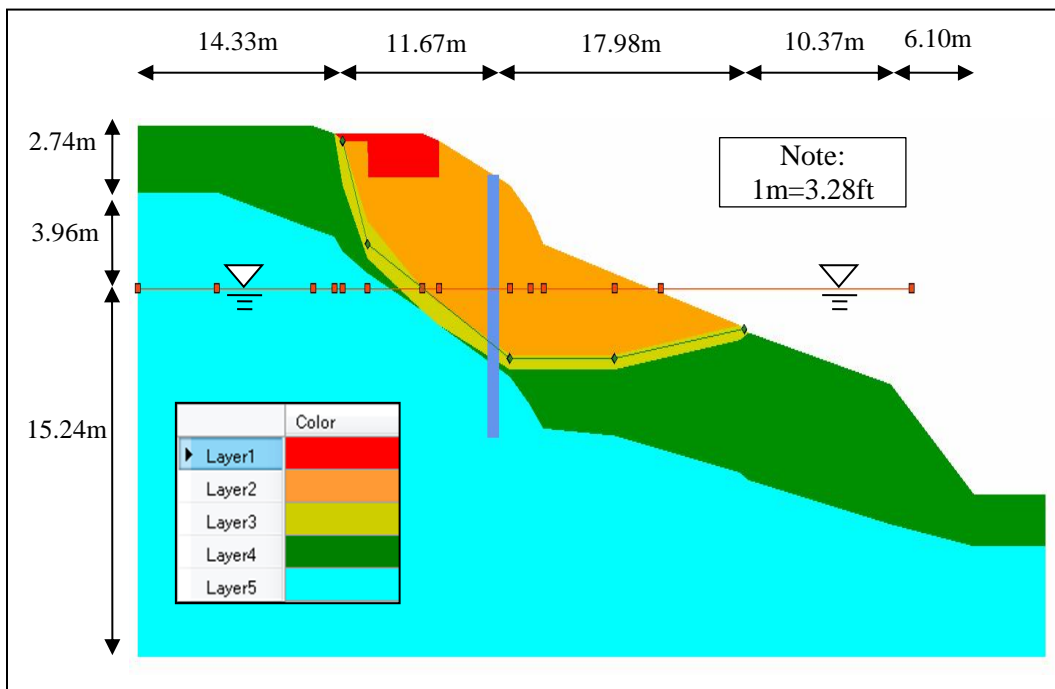


Figure 0-13: Slope geometry for ATH-124 slope (shaft location 26 m)

Table 0-2: Soil properties at the slope of ATH-124 project

Layer No.	Mean					C.O.V.
	1	2	3	4	5	
c (kN/m²)	3.35 (70psf)	3.35 (70psf)	0 (0psf)	3.35 (70psf)	7.42 (155psf)	0.2
φ (degree)	24	24	11.5	24	35	0.1
γ (kN/m³)	23.56 (150pcf)	21.21 (135pcf)	20.42 (130pcf)	21.21 (135pcf)	24.35 (155pcf)	0.01

3.5.3.1. Step-by-Step Design Procedure for Example 2

The step-by-step design procedure for the slope in Example 2 is as follows:

- Step 1: Collect data (i.e. the geometry of the slope, soil parameters, ground water table, critical slip surface, etc.) and generate random variables. All parameters are provided in Figure 3-13 and Table 3-2.
- Step 2: Set the target reliability index at 3.0.
- Step 3: Select different drilled shaft locations. The allowable locations for drilled shafts are between 23 m and 30.5 m horizontally from the top of the slope (the upper left corner shown in Figure 3-13). The slope/shaft system will be analyzed for different shaft locations starting from $X = 23$ m (75 ft) to $X = 30.5$ m (100 ft) in 1.5-m (5.0 ft) increments.

- Step 4: Select different pairs of clear spacing S and shaft diameter D combinations within the permissible range. The range for D can be selected between 0.6 m to 2.4 m (2 ft~8 ft), and the range of S/D can be selected to be between 1.0~3.0. The following combinations for (S, D) are selected: (0.6m (2.0ft), 0.6m (2.0ft)), (1.2m (4.0ft), 0.6m (2.0ft)), (1.8m (6.0ft), 0.6m (2.0ft)), (1.2m (4.0ft), 1.2m (4.0ft)), (2.4m (8.0ft), 1.2m (4.0ft)), (1.8m (6.0ft), 1.8m (6.0ft)), and (2.4m (8.0ft), 2.4m (8.0ft)). All units in the parentheses are in meters.
- Step 5: For each (S, D) combination, plot the relationship between the computed reliability index and the shaft location, as shown in Figure 3-14.
- Step 6: For each (S, D) combination, plot the relationship between the computed net forces on the drilled shaft and shaft location, as shown in Figure 3-15.

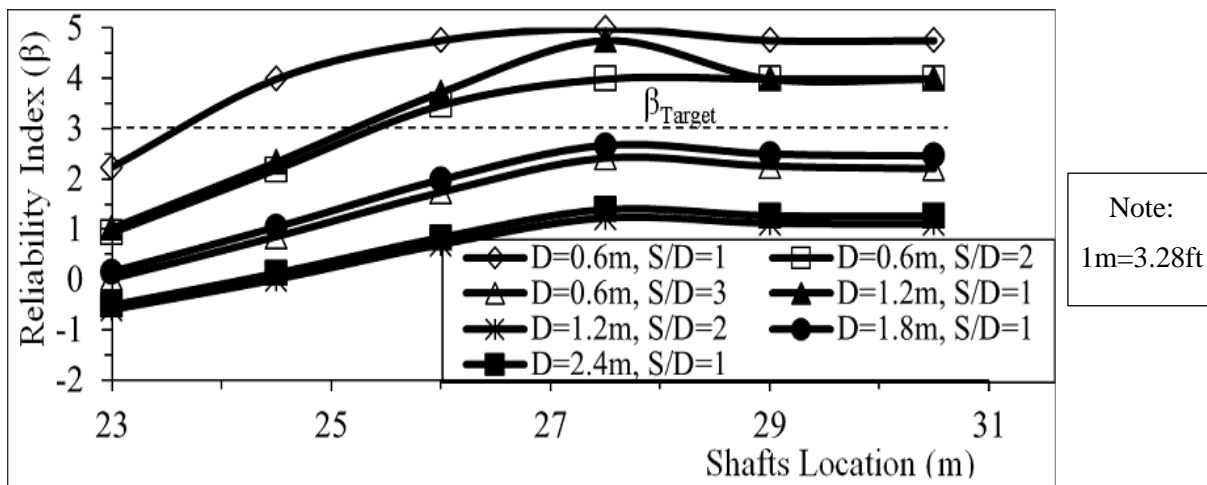


Figure 0-14: Reliability index of the shaft-slope system versus shaft location for different (S, D) combinations

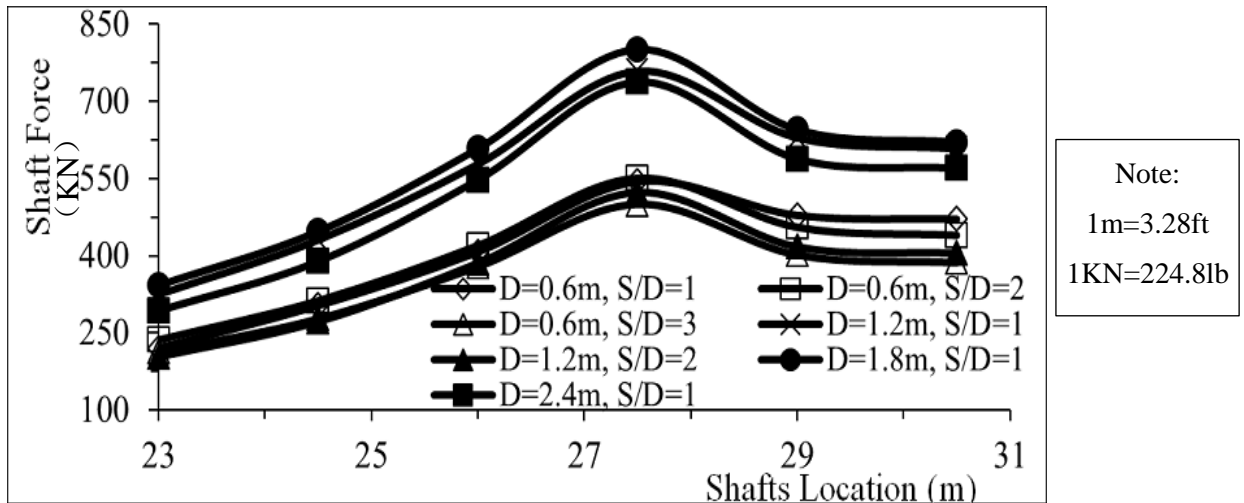


Figure 0-15: Shaft force versus shaft location for different (S, D) combinations

- Step 7: Optimize the design parameters. As can be seen in Figure 3-14, the reliability index β tends to increase with distance from the top of slope and then decreases slightly. The location of 27.5 m provides the highest reliability index for the given shaft diameter and spacing. In addition, it can be seen that the following foundation dimensions would satisfy the chosen target reliability: (a) location $X = 27.5$ m (90 ft), $D = 0.6$ m (2.0 ft), $S/D = 1.0$, (b) $X = 27.5$ m (90ft), $D = 0.6$ m (2.0 ft), $S/D = 2.0$, and (c) $X = 27.5$ m (90 ft), $D = 1.2$ m (4.0ft), $S/D = 1.0$. However, as shown in Figure 3-15, the shafts at the location equal to 27.5 m (90 ft) are also subjected to the largest net forces, which would have resulted in higher internal moments and shears in the shaft and a higher reinforcement ratio as well. It appears that the force on the shafts would decrease after the location 27.5 m (90 ft), and the computed reliability index β would still satisfy the target reliability index. Furthermore, the required length of drilled shafts could be reduced if the location of the drilled shafts is moved further downslope. From these considerations, three different combinations are selected: (a) location $X = 30.5$ m (100 ft), $D = 0.6$ m (2.0

ft), $S/D = 1.0$; (b) $X = 30.5$ m (100 ft), $D = 0.6$ m (2.0 ft), $S/D = 2.0$; (c) $X = 30.5$ m (100 ft), $D = 1.2$ m (4.0ft), $S/D = 1.0$.

- Step 8: The software *LPILE* was used for the structural analysis of the shaft. The three combinations obtained from Step 7 (i.e., (a) $D = 0.6$ m (2.0 ft), $S/D = 1.0$, $F = 470$ kN (106 kips); (b) $D = 0.6$ m (2.0 ft), $S/D = 2.0$, $F = 440$ kN (99 kips); (c) $D = 1.2$ m (4.0 ft), $S/D = 1.0$, $F = 620$ kN (140 kips)) can be taken into *LPILE* program to calculate the lateral deflection and the internal forces and moments on the shaft. The soil and rock properties were used as input in the computer code *LPILE*. In such a case, typically the p - y curves were internally generated in the computer code based on the input soil and rock properties. After calculation with *LPILE*, the lateral deflections on the top of the shaft are 0.008 m, 0.075 m, and 0.015 m, respectively, for the three combinations (a, b, and c), and the total shaft lengths for the three combinations are 11.0 m (36 ft), 11.0 m (36 ft), and 10 m (32 ft), respectively. Meanwhile, if we set up the allowable deflection as half an inch (12.7 mm), then Combination (c) needs to be excluded. Finally, Combination (b) (with $X = 30.5$ m (100 ft), $D = 0.6$ m (2.0 ft), $S/D = 2.0$, $F = 440$ kN (99 kips)) can be chosen as the optimized design, considering both the construction cost (the least amount of concrete volume per unit width of slope) and performance requirements (i.e., target reliability of the system and lateral deflection at the top of the drilled shaft).

3.5.3.2. Reliability Index and Factor of safety

The difference between the deterministic version *UA Slope* and the probabilistic version *P-UASLOPE* is demonstrated in Table 3-3 for a case where the shaft diameter is equal to 0.6 m (2.0 ft) and the shaft location is at 23.0 m (75 ft) for the slope geometry and soil properties in

Example 2. It can be seen that the computed reliability index for this case does not satisfy the target reliability index ($\beta_{\text{Target}} = 3.0$), even though the calculated FS is greater than one. For the case presented in Table 3-3, the factor of safety should be close to 1.5 if the chosen target reliability is 3.0. The case presented in Table 3-3 provides insight on the importance of using a reliability-based design approach for the slope stability problem, as a single value of FS cannot be properly chosen to reflect the uncertainties associated with soil properties and the computational methods.

Table 0-3: Comparison between Reliability Index and Factor of Safety ($D = 0.6 \text{ m (1.97ft)}$)

Shaft Location		23.0m	24.5m	26.0m	27.5m	29.0m	30.5m
		(75ft)	(80ft)	(85ft)	(90ft)	(95ft)	(100ft)
S/D=1	Reliability Index (β)	2.23	3.98	4.75	4.75	4.75	4.75
	FS	1.31	1.64	2.24	3.62	3.28	3.16
S/D=2	Reliability Index (β)	0.93	2.19	3.46	3.98	3.98	3.99
	FS	1.16	1.31	1.53	1.81	1.69	1.64
S/D=3	Reliability Index (β)	0.02	0.86	1.74	2.42	2.26	2.21
	FS	1.06	1.14	1.25	1.36	1.31	1.29

3.6. Summary and Conclusions

In this chapter, a reliability-based computational algorithm for the design of a row of equally spaced drilled shafts to stabilize an unstable slope was presented. The computational algorithm was based on the deterministic approach using a modified limiting equilibrium method of slices incorporating the drilled shaft-induced soil arching effects in calculating the global factor of

safety of a drilled shaft/reinforced soil slope system. The uncertainties of soil parameters and the model errors of a semi-empirical equation for predicting the load transfer factor in characterizing the soil arching effects were taken into consideration in the new computer program, *UA Slope 3.0*, by using Monte Carlo simulation techniques. The ziggurat algorithm was used for pseudo-random generation of random numbers for the uncertain variables of the system, including soil cohesion, soil friction angle, soil unit weight for each soil layer, and bias of the load transfer factor. The *UA Slope 3.0* program was used in two design examples to illustrate the design procedure for achieving the required target reliability index while using the most economical drilled shaft combinations in terms of location of the drilled shafts on the slope as well as the diameter, length, and spacing of the drilled shafts. Finally, a sensitivity analysis of model error on the computed probability of failure of the drilled shaft/slope system for a design example was presented to demonstrate the need to refine the predictive model of the semi-empirical equation for the load transfer factor. Specific conclusions based on the design example and sensitivity study can be made as follows:

1. The design of a single row of equally spaced drilled shafts for stabilizing an unstable slope involves consideration of both geotechnical global factor of safety (or reliability index) as well as structural performance of the drilled shafts in terms of meeting the requirements of limiting the drilled shaft deflection and the necessary reinforcements for sustaining the internal forces and moments. This chapter presented reliability-based methodologies for computing reliability index of a drilled shaft/slope system as well as the loads on the drilled shaft for determining internal forces and moments for structural design of a drilled shaft.

2. The location, spacing, diameter, and length of the drilled shafts are the fundamental design variables that can be varied in different combinations to achieve the target reliability index. The final selection of the design combination should be based on economic analysis and consideration of constructability of the drilled shafts.
3. Bias in the semi-empirical load transfer prediction equation, or the model error, can affect the computed probability of failure of a drilled shaft/reinforced slope system. There is an incentive for conducting additional 3D finite element simulations covering more simulation conditions so that the bias of the semi-empirical predictive equation can be reduced.
4. The case presented in Table 3-3 provides insight on the importance of using the reliability based design approach for slope stability problems, as a single value of FS cannot be properly chosen to reflect uncertainties associated with soil properties and model errors of the computational methods.

4. ADVANCED PROBABILISTIC TECHNIQUE IN A DRILLED SHAFT/SLOPE SYSTEM

4.1. Introduction

Traditional brute force Monte Carlo simulation (MCS) typically presents a sloppy process for calculating the probability of failure, since it needs a large number of samples to obtain the required accuracy. In this chapter, a more advanced methodology known as the importance sampling technique (IST) is proposed for determining the probability of failure and the reliability index of a drilled shaft/slope system.

Recently, Li and Liang (2012, 2013) developed an approach based on MCS to extend the deterministic *UA Slope* program into a probabilistic version in which uncertainties of the soil parameters such as strength parameters and unit weight of soils are considered. In addition, the modeling error of the semi-empirical equation for quantifying the load transfer factor was considered by introducing a bias factor for the load transfer factor. However, the brute force MCS process draws samples “randomly” when calculating the estimator for the probability of failure (P_f). If the estimator P_f is quite small, then a large number of samples will need to be drawn, as illustrated in Figure 4-1. Since the use of brute force MCS requires a large number of samples and intensive use of computational power, there is a need to develop a computationally efficient MCS approach for assessing the probability of failure of the described drilled shaft/slope system.

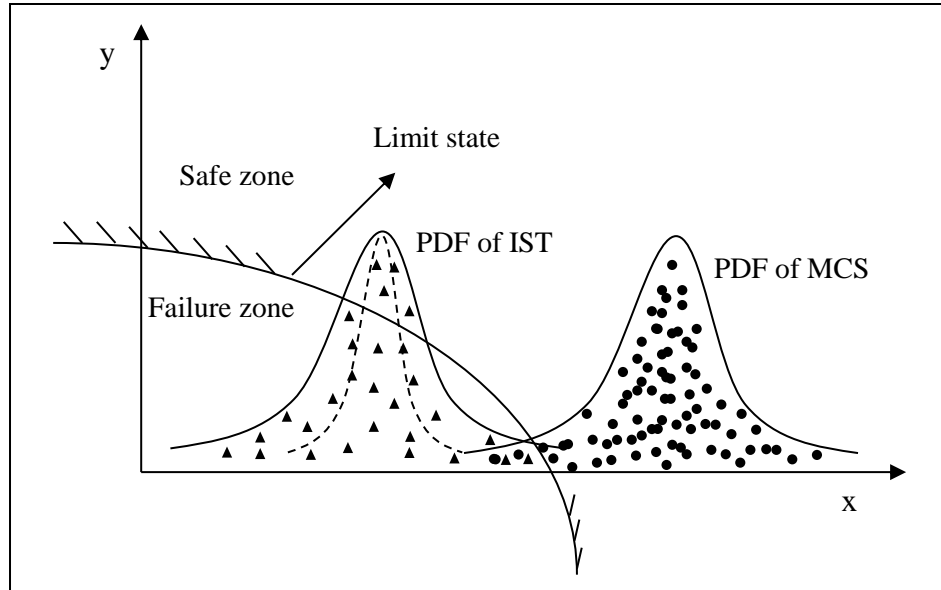


Figure 4-1: Sketch of PDF Comparison between MCS and IST (1D)

The objective of this chapter is to provide a computationally efficient algorithm that can accurately and efficiently calculate the probability of failure and the reliability index for a drilled shaft/slope system. The basic concept of the method of slices, incorporating the arching effects of the drilled shafts, has been described in Chapter 3. In this chapter, a creative method to form the performance function of the system is developed, from which the design point can be determined. The importance function (i.e., $IS(x)$), which is within the context of importance sampling techniques, is developed based on the design point. A more efficient random sample generation scheme based on the importance function $IS(x)$ is implemented in the probabilistic PC-based program, *UA Slope 3.0*, to efficiently compute the P_f of a drilled shaft/slope system. A computational example of a real-world slope stabilization project is presented at the end of the chapter.

4.2. Basic Concept of Importance Sampling Technique

Brute force MCS provides the most robust way for computing the probability of failure (Robert and Casella, 2004); however, the tremendous computation demand of this method may pose severe limitations to its adoption by practicing engineers, especially when P_f is small. The importance sampling technique (IST) is a variance reduction technique in which the P_f is calculated by the samples generated from a different distribution rather than from the original distribution. If these “important” values are emphasized by sampling them more frequently, then the variance of the estimator (i.e., P_f) can be reduced. In other words, the computing of the estimator (P_f) will be converged faster while reaching a more accurate value. Figure 4-1 shows the contrast of the one-dimensional probability density function (PDF) between the brute force MCS and the IST.

Concerning Equation 3-12 of the MCS algorithm, the P_f can be considered as the ratio between the number of failure events (i.e., the number of events when the computed FS is less than 1) and the total sample number (i.e., N). The mathematical equation of probability of failure can be written as Equation 4-1 by introducing an importance function $IS(x)$:

$$\begin{aligned}
 P_f &= E_f(I[FS < 1]) = \int I[FS < 1] \cdot f(x) dx = \int I[FS < 1] \cdot \frac{f(x)}{IS(x)} IS(x) dx \\
 &= E_{IS} \left(I[FS < 1] \frac{f(x)}{IS(x)} \right) \approx \frac{1}{N} \sum_{i=1}^N I_i[FS < 1] \frac{f(x_i)}{IS(x_i)}
 \end{aligned}
 \tag{4-1}$$

where

P_f = the probability of failure of the drilled shaft/slope system;

$I[FS < 1]$ = the indicator function of the specified failure mode (with a factor of safety that is less than 1);

$f(x)$ = the original probability distribution function of the parameters;

$IS(x)$ = the importance function;

i = the i -th random number; and

N = total number of randomly generated samples.

Equation 4-1 represents the basic concept of IST for one dimension. As can be seen from this equation, the distribution of random numbers (x_i) has been transferred from the original probability distribution function, $f(x)$, to the importance function, $IS(x)$. Use of an appropriate importance function can make the P_f calculation converge quickly. Therefore, the key is to choose the appropriate importance function to enable fast and accurate convergence on the calculated P_f .

4.3. Importance Sampling Technique for the Drilled Shaft/Slope System

4.3.1. Design point of importance function

Typically, the appropriate expression of importance function $IS(x)$ is very difficult to determine. Au and his research team (Au and Beck, 1999; Au et al. 2003) suggested that the PDF of the importance function $IS(x)$ can be determined using “design points” for high dimensional cases. For example, Ching et al. (2009, 2010) utilized the ordinary method of slices (OMS) to obtain the performance function ($g(x)$) of a slope without the drilled shafts, from which the design point

\bar{z}_w^{OMS} was calculated by using the first-order algorithm on $g(x)$. In our drilled shaft/slope system, however, there is no functional expression for $g(x)$. A new method to determine the performance function ($g(x)$) as well as the design point for the drilled shaft/slope system will be developed in the following subsections.

Since the calculation of the factor of safety for the drilled shaft/slope system is an iterative computation algorithm using the method of slices, which is different from those of a functional expression such as Bishop's method (Bishop, 1955) or Chen's method (Chen, 1975) for slope stability analysis. Consequently, there is no direct expression of performance function if Equations 3-1 to 3-3 are used. However, considering that OMS is the only noniterative method dealing with a homogeneous slope (Ching et al., 2009), the determination of the performance function is proposed by combining OMS and arching theory. Based on Equation 2-2, the performance function can be written as:

$$\begin{aligned}
 g(x) &= F_R - F_D + (\Delta F_D)_{\text{arching}} \\
 &= \left\{ \sum_i c_i \Delta l_i + (W_i \cos \alpha_i - u_i \Delta l_i) \tan(\varphi_i) \right\} - \left\{ \sum_i W_i \sin \alpha_i \right\} + (1 - \eta) P_{i-1}^L
 \end{aligned} \tag{4-2}$$

where, c_i and φ_i = cohesion and friction angle at the base of the i th slice; W_i = total weight of the i th slice; u_i = pore water pressure at the middle point of the i th slice base; Δl_i = length of the slice base; α_i = inclination angle of the slice base; η = load transfer factor; and P_{i-1}^L = the left interslice force on Slice $i-1$. All these parameters are depicted in Figures 3-1(a) and 3-1(b). If the performance function $g(x) < 0$, the drilled shaft/slope system fails, and vice versa. Assuming the critical slip surface passes through n soil layers, the performance function can be rewritten as follows:

$$g(x) = \sum_{j=1}^n \left\{ c_j \sum_i \Delta l_i + \psi_j \left[\gamma_j \sum_i h_i \cos \alpha_i - \sum_i u_i \Delta l_i \right] - \gamma_j \sum_i h_i \sin \alpha_i \right\} + (1-\eta) P_{i-1}^L \quad (4-3)$$

where j = soil layer number; i = slice number; $\psi_i = \tan(\phi_i)$; γ_j = unit weight of j th layer; and the remaining parameters were defined previously in Equation 4-2. The design point of the drilled shaft/slope system can be written as:

$$\mu_i^* = - \frac{\left(\frac{\partial g}{\partial X_i} \right)}{\sqrt{\sum_i \left(\frac{\partial g}{\partial X_i} \right)^2}} \beta \quad (4-4)$$

where X_i is the i -th parameter of the performance function; μ_i^* is the design point of the i -th parameter; and β is the reliability index of the drilled shaft/slope system, which is:

$$\beta = \frac{\mu_{g(x)}}{\sigma_{g(x)}} = \frac{\mu_{F_R} - \mu_{F_D} + \mu_{(\Delta F_D)_{\text{arching}}}}{\sqrt{\sigma_{F_R}^2 + \sigma_{F_D}^2 + \sigma_{(\Delta F_D)_{\text{arching}}}^2}} \quad (4-5)$$

where $\mu_{F_R}, \mu_{F_D}, \mu_{(\Delta F_D)_{\text{arching}}}$ are the means of F_R, F_D , and $(\Delta F_D)_{\text{arching}}$, respectively; and

$\sigma_{F_R}, \sigma_{F_D}, \sigma_{(\Delta F_D)_{\text{arching}}}$ are the standard deviations of F_R, F_D , and $(\Delta F_D)_{\text{arching}}$, respectively.

It should be noted that the load transfer factor η and the slice force P_{up} in Equation 4-3 change based on different combinations of (c_i, ψ_i, γ_i) during the analysis. The important simplifications in Equation 4-3 are: (a) the critical slip surface of the slope, which has been confirmed prior to installation of the drilled shafts, does not change after the drilled shafts are installed; and (b) the interslice force exists only in the calculation of the $(\Delta F_D)_{\text{arching}}$, and there is no interslice force in

the calculation of OMS. Of course, the performance function (Equation 4-3) cannot precisely represent the actual function of the drilled shaft/slope system; nevertheless, we are only looking for an approximate location of the actual design point to build a new PDF of the importance function $IS(x)$.

Once the importance sampling design point μ_i^* is obtained, it can be employed in constructing a new PDF of importance function ($IS(x)$). The random numbers (i.e., c_i, ψ_i, γ_i) are generated based on the new PDF of $IS(x)$. Finally, the probability of failure P_f can be calculated based on Equation 4-1.

4.3.2. The ratio between $f(x)$ and $IS(x)$

In the drilled shaft/slope system, the variability of three soil parameters (cohesion c , friction angle ϕ , and unit weight γ) typically occurs simultaneously. For example, in one layer slope, there are three variables that comprise the variable matrix \bar{x} : (c, ψ, γ) (note: $\psi = \tan(\phi)$), and in a two-layer slope there are six variables: ($c_1, \psi_1, \gamma_1, c_2, \psi_2, \gamma_2$), and so on. All soil parameters are assumed to be independent and identically distributed; therefore, the correlation matrix associated with every soil parameter is the identical matrix: \bar{E} .

where $\bar{E} = \begin{bmatrix} 1 & & & \\ & 1 & & \\ & & \ddots & \\ & & & 1 \end{bmatrix}_{M \times M}$, where $M =$ The number of soil parameters.

In IST, the most important calculation for Equation 4-1 is the ratio between the original PDF, $f(x)$, and the importance sampling PDF, $IS(x)$, i.e., $f(x)/IS(x)$. In practical application, the use of the lognormal distribution ensures that soil properties (i.e., cohesion, friction angle, and unit weight) are always non-negative. Therefore, in this paper, the original function of $f(x)$ and $IS(x)$ are assumed to follow a lognormal distribution. For mathematical simplification, the normal distribution is preferable for calculating the ratio, $f(x)/IS(x)$. The transformation from a normal distribution to a lognormal distribution is shown in the following equations.

$$f(x) = \frac{1}{x\sigma\sqrt{2\pi}} \exp\left[-\frac{1}{2} \frac{(\ln x - \mu)^2}{\sigma^2}\right] \quad (4-6)$$

$$\sigma = \sqrt{\ln\left(1 + \frac{\sigma_0^2}{\mu_0^2}\right)} \quad (4-7)$$

$$\mu = \ln \mu_0 - \frac{1}{2} \sigma^2 \quad (4-8)$$

where σ = standard deviation of a lognormal distribution;

μ = mean of a lognormal distribution;

σ_0 = standard deviation of a normal distribution;

μ_0 = mean of a normal distribution;

By using Equations 4-6 to 4-8, the normal variable can be transformed to lognormal distributed random variable. Assuming that variables in $f(x)$ and $IS(x)$ are independent, then the ratio of $f(x)/IS(x)$ can be written as Equation 4-9.

$$\begin{aligned}
\frac{f(x)}{IS(x)} &= \frac{(2\pi)^{-\frac{M}{2}} |\bar{\Sigma}|^{-\frac{1}{2}} \exp\left[-\frac{1}{2}(\bar{x} - \bar{\mu})^T \Sigma^{-1} (\bar{x} - \bar{\mu})\right]}{(2\pi)^{-\frac{M}{2}} |\bar{\Sigma}^*|^{-\frac{1}{2}} \exp\left[-\frac{1}{2}(\bar{x} - \bar{\mu}^*)^T (\Sigma^*)^{-1} (\bar{x} - \bar{\mu}^*)\right]} \\
&= \frac{\exp\left[-\frac{1}{2}(\bar{x})^T (\bar{x})\right]}{|\bar{\Sigma}^*|^{-\frac{1}{2}} \exp\left[-\frac{1}{2}(\bar{x} - \bar{\mu}^*)^T (\Sigma^*)^{-1} (\bar{x} - \bar{\mu}^*)\right]} \\
&= \prod_{i=1}^M (\sigma_i^*) \exp\left\{-\frac{1}{2} \sum_{i=1}^M \left[x_i^2 - (x_i - \mu_i^*)^2 (\sigma_i^*)^{-2}\right]\right\}
\end{aligned} \tag{4-9}$$

where \bar{x} = The $M \times 1$ variable matrix of soil parameters, i.e., $\bar{x} = (x_1, x_2, \dots, x_M)^T$, for example, in a

two-layer slope, $\bar{x} = (C_1, \psi_1, \gamma_1, C_2, \psi_2, \gamma_2)^T$;

x_i = the i -th soil parameter;

M = the number of parameters;

$\bar{\Sigma}$ = $M \times M$ covariance matrix of original PDF $f(x)$, which is equal to 1 for a standard normal distribution;

$\bar{\mu}$ = $M \times 1$ mean matrix of original PDF $f(x)$, which is equal to 0 for a standard normal distribution;

$\bar{\Sigma}^*$ = $M \times M$ covariance matrix of importance sampling function $IS(x)$;

$\bar{\mu}^*$ = $M \times 1$ design point matrix of importance sampling function $IS(x)$;

μ_i^* = Design point of the i -th parameter; and

σ_i^* = The i -th standard deviation of the importance sampling function.

4.4. Procedure of Importance Sampling Calculation using the Design Point

Typically, few samples generated from the original PDF can fall into the failure zone in the brute force MCS. If we reduce the mean of the original PDF, which means we horizontally move the original PDF to the left side, then it can generate more samples falling into the failure zone, as shown in Figure 4-1. Mathematically, the above theory can be used as the basis for building the importance function (IS(x)) by using the design point. In addition, if we reduce the variance of the PDF of IS(x), the PDF curve will “shrink,” which might produce more failure events, as shown in Figure 4-1. In our approach, the “design point” method is employed, and for comparison, the standard deviation of IS(x) will be slightly reduced in order to analyze the accuracy and efficiency of importance sampling.

From Equations 4-1 and 4-9, the probability of failure for a drilled shaft/slope system can be computed using the following equation:

$$\begin{aligned}
 P_f &\approx \frac{1}{N} \sum_{i=1}^N \left\{ I_i [FS < 1] \frac{f(x_i)}{IS(x_i)} \right\} = \frac{1}{N} \sum_{i=1}^N \left\{ I_i \left[\frac{F_R}{F_D - (\Delta F_D)_{arching}} < 1 \right] \frac{f(x_i)}{IS(x_i)} \right\} \\
 &= \frac{1}{N} \sum_{i=1}^N \left\{ I_i \left[\frac{F_R}{F_D - (\Delta F_D)_{arching}} < 1 \right] \prod_{i=1}^M (\sigma_i^*) \exp \left\{ -\frac{1}{2} \sum_{i=1}^M \left[x_i^2 - (x_i - \mu_i^*)^2 (\sigma_i^*)^{-2} \right] \right\} \right\}
 \end{aligned} \tag{4-10}$$

The corresponding c.o.v. of the estimator P_f is:

$$c.o.v.(P_f) = \frac{\sigma_{P_f}}{\mu_{P_f}} \approx \sqrt{\frac{1}{N} \sum_{i=1}^N \left\{ I_i \left[\frac{F_R}{F_D - (\Delta F_D)_{arching}} < 1 \right] \frac{f(x_i)}{IS(x_i)} - P_f \right\}^2} / P_f \tag{4-11}$$

where all variables have been defined previously. The flowchart of the proposed IST for a drilled shaft/slope system is shown in Figure 4-2. The detailed procedure is described in the following steps:

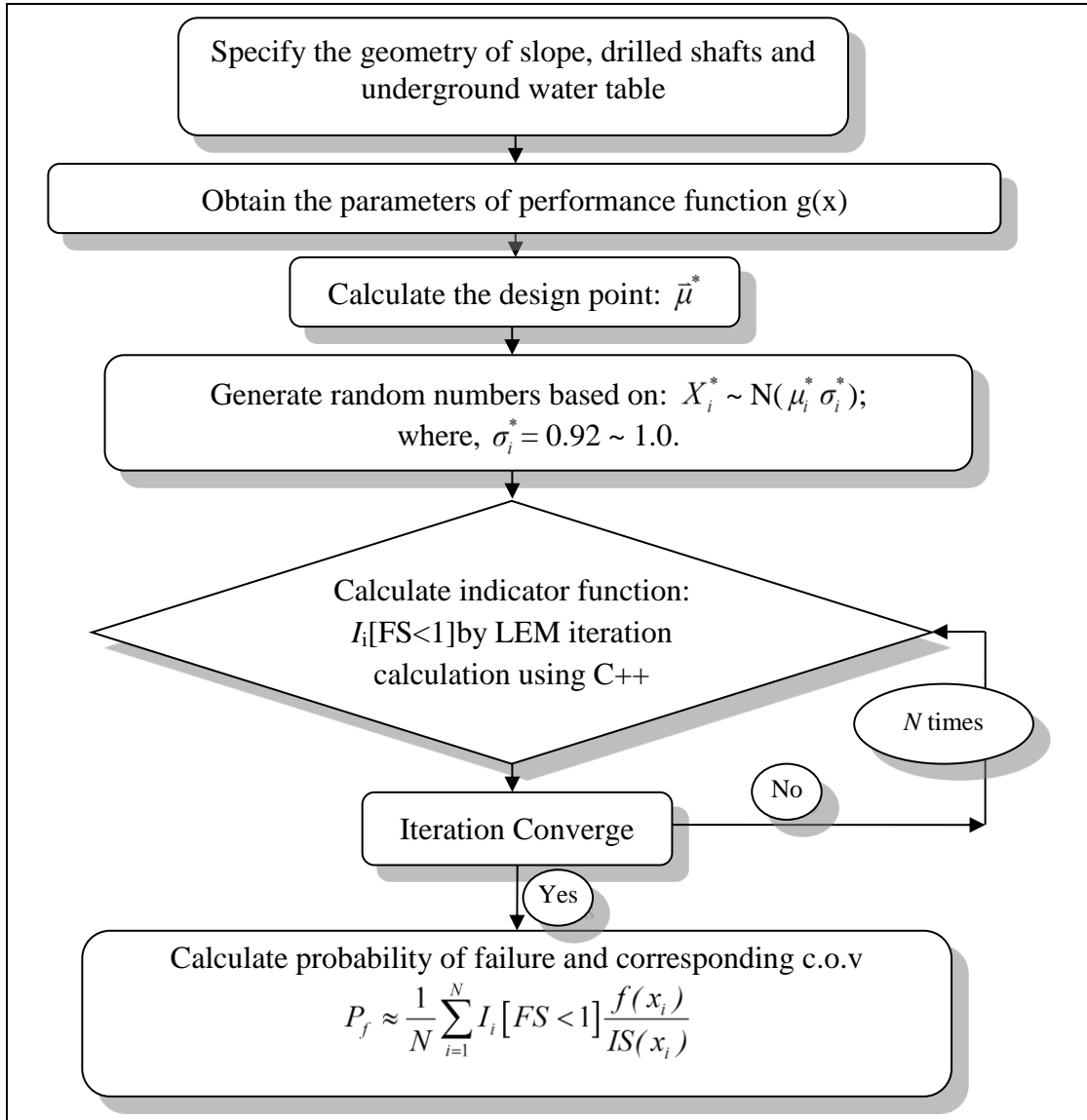


Figure 4-2: Flowchart of importance sampling technique in a drilled shaft/slope system

- Step 1: Specify the geometry and slope profile with soil parameters, including the location of the groundwater table and the relevant drilled shafts information (e.g., diameter D , clear spacing S , and shaft location ζ_x);
- Step 2: Determine the parameters of performance function $g(x)$ in Equation 3-3 by using ordinary method of slices and arching theory;

- Step 3: Calculate each component of the design point μ_i^* using Equations 3-3, 3-4 and 3-5;
- Step 4: Generate N random samples based on $X_i^* \sim N(\mu_i^*, \sigma_i^*)$, where, μ_i^* is the design point component calculated by Step 3, and σ_i^* is chosen as five cases: 0.92, 0.94, 0.96, 0.98, and 1.0;
- Step 5: Calculate the indicator function $I_i[\text{FS} < 1]$ and the ratio of $f(x_i)/IS(x_i)$ by using Equation 4-9 based on the new samples generated in Step 4;
- Step 6: Calculate the P_f by using Equation 4-10.

4.5. Illustrative Example of Application

Slope ATH-124 on State Route 124 in Athens County, Ohio, is presented to illustrate the computational efficiency of the developed IST for a slope reinforced by using a drilled shaft. The soil parameters (c_i , ψ_i , γ_i) are assumed to be independent and identically distributed for each layer. In addition, all soil parameters are considered to follow a lognormal distribution. The bias of the semi-empirical equation for the load transfer factor is considered to follow a lognormal distribution. The critical slip surface for the failed slope was determined from interpretation of an inclinometer reading obtained in the field. This interpreted slip surface is a dominant failure surface used in computing the reliability of a slope reinforced with a row of spaced drilled shafts.

The detailed parameters of ATH-124 slope (including the slope geometry and simplified soil layer information) are presented in Figure 3-12. The location of a single row of drilled shafts is selected at 25.91 m horizontally from the top of the slope. The diameter and clear spacing of the

drilled shafts are 0.8 m and 1.8 m, respectively. The soil parameters for each soil layer and the assumed c.o.v. have been summarized in Table 3-2. After 40,000 samples of brute force Monte-Carlo simulation, the probability of failure for this slope with the described drilled shafts layout is computed as 2.8%, with a corresponding c.o.v. of 0.06.

To consider the “variance effect” of the importance function $IS(x)$, the value of standard deviation (SD) σ_i^* (shown in Equation 4-9) is varied from 0.92 to 1.0 with an increment of 0.02. Using the importance sampling technique proposed in this paper, the P_f values calculated by MCS and IST are compared in Figure 4-3. As can be seen in this figure, the P_f value of the calculation using SD = 1.00 is the closest curve to the true value (i.e., P_f equals 2.8% after 40,000 samples of brute force MCS). It is noted that the convergence rate is fast as well. Figure 4-4 shows the comparison of c.o.v. of P_f calculated by brute force MCS and IST. By using IST, one can obtain a smaller c.o.v. of P_f than brute force MCS during sample calculations. Therefore, it seems that reducing the SD value in the IST computation can possibly lead to a relatively smaller c.o.v. of P_f . Figure 4-5 presents the number of failure events versus the number of sample calculations for different SD values. It can be seen that after 5,000 sample calculations, the number of failure events is 147 using brute force MCS, and it is 384 when using IST (SD = 1.00). Obviously, using IST can draw more failure events than brute force MCS. However, having more failure events does not automatically mean that the estimator (i.e., P_f) is more accurate. As shown in Figure 4-5, reducing the SD value from 0.98 to 0.92 can indeed help in obtaining more failure events. Nevertheless, the calculated result for P_f deviates from the true value too much, if we choose an SD between 0.92 and 0.98, as shown in Figure 4-4. In summary, the best choice for the importance sampling function $IS(x)$ is to use an SD value of 1.00 in Equation 4-9.

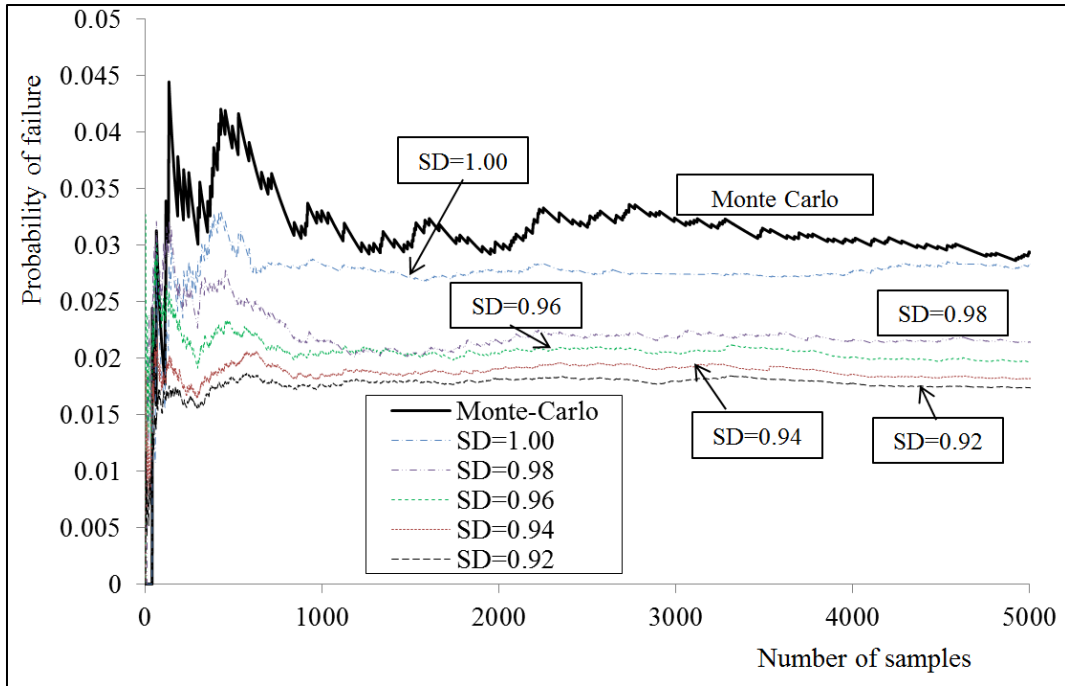


Figure 4-3: Comparison of P_f between MCS and IST ($P_f = 2.8\%$ after 40,000 MCS)

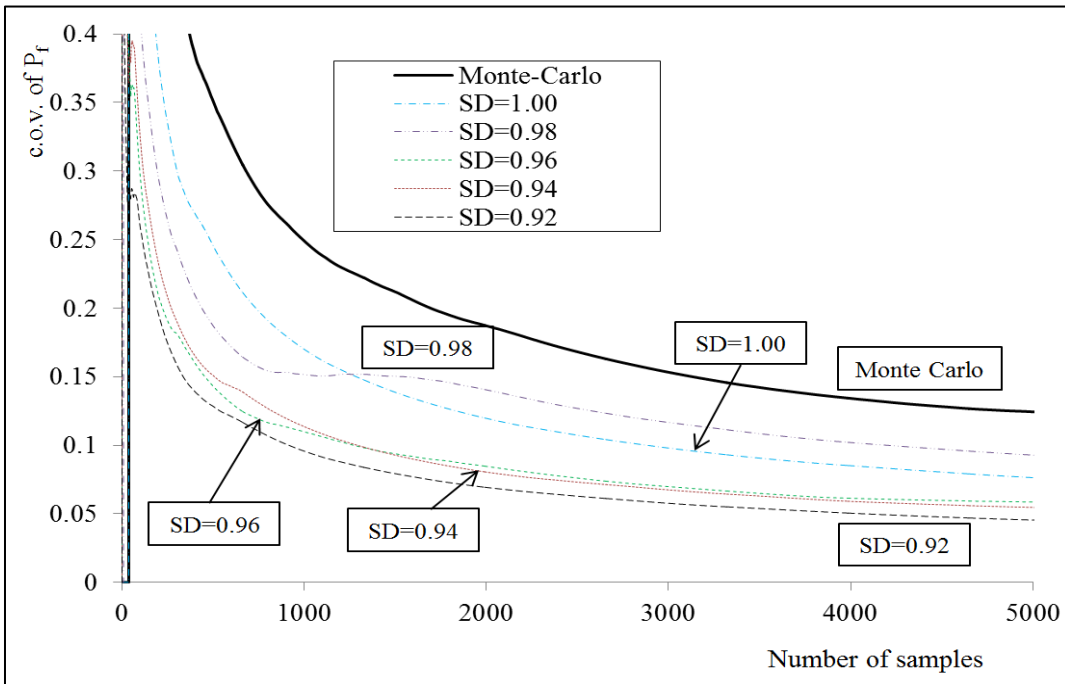


Figure 4-4: c.o.v. of P_f for MCS and IST with different standard deviations

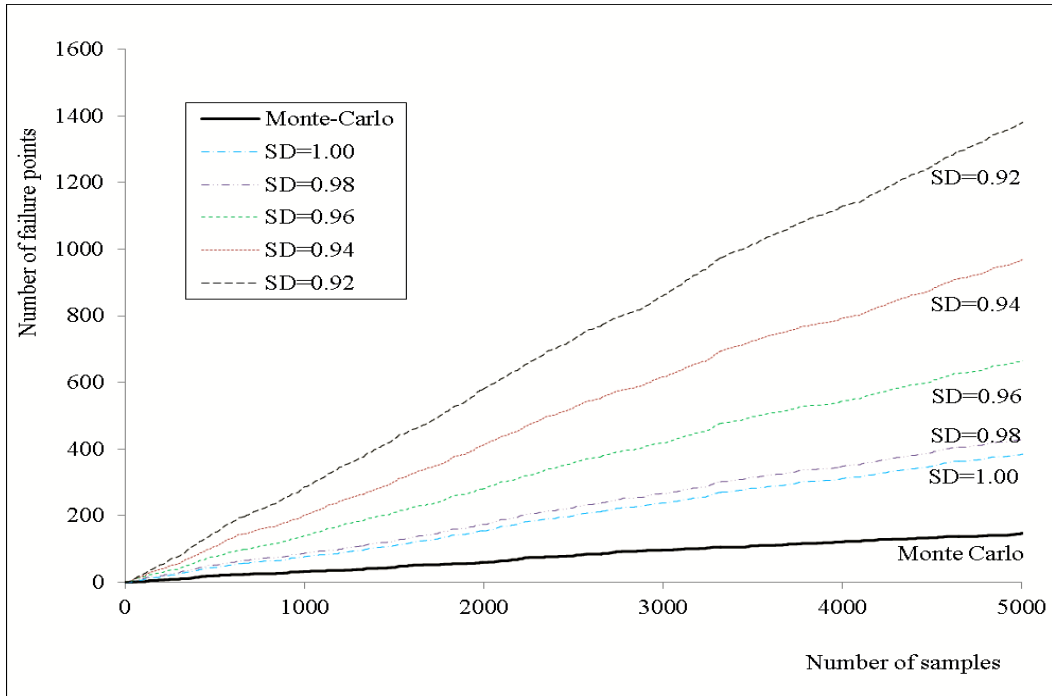


Figure 4-5: Number of failure events for MCS and IST with different standard deviations

Table 4-1 shows the convergence analysis between IST and brute force MCS. As can be seen from this table, only 307 sample calculations are required when using IST (SD = 1.00) to make the c.o.v. of P_f reach 0.3, but 686 sample calculations are required when using brute force MCS. Also, as shown in Table 4-2, after 307 IS calculations, the relative error of P_f is only 2.68% compared with the true value (i.e., $P_f = 2.8\%$ after 40,000 samples of brute force MCS). However, a total of 5,216 brute force MCS calculations are needed to reach the same accuracy, as shown in Table 4-2. The same trends are seen in the results of “c.o.v. (P_f) ≤ 0.2 ” presented in Tables 4-1 and 4-2. Therefore, using the importance sampling technique (IST) to calculate P_f is not only more efficient but also more accurate than using brute force MCS for a drilled shaft/slope system.

Table 4-1: Convergence analysis between IST and MCS

	SD reduction	c.o.v. (P_f) ≤ 0.3		c.o.v. (P_f) ≤ 0.2	
		Required sample calculations (N)	P_f (%)	Required sample calculations (N)	P_f (%)
IST	0.92	169	1.702	380	1.745
	0.94	122	1.879	276	1.720
	0.96	103	2.372	228	2.156
	0.98	199	2.615	443	2.660
	1.00	307	2.725	682	2.821
MCS		686	3.51	1698	3.13

Note: The probability of failure is 2.8% after 40,000 Monte Carlo simulations, and the corresponding c.o.v. of P_f is 0.06.

Table 4-2: Accuracy analysis between IST and MCS

Method	Required sample calculations (N)	Relative error	Required sample calculations (N)	Relative error
IST (SD=1.00)	307	2.68%	682	0.75%
MCS	5216	2.68%	22958	0.75%

Note: The probability of failure is 2.8% after 40,000 Monte Carlo simulations, and the corresponding c.o.v. of P_f is 0.06.

4.6. Summary and Conclusions

This chapter presents a novel methodology, the importance sampling technique (IST), which can be used in conjunction with the design point to perform the reliability analysis of a drilled shaft/slope system. Considering uncertainties of soil parameters and the bias of the semi-empirical equation for the load transfer factor (η), the reliability analysis using brute force MCS is not efficient due to its requirement of a large number of samples. Compared with brute force MCS, IST offers advantages in terms of achieving computational efficiency and accuracy, especially when the estimator (P_f) is small. The illustrative application example provides evidence of the capability of the proposed IST. The following conclusions can be drawn from this paper:

1. Importance sampling using the design point was developed to compute the probability of failure for a drilled shaft/slope system. The proposed ordinary method of slices (OMS), together with the arching theory, was shown to be able to efficiently determine the performance function $g(x)$ and the design point.

2. The standard deviation (SD) of importance function ($IS(x)$) should be chosen very carefully. Reducing the SD value of $IS(x)$ may be able to produce more failure events; however, it does not automatically guarantee that the estimator P_f is more accurate. In this paper, a standard deviation equal to 1.00 for the importance function is suggested for determining the importance function $IS(x)$ in the drilled shaft/slope system.

5. LIMIT EQUILIBRIUM BASED DESIGN APPROACH FOR SLOPE STABILIZATION USING MULTIPLE ROWS OF DRILLED SHAFTS

Use of a single row of drilled shafts for stabilization of an unstable or failed slope has been employed for many years. However, there may be conditions under which the use of a single row of drilled shafts may not be feasible: these situations may occur in cases where there is an inability to provide the required global factor of safety, a high force is imparted on the shaft (with the attendant high reinforcement requirement that is not constructible), or where the deflection of the drilled shaft is too high to meet the service limit requirement. In the past, no design method has been developed to permit systematic design for optimizing multiple rows of drilled shafts for slope stabilization. In this chapter, a limiting equilibrium–based method of slices procedure, incorporating the arching effects of the drilled shafts, is developed for optimizing the use of multiple rows of drilled shafts, in terms of the number of rows, the location of each row, and the dimension and spacing of the drilled shafts in each row. Two design criteria are used for optimization: 1) the target global factor of safety and constructability and 2) the service limit. A PC-based research version program called *UA Slope 2.2* has been coded to allow for handling of complex slope geometry, soil profiles, and groundwater conditions. A design example is presented in this chapter to illustrate the application of the *UA Slope 2.2* program in the optimized design of multiple rows of drilled shafts for stabilizing an example slope.

5.1. Introduction

The practice of using drilled shafts to stabilize an unstable slope has been widely and successfully adopted (e.g., Fukumoto, 1972, 1973; Sommer, 1977; Ito and Matsui, 1975; Ito et al., 1981, 1982; Nethero, 1982; Morgenstern and Price, 1965; Morgenstern, 1982; Gudehus and Schwarz, 1985; Reese et al., 1992; Rollins and Rollins, 1992; and Poulos 1995, 1999). However, most of the analyses and design methods are based on the limiting equilibrium approach, which considers the effect of drilled shafts to be an increase in resistance. The estimation of resistance from drilled shafts has been based on ultimate soil reaction pressure or displacement-based finite element analysis or a computational program such as *LPILE* (Reese et al., 2004) to determine the displacement-dependent soil pressures against the drilled shafts. The alternative approach, within the concept of the limiting equilibrium method of slices, has been proposed and developed by several researchers (Zeng and Liang, 2002; Yamin, 2007; Yamin and Liang, 2010; Liang et al., 2010; Al Bodour, 2010; Joorabchi, 2011; Liang and Joorabchi, 2013), in which the effects of the drilled shafts are considered as the reduction in the driving forces due to the soil arching between the adjacent drilled shafts. The estimate of the reduction in the driving force is based on an empirical load transfer factor equation. The equation was derived from regression analysis of more than 40 cases of three-dimensional (3D) finite element simulation results. This method has been coded into a PC-based computer program (*UA Slope 2.1n*) for design applications.

When looking at the various methods proposed for slope stabilization using drilled shafts, it was found that all of them were concerned with the design of a single row of drilled shafts. The method proposed by Liang (2010) allows for optimization of the size (diameter and length) of the drilled shafts, the spacing between the adjacent drilled shafts, and the location of the row of drilled shafts on the slope. However, in reality, the use of a single row of drilled shafts may not

be feasible due to the dimensions of the failed slope and because of the large earth thrust applied to the drilled shafts, which would render the structural design of the drilled shafts nearly impossible. Under these difficult conditions, the use of multiple rows of drilled shafts could be a feasible solution to both ensure that the global factor of safety of the stabilized slope meets the target factor of safety and that the size of drilled shafts and the amount of reinforcement used in the drilled shafts is constructible and economical. Specifically, multiple rows of drilled shafts are needed to arrest slope movement and enhance the safety margin of the failing slope for the following two scenarios: (1) one row of drilled shafts cannot satisfy the target factor of safety (FS_{Target}), regardless of the dimension of the drilled shafts and location of the drilled shafts; and (2) although the use of single row of drilled shafts can increase the global factor of safety of the slope to the target value, the net force applied to the drilled shafts is excessively large, which either precludes the design of a constructible reinforcement or produces a deflection of the shaft that may be too large to meet the service limit requirements.

In this chapter, an analysis and design approach for using multiple rows of drilled shafts to stabilize an unstable slope is presented. The method is based on the limit equilibrium method of slices, incorporating the concept of soil arching in determining the reduction of the driving force in the stability analysis. The formulation of this method, together with the empirical equations for determining the arching-induced reduction in the driving forces, is described in detail. Optimization of the number of the rows, the dimensions of the drilled shafts, and the locations of each row of drilled shafts to achieve safety and service limit requirements is discussed. An example is presented to demonstrate the use of the proposed method to optimally design multiple rows of drilled shafts for the purpose of slope stabilization.

5.2. Using Multiple Rows of Drilled Shafts for Stabilizing a Slope

Ideally, one would like to use only a single row of drilled shafts to stabilize an unstable slope. However, conditions exist that may require use of more than one row of drilled shafts. Usually, there are two major circumstances where multiple rows of drilled shafts are necessary: 1) cases where using one row of drilled shafts cannot satisfy the target FS regardless of the chosen dimension of the drilled shafts, the spacing of drilled shafts, and location of the row of drilled shafts, and 2) cases where the forces applied to the drilled shaft are excessively large such that either the reinforcement cannot be practically provided without causing constructability issues or the drilled shaft deflection is too excessive to meet the service limit requirements. Therefore, to address situations like these, there is a need to use multiple rows of drilled shafts.

5.2.1. Method of Slices for a Two-Row Drilled Shaft/Slope System

The global factor of safety of two or more rows in a drilled shaft/slope system can be calculated based on the limit equilibrium method of slices. The method of slices for two rows of drilled shafts incorporating the arching-induced reduction in driving force on the downslope side of drilled shafts is formulated herein. The basic assumptions made in the calculation of the method of slices are listed below:

- 1) FS was considered to be identical for all slices;
- 2) A normal force on the base of the slice was applied at the midpoint of the slice base;
- 3) The location of the thrust line of the interslice forces was placed at one-third of the average interslice height above the failure surface, as in the study by Janbu (1973);

- 4) The inclinations of the interslice forces were assumed as follows: the right interslice force (P_i^R) was assumed to be parallel to the inclination of the preceding slice base (i.e., α_{i-1}), and the left interslice force (P_i^L) was assumed to be parallel to the current slice base (i.e., α_i);
- 5) There is no group pile effect between the two adjacent rows of drilled shafts; and
- 6) There is no soil arching influence between the two adjacent rows of drilled shafts.

Figure 5-1 shows a typical slice with all force components acting on the slice. The load in the drilled shaft/slope system is generated by gravity and friction and then transferred slice-by-slice through the interslice force P_i^L . For a typical slice without drilled shafts on the slope, the interslice force P_i^L can be expressed as an equilibrium equation given in Equation 5-1.

$$P_i^L = w_i \sin \alpha_i - \left[\frac{c_i l_i}{FS} + (w_i \cos \alpha_i - u_i l_i) \frac{\tan \varphi_i}{FS} \right] + k_i P_i^R \quad (5-1)$$

After the drilled shafts are inserted into the slope, the interslice force on the downslope side of the drilled shaft will be reduced due to soil arching, i.e., it will be reduced by a multiplier called the load transfer factor (η) from the previous interslice force P_i^R . Referring to Figures 5-1, 5-2 and 5-3 and applying the force equilibrium while invoking Mohr-Coulomb's strength criterion for any slice i of the slope, the interslice force shown in Figure 5-3 can be written using the following expressions:

$$P_i^L = w_i \sin \alpha_i - \left[\frac{c_i l_i}{FS} + (w_i \cos \alpha_i - u_i l_i) \frac{\tan \varphi_i}{FS} \right] + k_i \eta_1 P_{i-1}^L \quad (5-2)$$

$$P_j^L = w_j \sin \alpha_j - \left[\frac{c_j l_j}{FS} + (w_j \cos \alpha_j - u_j l_j) \frac{\tan \varphi_j}{FS} \right] + k_j \eta_2 P_{j-1}^L \quad (5-3)$$

$$k_i = \cos(\alpha_{i-1} - \alpha_i) - \sin(\alpha_{i-1} - \alpha_i) \frac{\tan \varphi_i}{FS} \quad (5-4)$$

$$k_j = \cos(\alpha_{j-1} - \alpha_i) - \sin(\alpha_{j-1} - \alpha_i) \frac{\tan \varphi_j}{FS} \quad (5-5)$$

where $i < j$; P_i^L and P_j^L are the interslice forces acting on the downslope side of Slices i and j ; w_i and w_j are weight of Slices i and j ; α_i and α_j are inclinations of the bases of Slices i and j ; c_i and c_j denote the soil cohesion at the bases of Slices i and j ; φ_i and φ_j are the soil friction angles at the bases of Slices i and j ; u_i and u_j are the pore water pressures at Slices i and j ; and η_1 and η_2 are the load transfer factors for Row 1 and Row 2.

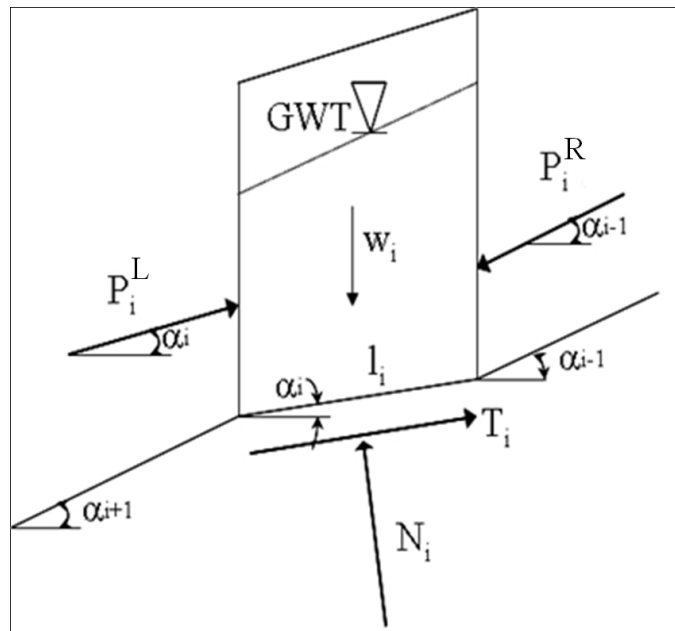


Figure 5-1: A typical slice showing all force components

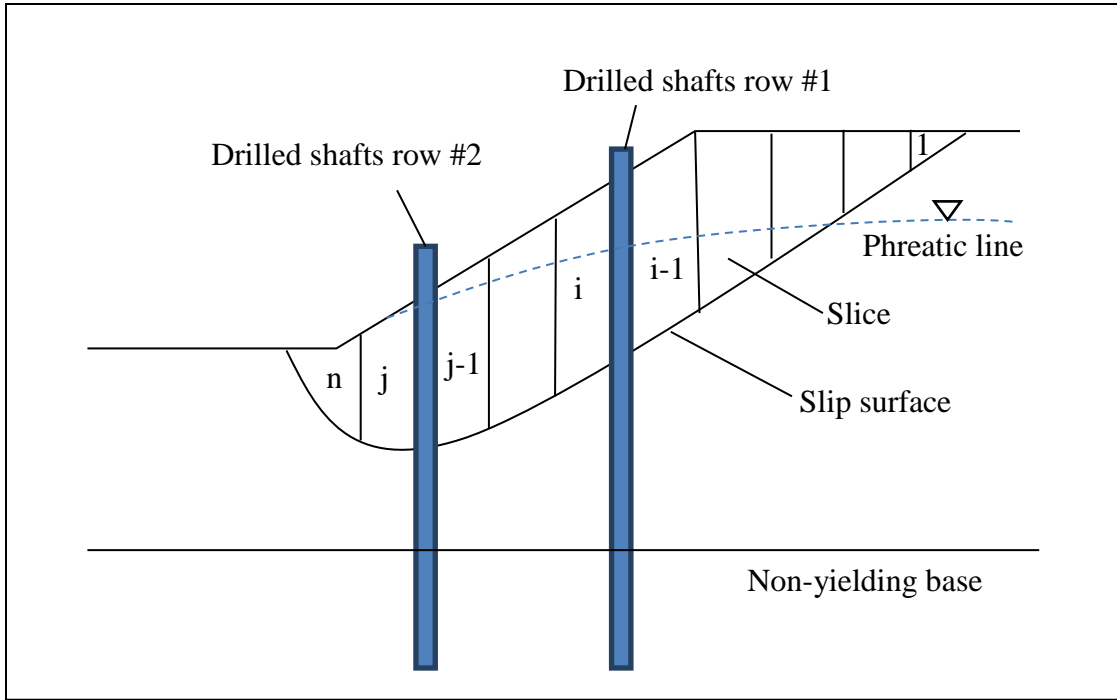


Figure 5-2: A typical cross-section divided into slices for a slope reinforced with two rows of drilled shafts

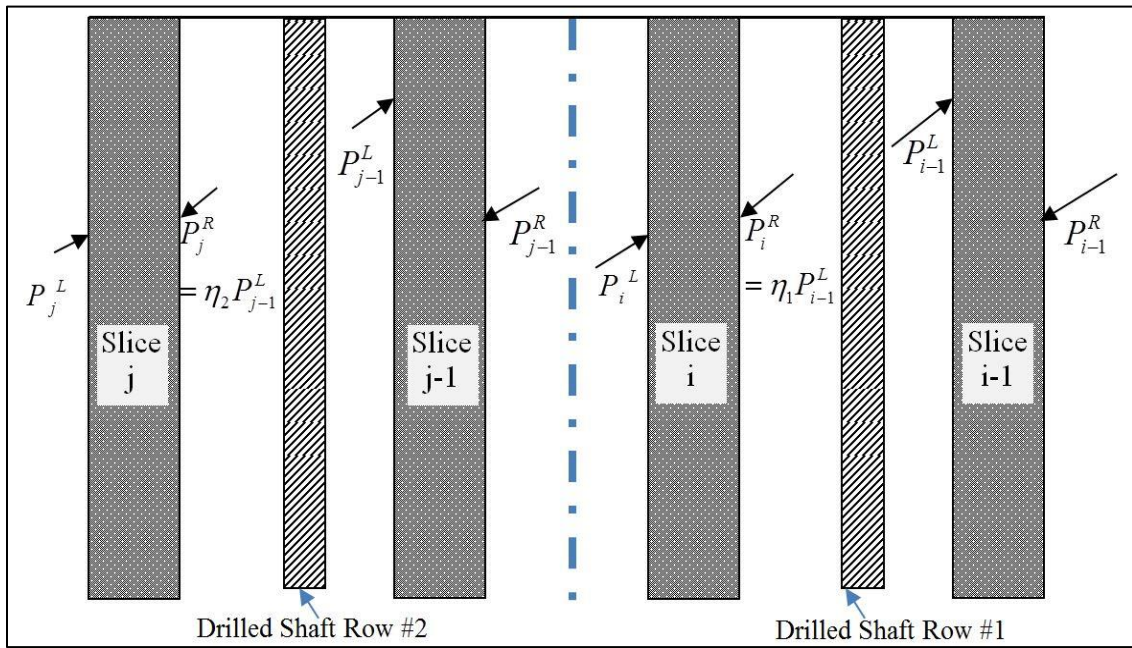


Figure 5-3: Method of slices using two rows of drilled shafts

The net force applied to the two rows of drilled shafts, which is due to the difference in the interslice forces on the upslope and downslope sides of the drilled shaft can be calculated as follows:

$$F_{shaft-row1} = (1 - \eta_1) P_{i-1}^L S_{01} \quad (5-6)$$

$$F_{shaft-row2} = (1 - \eta_2) P_{j-1}^L S_{02} \quad (5-7)$$

where S_{01} and S_{02} are the center-to-center spacing between two adjacent drilled shafts of the two rows (Figure 5-2), P_{i-1}^L and P_{j-1}^L are the interslice forces acting on the upslope side of Slice $i-1$ and $j-1$ (Figure 5-3) and $F_{shaft-row1}$ and $F_{shaft-row2}$ are the net forces on the drilled shaft in Row 1 and Row 2, respectively. Based on Equations 5-2 to 5-5, the global factor of safety for two rows in a drilled shaft/slope system can be calculated in an iterative computational algorithm. For multiple rows of drilled shafts, the calculation principles of the global factor of safety and the net force for each row of shafts are the same as in the case of two rows of drilled shafts. A PC-based computer program, *UA Slope 2.2*, has been developed based on the above computational algorithm to calculate the global factor of safety for multiple rows of a drilled shaft/slope system and the net force imparted on each drilled shaft for each row of drilled shafts.

In Equations 5-2 to 5-7, the load transfer factor η is defined as the ratio between the horizontal force on the downslope side of the vertical plane at the interface between the drilled shaft and soil (i.e., $P_{downslope}$) to the horizontal force on the upslope side of the vertical plane at the interface between the drilled shaft and soil (i.e., $P_{upslope}$). For the expression of the load transfer factor, Joorabchi (2011) proposed a semi-empirical equation, given in Equation 2-15 in Chapter 2, to compute the load transfer factor using regression analysis techniques on more than 40 cases

of 3D finite element model simulation results that were conducted by Al Bodour (2010). Assuming that a sufficient length of the drilled shaft is socketed into the rock layer, the other important influencing factors on the load transfer factor consist of the following six parameters: soil cohesion c , friction angle φ , drilled shafts diameter D , center to center shaft spacing S_0 , shaft location on slope ζ_x , and slope angle β .

5.2.2. Optimization Strategy and Criteria

The following principles are used for optimization of multiple drilled shafts on a slope:

- 1) The global FS should be equal to or bigger than FS_{Target} . For example, $FS_{Target} = 1.5$ is used in the example given below;
- 2) The lateral deflection of each drilled shaft should not exceed the prescribed service limit, say, 12.7 mm (0.5 inch) on the top of the shaft; and
- 3) The location of drilled shafts should depend on site accessibility and on the local availability of appropriate construction equipment.

After satisfying the above principles, further steps in the optimization strategy are taken to ensure constructability for practical reinforcement placements (such as rebar spacing, cover thickness, etc.) and to determine the drilled shaft with the minimum volume, as suggested below:

- 4) To minimize the cost of reinforcement, the net force of drilled shafts should be as low as possible;
- 5) To minimize the total cost of concrete, the total volume of drilled shafts for each

combination (shaft diameter D , shaft clear spacing S , and shaft length L) should be calculated and compared to find which shaft has the smallest volume.

5.3. Illustrative Design Example

An example slope is used to demonstrate the design approach for using multiple rows of drilled shafts in stabilizing the slope to the target global factor of safety. During the design procedure, one row of drilled shafts was analyzed first to demonstrate that it is not sufficient to stabilize the slope. Next, two rows of drilled shafts were considered in the design of the slope stabilization. Finally, if the need is demonstrated, three rows of drilled shafts are considered.

The slope shown in Figure 5-4 consists of six soil layers, and the soil properties for each layer are summarized in Table 5-1. The critical slip surface for the slope was determined by a conventional slope stability analysis program, *STABL*, with the computed FS equal to 1.00. The identified critical slip surface is represented by connecting seven points. In the majority of design problems involving the reinforcement of an unstable slope, the slip surface of the failed slope is typically identified during field monitoring through the use of an inclinometer. Therefore, in the present study, the slip surface determined by the slope stability analysis is treated as a pre-existing failure surface and is used in the subsequent design of drilled shafts for stabilization of this particular slope. In this example, we will provide a rock socket in Layer 6, which is a rock layer. The groundwater table is assumed at an elevation of -33.0 m (-108 ft), as shown in Figure 5-4. It is noted that effective stress approach is used in the stability analysis.

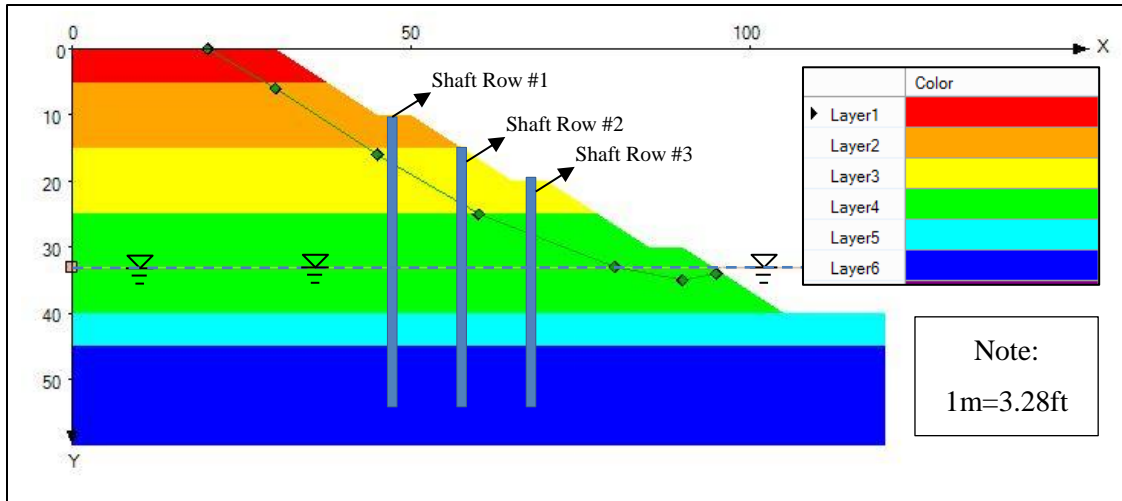


Figure 5-4: Geometry of illustrative example (Unit: meter)

Table 5-1: Soil Properties of Illustrative Example

Layer No.	Layer 1	Layer 2	Layer 3	Layer 4	Layer 5	Layer 6
c (kN/m²)	10.0 (208psf)	11.0 (229psf)	25.0 (522psf)	20.0 (417psf)	30.0 (626psf)	50.0 (1044psf)
φ (degree)	3.0	5.0	6.0	3.0	18.0	30.0
γ (kN/m³)	5.0 (32pcf)	7.0 (45pcf)	8.0 (51pcf)	12.5 (80pcf)	16.0 (102pcf)	19.9 (127pcf)

5.3.1. Step-by-Step Design Procedure

The step-by-step procedure for the design of the illustrative example is as follows:

- Step 1: Collect data concerning the geometry of the slope, soil profile, soil parameters, groundwater table conditions, location of the slip surface, and other necessary

information. For this example, the relevant information is presented in Figure 5-4 and listed in Table 5-1. It is noted that the slip surface identified for the original slope will be used for the subsequent calculation and design, as this surface is considered to be the weakest surface for subsequent slope movement to occur.

- Step 2: Choose a target factor of safety (FS_{Target}) for the drilled shaft/slope system equal to 1.5.
- Step 3: Select feasible locations for drilled shafts, which may depend on the site situation and the local availability of construction equipment suitable for drilling shafts. The feasible locations for drilled shafts are between 30.0 m (98ft) and 90.0 m (295ft) horizontally from the left side of the slope (as shown in Figure 5-4). In the current design, we analyze the location starting at $X = 30$ m (98ft) and ending at $X = 90$ m (296ft), in increments of 5.0 m (16.5 ft).
- Step 4: Perform analysis and design using one row of drilled shafts, considering different combinations of clear spacing S and shaft diameter D within the permissible range. In this example, the range for D is selected to be between 0.6 m to 2.4 m (2 ft~8 ft), and the range of S/D is selected to be between 1.0 and 3.0. The following combinations for (S, D) are selected for computation: (0.6m (2.0ft), 0.6m (2.0ft)), (1.2m (4.0ft), 0.6m (2.0ft)), (1.8m (6.0ft), 0.6m (2.0ft)), (1.2m (4.0ft), 1.2m (4.0ft)), (2.4m (8.0ft), 1.2m (4.0ft)), (3.6m (12ft), 1.2m (4.0ft)), (1.8m (6.0ft), 1.8m (6.0ft)), (3.6 (12ft), 1.8 (6.0ft)), (5.4 (18ft), 1.8 (6.0ft)), (2.4m (8.0ft), 2.4m (8.0ft)), (4.8 (16ft), 2.4 (8.0ft)), and (7.2 (24ft), 2.4 (8.0ft)).

- Step 5: Calculate global FS and shaft net force using the described method and the computer program *UA Slope 2.2*. For each (S, D) combination, it is necessary to plot the relationship between the computed global FS and different shaft locations, as well as to plot the relationship between the net force on the drilled shaft and the different shaft locations, as shown in Figures 5-5 and 5-6, respectively.

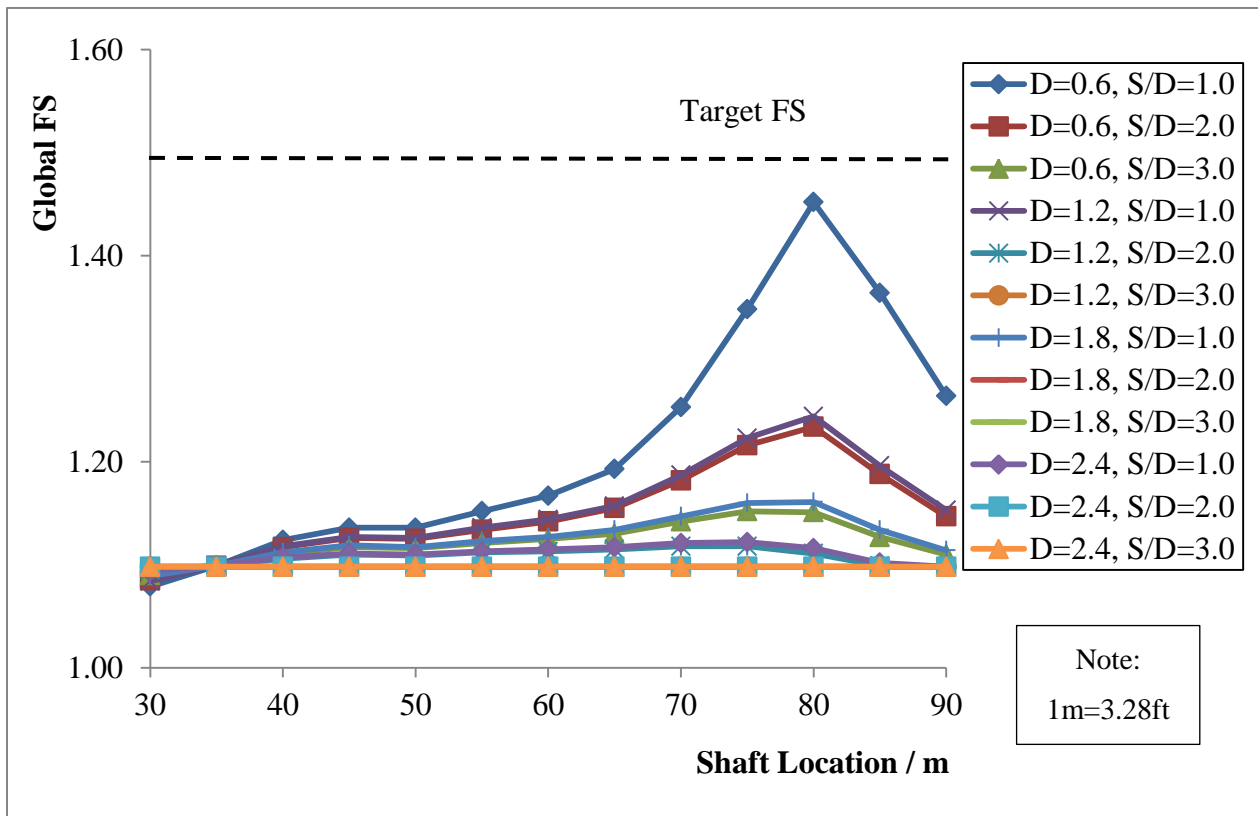


Figure 5-5: Global FS versus shaft location for different (S, D) combinations using one row of drilled shafts

As can be seen from Figure 5-5, the computed global FS for all combinations and shaft locations considered do not satisfy the target FS of 1.5. The next highest FS is 1.452, corresponding to the drilled shaft located at 80 m and the (S, D) combination of (0.6 m (2.0 ft), 0.6 m (2.0 ft)). Therefore, we need to consider the use of two rows of drilled shafts.

- Step 6: Perform analysis and design using two rows of drilled shafts, considering different combinations of clear spacing S , shaft diameter D , and various drilled shaft locations. For the (S, D) combinations and the drilled shaft locations, we choose the same range as was discussed in Steps 3 and 4.

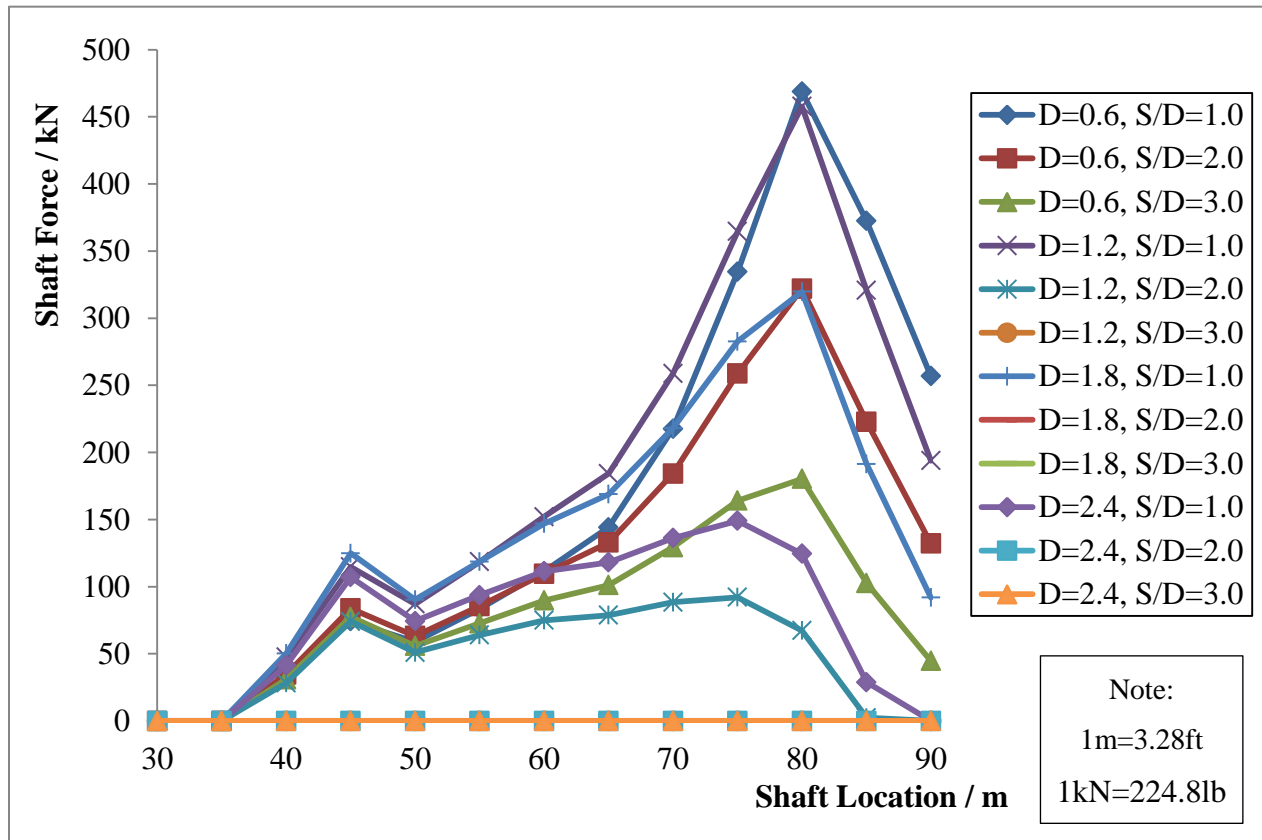


Figure 5-6: Shaft force versus shaft location for different (S, D) combinations using one row of drilled shafts

At the beginning of Step 6, we place the location of the first row of drilled shafts on the slope crest; next, we change the location of the second row of drilled shafts from the slope crest to the slope toe. Thereafter, we place the first row 5.0 m further to the downslope direction, and we

change the location of the second row from the slope crest to the slope toe. We repeat the above procedure until the location of the first row reaches to the slope toe.

- Step 7: Calculate the global FS and the shaft net force by using the computer program *UA Slope 2.2*. Since there are many possible combinations and it is hard to display all of the data in one figure, only those combinations that provide a global FS larger than FS_{Target} of 1.5 and a shaft net force less than 400 kN (90 kips) are presented in Table 5-2. As can be seen in this table, only five feasible combinations are obtained for the case of using two rows of drilled shafts.

Table 5-2: Design Results using Two Rows of Drilled Shafts

No.	FS	Row #1				Row #2			
		Force (kN)	Location (m)	<i>D</i> (m)	<i>S</i> (m)	Force (kN)	Location (m)	<i>D</i> (m)	<i>S</i> (m)
1	1.500	176.3 (39.6kip)	50 (160ft)	0.6 (2.0ft)	0.6 (2.0ft)	322.1 (72.4kip)	85 (280ft)	0.6 (2.0ft)	0.6 (2.0ft)
2	1.655	269.1 (60.5kip)	55 (180ft)	0.6 (2.0ft)	0.6 (2.0ft)	358.8 (80.6kip)	80 (260ft)	0.6 (2.0ft)	0.6 (2.0ft)
3	1.554	241.4 (54.3kip)	55 (180ft)	0.6 (2.0ft)	0.6 (2.0ft)	304.7 (68.5kip)	80 (260ft)	0.6 (2.0ft)	0.6 (2.0ft)
4	1.529	328.1 (73.8kps)	60 (200ft)	0.6 (2.0ft)	1.2 (2.0ft)	312.8 (70.3kip)	85 (280ft)	0.6 (2.0ft)	0.6 (2.0ft)
5	1.509	381.3 (85.7kip)	75 (240ft)	0.6 (2.0ft)	1.8 (2.0ft)	319.5 (71.8kip)	85 (280ft)	0.6 (2.0ft)	0.6 (2.0ft)

Note: *D* is the diameter of drilled shaft; *S* is the clear spacing between adjacent drilled shafts.

- Step 8: Use the p - y method based software, *LPILE* v.5.0 (developed by Reese et al., 2004), to determine the internal forces and moments in the drilled shaft and the shaft deflections under the net shaft force given in Table 5-2. The calculation results of the analysis using *LPILE* indicate that the lateral deflections on the top of the shaft are very high, such that the program cannot even converge if the shaft net force exceeds 300 kN (67 kips). Although the use of two rows of drilled shafts can ensure that the global FS will be greater than the target FS, the *LPILE* analysis shows excessive deflections that do not meet the service limit requirements. Consequently, three rows of drilled shafts are considered for the subsequent analysis and design.
- Step 9: Perform analysis and design using three rows of drilled shafts, considering the same range for the shaft location, shaft clear spacing S , and shaft diameter D as in Step 6. In the current step, we follow the same logic in trying different combinations of drilled shaft locations as described before.
- Step 10: Calculate the global FS and shaft net force for each drilled shaft by using *UA Slope 2.2*, using the same methodology discussed in Step 7 and outputting only the combinations that provide the global FS larger than FS_{Target} of 1.5. In the meantime, only combinations showing net forces on drilled shaft that are less than 200 kN (45 kips) are considered. Table 5-3 shows the design results using three rows of drilled shafts. Two combinations can satisfy the requirements on the FS_{Target} , and the computed shaft net forces are less than 200 kN (45 kips) for both.

Table 5-3: Design Results using Three Rows of Drilled Shafts

No	FS	Row #1				Row #2				Row #3			
		Force (kN)	Location (m)	<i>D</i> (m)	<i>S</i> (m)	Force (kN)	Location (m)	<i>D</i> (m)	<i>S</i> (m)	Force (kN)	Location (m)	<i>D</i> (m)	<i>S</i> (m)
1	1.536	184.85 (41.6kip)	50 (160ft)	0.6 (2.0ft)	0.6 (2.0ft)	169.10 (38.1kip)	65 (220ft)	0.6 (2.0ft)	0.6 (2.0ft)	140.48 (31.7kip)	75 (240ft)	0.6 (2.0ft)	0.6 (2.0ft)
2	1.504	177.23 (39.8kip)	50 (160ft)	0.6 (2.0ft)	0.6 (2.0ft)	184.35 (41.4kip)	65 (220ft)	0.6 (2.0ft)	1.2 (4.0ft)	169.94 (38.2kip)	75 (240ft)	0.6 (2.0ft)	0.6 (2.0ft)

Note: *D* is the diameter of drilled shaft; *S* is the clear spacing between adjacent drilled shafts.

- Step 11: Optimize design results by using the strategy of minimum concrete volume. As shown in Table 5-3, both combinations (No. 1 and No. 2) yield a similar shaft net force; however, the clear spacing for Row 2 of Combination No. 2 (i.e., $S = 1.2$ m (4.0 ft)) is larger than that for Combination No. 1 (i.e., $S = 0.6$ m (2.0 ft)), meaning that less concrete material is needed in Combination No. 2. Further structural analysis and total volume of drilled shafts are considered in Step 12.
- Step 12: Perform soil-structure interaction analysis for the drilled shaft using the computer program *LPILE* (Reese et al., 2004). Assuming that at least 20% of the length of drilled shaft is embedded into the rock layer (Layer 6) below the slip surface, the shaft parameters of the two combinations obtained from Step 11 with the corresponding net forces for each drilled shaft can be used as inputs in *LPILE* to calculate the lateral deflection and the internal forces and moments on the drilled shaft.

In the *LPILE* analysis, the boundary conditions at the top of the drilled shaft are zero shear and moment. The net force is distributed as a triangularly distributed shear force acting on the drilled shaft above the slip surface. The total net force is taken from Table 5-3. After calculation with *LPILE*, the lateral deflections on the top of the shaft for each row are summarized in Table 5-4, and the total shaft lengths of the two combinations are summarized in Table 5-4 as well. All the lateral deflections on the top of the shaft can be considered to be within the allowable deflection (say, half an inch, or about 12.7 mm). If we perform the quantitative analysis of the volume of the required drilled shafts, the drilled shaft volume per unit width of a slope for the two combinations can be determined (the results are shown in Table 5-5). Clearly, Combination No. 2 requires less total concrete volume than Combination No. 1. Thus, Combination No. 2 can be chosen as the most economical design with the least amount of drilled shaft volume while meeting the target global factor of safety.

Table 5-4: Design Results of the Two Combinations Shown in Table 5-3

Combination	Row #1		Row #2		Row #3	
	δ (m)	L (m)	δ (m)	L (m)	δ (m)	L (m)
No. 1	0.0115	44.0	0.0102	32.0	0.0085	29.0
	(0.45inch)	(144ft)	(0.40inch)	(105ft)	(0.33inch)	(95ft)
No. 2	0.0105	44.0	0.0113	32.0	0.0103	29.0
	(0.41inch)	(144ft)	(0.44inch)	(105ft)	(0.41inch)	(95ft)

Note: δ is the deflection on the top of drilled shaft; L is the shaft length.

Table 5-5: Total Volume per Unit Width for the Four Combinations

Combination	Row #1	Row #2	Row #3	Sum
No. 1	10.36 m ³	7.54 m ³	6.83m ³	24.73m ³
	(365.9ft ³)	(266.3ft ³)	(241.2 ft ³)	(873.3 ft ³)
No. 2	10.36 m ³	5.02 m ³	6.83 m ³	22.22 m ³
	(365.9ft ³)	(177.3ft ³)	(241.2ft ³)	(784.7ft ³)

The specific reinforcement requirements for the drilled shaft were not discussed here. Suitable reinforcements can be designed by a qualified structural engineer, based on the computed internal forces and moments.

5.4. Summary and Conclusion

In this chapter, a design procedure for using multiple rows of drilled shafts to stabilize a slope is presented. The limiting equilibrium based slope stability analysis method, modified to incorporate the induced arching effects of multiple rows of drilled shafts through a semi-empirical load transfer factor, is coded into a general slope stability computer program (*UA Slope 2.2*) for handling complex slope geometry, soil profile, and groundwater table conditions. Optimization principles for designing multiple rows of drilled shafts are discussed. A step-by-step design procedure is given to illustrate the use of the design methodology. Specific conclusions drawn from the illustrative design examples are as follows:

- The need for using multiple rows of drilled shafts to stabilize a large slope was illustrated by the design example. It was shown that as compared to one row of drilled shafts, multiple rows of drilled shafts can effectively increase the global factor of safety and at the same time reduce the net force imparted on the shaft, thus making the reinforcement design more constructible and meeting the service limit.
- Different combinations of shaft diameter, shaft spacing, and shaft location for each row can affect the global factor of safety. However, the final design recommendation should follow the principle of using the least amount of reinforcement, as well as minimizing the total volume of concrete.
- Although the limit equilibrium method of slices is expressed as a two-dimensional calculation, the load transfer factor was derived from 3D finite element simulation results, indicating that this method is capable of representing three-dimensional soil arching effects.

6. SUMMARY AND CONCLUSIONS

A reliability-based optimization design for using drilled shafts to stabilize a failed slope has been developed in this research, which can be used to achieve both safe and economical design outcomes. The corresponding preliminary research version of *UA Slope* has been updated as “*UA Slope 3.0*” to calculate the probability of failure and the reliability index for a drilled shaft/slope system. As an extension of this research, three additional subjects have been developed, including (1) a more advanced probabilistic algorithm than brute force Monte-Carlo simulation, and (2) the use of multiple rows of drilled shafts for stabilizing a large slope. During the development process, the corresponding preliminary research version programs for all theoretical work have been coded and debugged. The recommendations for implementation and future research are presented at the end of this chapter.

6.1. Summary of Work Accomplished

This research encompassed both program coding and design methodology development. The program coding consists of a limit equilibrium method of slices, a semi-empirical equation of load transfer factor, and techniques to account for uncertainties of soil parameters and load transfer factor parameters. On the design methodology side, the Ohio ATH-124 slope has been adopted to perform a Monte-Carlo reliability-based design using a single row of drilled shafts (*UA Slope 3.0*). The design methodology also includes the use of multiple rows of drilled shafts in stabilizing a failed slope (*UA Slope 2.2*). Specific contributions obtained from these program coding and design methodologies include the following:

- The state-of-the-art literature review clearly supported the need for conducting this research, which revealed that there was no reliability-based design and analysis on a drilled shaft/slope system with assured safety and economy. It was observed that in the past, most of the designs involving the use of drilled shafts tended to be ultra-conservative, or they did not reach the reliability even though the factor of safety has satisfied the target. This situation, which is primarily due to a lack of adequate knowledge in probabilistic algorithms, can result in transportation agencies, such as ODOT, dedicating an excessive amount of financial resources to mitigate damage caused by landslides.
- The next generation of slope stability design methodology, a true reliability-based optimization design method using Monte-Carlo simulation, has been developed for analyzing and designing a drilled shaft/slope system with a complex slope profile and groundwater activity.
- The major contributions of this research include not only the development of improved methodology but also the accompanying computer program to solve a challenging design problem with no prior universally accepted solutions. This research-grade probabilistic computer program, *UA Slope 3.0*, has been developed in this research to calculate the probability of failure and the reliability index for a drilled shaft/slope system.
- The step-by-step design procedure using the *UA Slope 3.0* program for an optimized shaft/slope system presented in this report represents the first documented procedure where the design of the drilled shaft stabilized slope was treated as an optimization

process with an ultimate goal of achieving both the targeted reliability of the geotechnical system (including the structural components) and economy in construction costs.

- A more efficient and accurate methodology, which employs the importance sampling technique (IST), has been developed to deal with high-dimensional drilled shaft/slope systems. It is demonstrated that IST is feasible and highly efficient in performing a reliability analysis for a drilled shaft/slope system.
- A new deterministic methodology has been developed to analyze and design a system of multiple rows of drilled shafts to stabilize a large failed slope. A new limit equilibrium method of slices has been developed based on multiple load transfer factors in a slope. The optimization strategy and design criteria for how to choose the parameters (including the shaft diameter of each row, shaft clear spacing of each row, shaft location of each row, and shaft net force of each row) have been developed.
- A research-grade version of a computer program, *UA Slope 2.2*, has been coded in this report to calculate the global factor of safety and shaft net force for a reinforced slope system using multiple rows of drilled shafts. A step-by-step design procedure has been developed based on the above optimization strategy and design criteria.

6.2. Conclusions

The main conclusions of this study are summarized as follows.

- The reliability based methodologies for computing reliability index of a drilled shaft/slope system as well as the loads on the drilled shafts for determining internal forces and moments for structural design of a drilled shaft have been developed. A case study employing *UA Slope 3.0* shows that the location, spacing, diameter, and length of the drilled shafts are the fundamental design parameters that can be varied in different combinations to achieve the target reliability index. Furthermore, the model error of the semi-empirical load transfer prediction equation can affect the computed probability of failure in the drilled shaft/slope system.
- Importance sampling technique (IST) using the design point is able to compute the probability of failure for a drilled shaft/slope system in which the combination of ordinary method of slices (OMS) and arching theory are used to determine the performance function $g(x)$ and the design point.
- Multiple rows of drilled shafts can effectively increase the global factor of safety of a large failed slope and can reduce the net force imparted on the shaft, thus making the reinforcement design for drilled shafts more constructible while meeting the service limit requirement. The final design should follow the principle of using the least amount of reinforcement and minimizing the amount of total concrete required.

6.3. Recommendations for Implementation

The implementable outcome of this study is a research-grade version of a probabilistic program (*UA Slope 3.0*) that can be used by design engineers to analyze complex soil profiles and slope

conditions that are frequently encountered in real-world projects. The computer program can also effectively be used for the necessary iterative optimization design process in order to achieve the best combination of shaft location, shaft diameter, and shaft spacing, which would provide the target reliability index for the drilled shaft/slope system while minimizing construction costs. The following recommendations are made for possible implementation.

- The statistical values of soil properties (i.e. the mean and variance of cohesion, friction angle and unit weight) should be calculated based on measurements from field tests. However, the variance of soil properties can be adopted from Phoon and Kulhawy (1999) in cases where the field data is limited, a situation that would make the variance difficult to determine from the field data.
- In the research grade *UA Slope 3.0* program, the default distributions of soil parameters as well as the model error of semi-empirical equation follow a lognormal distribution. Other distributions are not included in *UA Slope 3.0* and will be incorporated into the next generation of the program.
- Following the successful completion of an initial stage of OGE's trial use of the program, it is recommended that the program be sent to selected qualified geotechnical consultants for trial use. This would broaden the number of test cases of the program so that the robustness of the program can be ascertained. Any comments from the selected user group of consultants should be summarized and provided to the UA research team for further debugging and improvement of the program, if necessary.
- Future implementation may include publishing the downloadable version of the *UA Slope 3.0* program, along with a user manual, on various pages of the ODOT website (such as

the pages for the Office of Geotechnical Engineering, the Office of Structures, and the Office of Research and Development) to allow for wide dissemination of the computer program to the professional community.

6.4. Recommendations for Future Research

The major development efforts of this study were concentrated on the reliability-based design optimization for a single row of equally spaced drilled shafts to stabilize a failed slope, as well as the probabilistic research version program, *UA Slope 3.0*. As an extension of this research, we have also developed the following methodologies and the accompanying computer programs: (a) an importance sampling technique applied to the probability-based methodology for a drilled shaft/slope system, and (b) a deterministic design method for the use of multiple rows of drilled shafts in stabilizing a slope. The following recommendations for future research are suggested:

- Extend the research-grade coding of *UA Slope 2.2* and *UA Slope 3.0* into three user-friendly programs.
- Develop a more accurate semi-empirical equation for the load transfer factor.
- Analyze the difference in the load transfer factor based on different configurations of drilled shafts, such as a staggered arrangement or an arched shape, as these placement configurations tend to offer more global stabilization benefits than a straight row of spaced drilled shafts.

- Develop a more efficient algorithm for using multiple rows of drilled shafts in stabilizing a large slope, in order to meet the target factor of safety and to minimize construction costs.

7. BIBLIOGRAPHY

- Al Bodour, W. (2010). "Development of Design Method for Slope Stabilization Using Drilled Shaft." Ph.D. Dissertation, Department of Civil Engineering, The University of Akron; Akron, Ohio.
- Abramson, L. W., Lee, T. S., Sharma, S., Boyce, G. M. (2002). *Slope Stability and Stabilization Methods, 2nd Ed.*, John Wiley & Sons, Inc., New York, pp. 427.
- Adachi, T., Kimura, M. and Tada, S. (1989). "Analysis on the preventive mechanism of landslide stabilizing piles." 3rd International Symposium on Numerical Models in Geomechanics, pp. 691-698.
- Ashour, M. Norris, G. & Pilling P. (1997) "Lateral loading of a pile in layered soil using the Akron load transfer model." *J. Geotechnical and Geoenvironmental Engineering*, V. 124, No. 4, p. 303-315.
- Ashour, M. Pilling, P. & Norris, G. (2002). "Akron load transfer Model Capability of Analyzing Behavior of Laterally Loaded Isolated Piles, Drilled Shafts, and Pile Groups." *J. Bridge Engineering*, V.7, No. 4, p. 245-254.
- Ashour, M. & Ardalan, H. (2012). "Analysis of pile stabilized slopes based on soil-pile interaction." *Computers and Geotechnics*, V.39, p.85-97.
- Au, S.K., Papadimitriou C., and Beck, J.L. (1999). "Reliability of uncertain dynamical systems with multiple design points." *Structural Safety* 21, 113-133.
- Au, S.K., and Beck, J.L. (2003). "Important sampling in high dimensions." *Structural Safety* 25, 139-163.

- Bicocchi, N. (2011). "Structural and geotechnical interpretation of strain gauge data from laterally loaded reinforced concrete piles." PhD Thesis, University of Southampton, Southampton, U.K.
- Bishop, A.W. (1955). "The use of the slip circle in the stability analysis of slopes." *Geotechnique* 5 (1), 7-17.
- Bosscher, P. J. and Gray, D. H. (1986). "Soil arching in sandy slopes." *Journal of Geotechnical Engineering*, Vol. 112, No. 6, pp. 626-645.
- Bransby, M.F., and Springman, S. (1999). "Selection of load transfer functions for passive lateral loading of pile groups." *Computers and Geotechnics*, Vol.24, pp. 155-184.
- Bulley, W.A. (1965). "Cylinder Pile Retaining Wall Construction - Seattle Freeway." Roads and Streets Conference, Seattle.
- Carrubba, P., Maugeri, M., Motta, E. (1989). "Esperienze in vera grandezza sul comportamento di pali per la stabilizzazione di un pendio." *Proc. Of XVII Convegno Nazionale die Geotechnics*, Assn. Geotec., Italiana.
- Chelapati, C. V. (1960). "Arching in soils due to the deflection of a rigid horizontal strip." *Proceedings, Symposium on soil-structural interaction*, Tucson, Ariz., 1960, pp. 356-377.
- Chen, W. F. (1975). *Limit analysis and soil plasticity*. Elsevier, Amsterdam.
- Chen, C.-Y., and Martin, G. R., (2002). "Soil-Structure interaction for landslide stabilizing piles." *Computers and Geomechanics. J.* Vol. 29:pp. 363-386

- Cheung, R. W. M. and Tang, W. H. (2005). "Reliability of deteriorating slopes." *J. Geotech. Geoenviron. Eng.* Vol. 131, No. 5, pp. 589-597.
- Ching, J.Y., Phoon, K.K. and Hu, Y.G. (2009). "Efficient evaluation of reliability for slopes with circular slip surfaces using importance sampling." *J. Geotech. Geoenviron. Eng.* 135 (6), 768-777.
- Ching, J.Y., Phoon, K.K. and Hu, Y.G. (2010). "Observations on limit equilibrium-based slope reliability problem with inclined weak seams." *J. Geotech. Geoenviron. Eng.* 136 (10), 1220-1233.
- Cornforth, D. H. (2005) *Landslides in Practice: Investigation, Analysis, and Remedial/Preventative Options in Soil*, John Wiley and Sons. ISBN 0-471-67816-3.
- De Beer, E. E. and Wallays, M. (1972). "Forces Induced in Piles by Unsymmetrical Surcharges on the Soil around the Pile." In *Proc. 5th European Conf. On Soil Mechanics and Foundation Engineering*, Vol 1, The Spanish Society for Soil Mechanics and Foundation, Madrid, Spain.
- Duncan, J.M. (1996). "State of the art: limit equilibrium and finite element analysis of slopes." *J. Geotech. Eng. Div. ASCE* 122 (7), 577-596.
- Durrani, I. K., Ellis, E. A., and Reddish, D. J. (2008). "Numerical modeling of lateral pile-soil interaction for a row of piles in a frictional soil." *Advances in Transportation Geotechnics - Proceedings of the 1st International Conference on Transportation Geotechnics 2008*, Pages 291-298.
- Esu, F. and D'Elia, B. (1974). "Interazione terreno-struttura in un palo sollecitato da una frana tipologica." *Rev. Ital di Geot.* III, pp. 27-38.

- Firat, S. (1998). "Critical assessment of existing slope stability formulae and application to slope stabilisation." Ph.D. Thesis, University of Glamorgan, Glamorgan, U.K.
- Fukumoto, Y. (1972). "Study on the behaviour of stabilization piles for landslides." *Journal of JSSMFE*, Vol. 12(2), pp. 61-73.
- Fukumoto, Y. (1973). "Failure condition and reaction distribution of stabilization piles for landslides." *Proc., 8th annual meeting of JSSM*, pp. 549-562.
- Fukuoka, M. (1977). "The effects of horizontal loads on piles due to Landslides." In *Proc. 10th Spec. Session, 9th Int. Conf. Soil Mechs and Fndn. Eng.*, Tokyo, pp. 27-42.
- Getzler, Z., Komornik, A., and Mazurik, A. (1968). "Model study on arching above buried structures." *Journal of Soil Mechanics and Foundations Division, ASCE*, Vol. 94, No. SM5, pp. 1123-1141.
- Ghee, E. H. (2009). "The behaviour of axially loaded piles subjected to lateral soil movements." Ph.D. Thesis, Griffith University, Southport, Australia.
- Griffiths, D. V., and Fenton, G. A. (2004). "Probabilistic slope stability analysis by finite elements." *J. Geotech. Geoenviron. Eng.* Vol. 130, No. 5, pp. 507-518.
- Gudehus, G. and Schwarz, W. (1985). "Stabilization of creeping slopes by dowels." *Proc. 11th International Conference on Soil Mechanics and Foundation Engineering*, San Francisco, Vol. 3, pp. 1679-1700.
- Guo, W.D. (2013). "P_u-based solutions for slope stabilising piles." *International J. of Geomechanics*, Vol. 13, No. 3, pp. 292–310.
- Hada, M. Fukuoka, M. & Anagnostopoulos, C. (1988). "Earth pressure during landslide." *Proc. 5th International Symposium on Landslides*, V.1, pp.179-185.

- Hassiotis, S., Chameau, J.L., and Gunaratne, M. (1997). "Design method for stabilization of slopes with piles." *J. Geotech. Geoenviron. Eng.* 3(4), 314-323.
- Hewlett, W. J., and Randolph, M. F. (1988). "Analysis of piled embankments." *Ground Engineering*, London, England, Vol. 21, No. 3, pp.12–18.
- Ho, K.K.S., and Lau, J.W.C. (2010). "Learning from slope failures to enhance landslide risk management." *Quarterly J. Engineering Geology & Hydrogeology*, V.43, p.33-68.
- Hong, H. P., and Roh, G. (2008). "Reliability Evaluation of Earth Slopes." *J. Geotech. Geoenviron. Eng.*, 134(12), 1700–1705.
- Ito, T., and Matsui, T. (1975). "Methods to estimate lateral force acting on stabilizing piles." *Soils and Foundations*, Vol. 15(4), pp. 43-59.
- Ito, T., Matsui, T. and Hong, P. W. (1981). "Design method for stabilizing piles against landslide—one row of piles." *Soils and Foundations*, Vol. 21(1), pp. 21-37.
- Ito, T., Matsui, T. and Hong, P. W. (1982). "Extended design method for multi-row stabilizing piles against landslide." *Soils and Foundations*, Vol. 22(1), pp. 1-13.
- Janbu, N. (1973). *Slope Stability Computations in Embankment-Dam Engineering*. R. C. Hirschfeld and S. J. Poulos, Eds. New York: Wiley, pp. 47-86.
- Jeong, S., Kim, B., Won, J., and Lee, J. (2003). "Uncoupled analysis of stabilizing piles in weathered slopes." *Computers and Geotechnics J.*, Vol. 30, pp. 671-682.
- Jiang, X. L., Li, L., Yuan, J., Yin, J.S. (2011). "Dynamic Analysis of Strata Horizontal Displacements Induced by Shield Construction of Deep Tunnel." *Journal of Rock and Soil Mechanics*, China, 32(4), pp. 1186-119.

- Joorabchi, A.E. (2011). "Landslide stabilization using drilled shaft in static and dynamic condition." Ph.D. Dissertation. The University of Akron; Akron, Ohio.
- Joorabchi, A. E., Liang, R. Y., Li, L. (2013). "Yield Acceleration and Permanent Displacement of a Slope Reinforced with a Row of Drilled Shafts." *International Journal of Soil Dynamic and Earthquake Engineering*. (Tentatively Accepted)
- Joorabchi, A. E., Liang, R. Y., Li, L. (2013). "Yield Acceleration of a Slope Reinforced with a Row of Drilled Shafts." *Geotechnical Special Publication*, ASCE, GSP 231, pp. 1994-2003.
- Kalteziotis, N., Zervogiannis, F.R., Seve, G. & Berche, J-C. (1993). "Experimental study of landslide stabilization by large diameter piles." *Geot. Eng. of Hard Soils-Soft Rocks*, Ed. A. Anagnostopoulos et al., Balkema, Rotterdam, p.1115-1124.
- Kanagasabai, S. (2010). "Numerical modelling of rows of discrete piles used to stabilise large landslides." PhD thesis, University of Southampton, UK.
- Kanagasabai, S. Smethurst, J.A. & Powrie, W. (2011). "Three dimensional modelling of discrete piles used to stabilise landslides." *Canadian Geotechnical Journal*, V.48(6), pp.1393-1411.
- Kellogg, C. G. (1987). "Discussions—the arch in soil arching." *Journal of Geotechnical Engineering*, ASCE, Vol.113, No. 3, pp. 269–71.
- Kourkoulis, R. (2009). "Interplay of mat foundations and piles with a failing slope." Ph.D. thesis, National Technical University of Athens; Athens, Greece.

- Kourkoulis, R. Gelagoti, F. Anastasopoulos, I. & Gazetas, G. (2012). "Hybrid method for analysis and design of slope stabilizing piles." *J. Geotechnical & Geoenvironmental Engineering*, V. 138, No.1, pp. 1-14.
- Leung, C.F., Chow, Y.K. & Shen R.F. (2000). "Behaviour of pile subject to excavation-induced soil movement." *Journal of Geotechnical and Geoenvironmental. Engineering*, ASCE, V.126, pp. 947-954.
- Li, L., and Liang, R.Y. (2012). "Reliability-Based Optimization Design for Drilled Shafts/Slope System." *Journal of Deep Foundations Institute*, 6 (2), pp. 48-56.
- Li, L., and Liang, R.Y. (2012). "Reliability Based Design for Drilled Shafts in Slope Stabilization." *The 17th Annual Great Lakes Geotechnical/Geoenvironmental Conference (GLGGC): GeoEngineering in Face of Energy and Sustainability Challenges*, Cleveland, Ohio, May24, 2012.
- Li, L., and Liang, R.Y. (2013). "Reliability Based Design for Slopes Reinforced with a Row of Drilled Shafts." *International Journal for Numerical and Analytical Methods in Geomechanics*. DOI: 10.1002/nag.2220.
- Li, L., and Liang, R. Y. (2013). "Efficient MCS Computational Algorithm for Reliability Assessment of a Drilled Shaft Stabilized Slope Using Importance Sampling Techniques." *Journal of Computing in Civil Engineering* ASCE. (Submitted)
- Li, L., and Liang, R. Y. (2013). "Limit Equilibrium Based Design Approach for Slope Stabilization Using Multiple Rows of Drilled Shafts." *Computers and Geotechnics*. (Submitted)

- Li, L., Jiang, X. L., Liang, R. Y. (2010). "A Numerical Case Study of Soil-Pile-Shield Tunneling Interaction for Guangzhou Subway Project." *GeoFlorida 2010*, GSP 199, ASCE, Reston, VA, pp. 1737-1746.
- Liang, R. Y., Nusier, O. K. and. Malkawi, A. H. (1999). "A reliability based approach for evaluating the slope stability of embankment dams." *Engineering Geology*, Vol. 54, pp. 271-285.
- Liang, R., and Zeng, S. (2002). "Numerical study of soil arching mechanism in drilled shafts for slope stabilization." *Soils and Foundations, Japanese Geotechnical Society*, 42(2), pp. 83-92.
- Liang, R. Y., and Li, L. (2012). "Design Method for Slope Stabilization Using Drilled Shafts." *Proc. International Conference on Ground Improvement and Ground Control*, Research Publishing, Singapore, Oct. 2012, vol. 2, pp. 1475-1480.
- Liang, R. Y., and Li, L. (2013). "Reliability Based Design for Drilled Shafts for Slope Stabilization." *Geotechnical Special Publication*, GSP 231, ASCE, Reston, VA, pp. 2004-2013.
- Liang, R. Y. (2010). "Field Instrumentation, Monitoring of Drilled Shafts for Landslide Stabilization and Development of Pertinent Design Method." 2010 Report for Ohio Department of Transportation. Report Number: FHWA/OH -2010/15.
- Liang, R. Y., Al Bodour, W., Yamin, M. and Joorabchi, A. E. (2010). "Analysis method for drilled shaft-stabilized slopes using arching concept." *Transportation Research Record: Journal of the Transportation Research Board* 2010; pp.38-46.

- Liang, R. Y., Joorabchi, A. E., Li, L. (2013). "Analysis and design method for slope stabilization using a row of drilled shafts." *Journal of Geotechnical and Geoenvironmental Engineering*. (Accepted).
- Liang, R. Y., Joorabchi, A. E., Li, L. (2013). "Design Method for Drilled Shaft Stabilization of Unstable Slopes." *Geotechnical Special Publication*, GSP 231, ASCE, Reston, VA, pp. 2024-2033.
- Liang, R. Y. and Yamin, M. (2010) "Three dimensional finite element study of arching behavior in slope/drilled shafts system", *International Journal of Numerical and Analytical Methods in Geomechanics*, Volume 34, Issue 11, pp. 1157–1168,
- Low, B. K., Gilbert, R. B. and Wright, S. G. (1998). "Slope reliability analysis using generalized method of slices." *J. Geotech. Geoenviron. Eng.*, Vol. 124, No. 4, pp. 350-362.
- Malkawi, A. I., Hassan, W. F., Abdulla, F. A. (2000). "Uncertainty and Reliability Analysis Applied to Slope Stability." *Structural Safety*, Vol. 22, pp. 161-187.
- Marsaglia, George and Tsang, Wai Wan (2000). "The Ziggurat Method for Generating Random Variables." *Journal of Statistical Software*, Vol. 5, No. 8, pp. 1-7.
- Merklin, C. M., Geiger, G., Liang, R., and Yamin, M (2007). "Design methodology for drilled shafts to stabilize a slope." First North American Conference on Landslides, CD-form.
- Morgenstern, N. R. and Price, V. E. (1965). "The analysis of the stability of general slip surfaces." *Geotechnique*, 15, pp. 70-93.
- Morgenstern, N. R. (1982). "The analysis of wall supports to stabilize slopes." *Proc., Application of Walls to Landslide Control Problems*, Edited by Reeves, R. B., ASCE, pp. 19-29.

- Mujah, D., Ahmad, F., Hazarika, H. and Watanabe, N. (2013). "Numerical analysis of the multirow arrangement of small diameter steel piles for landslide prevention." *International Journal of Current Engineering and Technology*, Vol. 3, No. 1, pp. 1-20.
- Nethero, M. F. (1982). "Slide control by drilled pier walls." *Proc., Application to Landslide Control Problems*, Edited by Reeves, R. B., ASCE, pp. 61-76.
- Ngwenya, K. (2007). "Advanced ground characterisation The Lloyds, Ironbridge." M.Sc. Thesis, University of Southampton, Southampton, U.K.
- Norris, G. (1986). "Theoretically based BEF laterally loaded pile analysis." *Proc. 3rd Inter. Conference on Numerical Methods in Offshore Piling*, Nantes, France, p.361-386.
- Offenberger, J.H. (1981). "Hillside stabilized with concrete cylinder pile retaining wall." *Public Works*, Vol. 112, No. 9, pp. 82-86.
- Oka, Y. and Wu, T. H. (1990). "System reliability of slope stability." *J. Geotech. Eng.*, Vol. 116, No. 8, pp. 1185-1189.
- Phoon, K. K., and Kulhawy, F. H. (1999). "Characterization of geotechnical variability." *J. Can. Geotech.* Vol. 36, 1999, pp. 612-624.
- Poulos H.G. (1973). "Analysis of piles in soil undergoing lateral movement." *J. Soil Mechanics and Foundations Division ASCE*, 1973, 99(SM5), pp. 391-406.
- Poulos, H. G. (1995). "Design of reinforcing piles to increase slope stability." *Canadian Geotechnical Journal*, Vol. 32, pp. 808-818.
- Poulos, H. G. (1999). "Design of slope stabilizing piles." In: Yagi, n., Yamagami, T., and Jiang, J.-C. *Slope Stability Engineering: Giotechnical & Geoenvironmental Aspects:*

- Proceedings of an International Symposium Is-Shohoku 1999, Matsuyama, Shohoku, Japan, November 8 - 11, 1999.* New York: Taylor and Francis.
- Qin, H. (2010). "Response of pile foundations due to lateral force and soil movements." PhD thesis, Griffith University, Australia.
- Reese, L. C., Wang, S. T. and Fouse, J. L. (1992). "Use of drilled shafts in stabilizing a slope." *Proc. Specialty Conference on Stability and Performance of Slopes and Embankments*, Berkeley.
- Reese, L. C., Wang, S. T., Isenhower, W. M., and Arrellaga, J. A. (2004). LPILE Plus 5.0 for Windows, Technical and User Manuals, *ENSOFT*, Inc., Austin, Texas.
- Reid, P.D. (2008). "Slope instability in the Ironbridge Gorge, Telford, United Kingdom – A study into the causes of slope instability of Ironbridge Gorge with particular emphasis on hydrological factors." MSc Thesis, University of Southampton.
- Richardson, T.M. (2005). "Experimental and analytical behavior of slide suppressor pile walls embedded in bedrock." West Virginia DOH Project RP-97.
- Robert, C.P., and Casella, G. (2004). *Monte Carlo statistical methods*, 2nd ed. Springer Science Business Media, Inc., New York.
- Rollins, K. M. and Rollins, R. L. (1992). "Landslide stabilization using drilled shaft walls." *Ground Movements and Structures*, Vol. 4, Edited by Geddes, J. D., Pentech Press, London, pp. 755-770.
- Smethurst, J.A. (2003). "Use of discretised piles for infrastructure slope stabilisation." Ph.D. Thesis, University of Southampton.

- Smethurst, J.A. and Powrie, W. (2007). "Monitoring and analysis of the bending behaviour of discrete piles used to stabilise a railway embankment." *Geotechnique* 57, No.8, pp. 663-677.
- Sommer, H. (1977). "Creeping slope in stiff clay." *Proc. Special Session No. 10, 9th International Conference on Soil Mechanics and Foundation Engineering*, Tokyo, pp. 113-118.
- Tang, W. H., Yucemen, M. S. and Ang, A. H. S. (1976) "Probability-based short term design of soil slopes." *J. Can. Geotech.*, Vol. 13, No. 3, pp. 201-215.
- Taniguchi, T. (1967) "Landslides in Reservoirs". In *Proc 3rd Asian Regional Conf. Soil Mech. and Fndns. Eng.*, Bangkok, Vol 1, pp. 258-261.
- Terzaghi, K. (1936). "Stress distribution in dry and saturated sand above a yielding trap-door." *Proceeding, 1st International Conference on Soil Mechanics*, Harvard University, Cambridge, Mass, Vol. 1, pp. 307-311.
- Terzaghi, K. (1943). *Theoretical Soil Mechanics*. John Wiley and Sons, New York.
- Viggiani, C. (1981). "Ultimate lateral load on piles used to stabilise landslides." *Proceedings of the 10th International conference on soil Mechanics and Foundation Engineering*, Stockholm, Sweden, 3, pp. 555-560.
- Wang, W.L. & Yen, B.C. (1974). "Soil arching in slopes." *J. Geotechnical Engineering*, V.100, No.GT1, pp. 61-78.
- Wei, W.-B. (2008). "Three dimensional slope stability analysis and failure mechanism." Ph.D. Thesis, The Hong Kong Polytechnic University.

- Wu, T. H., Tang, W. H., Sangrey, D. A. and Baecher, G. B. (1989). "Reliability of offshore foundations - State of the art." *J. Geotechnical Engineering*, Vol. 115, No. 2, pp. 157-178.
- Xinliang Jiang, Lin Li, Jie Yuan, Jiashun Yin. (2011). "Dynamic Analysis of Strata Horizontal Displacements Induced by Shield Construction of Deep Tunnel." *Journal of Rock and Soil Mechanics*, China, Vol. 32, No. 4, pp. 1186-1192.
- Yamin, M. M. (2007). "Landslide stabilization using a single row of rock-socketed drilled shafts and analysis of laterally loaded shafts using shaft deflection data." Ph.D. Dissertation, Department of Civil Engineering, The University of Akron, Akron, Ohio.
- Yamin, M. M., and Liang, R. Y. (2010). "Limiting equilibrium method for slope/drilled shaft system." *International Journal for Numerical and Analytical Methods in Geomechanics*, Vol. 34, No. 10, pp. 1063-1075.
- Yoon, B. S. (2008). "Centrifuge modelling of discrete pile rows to stabilise slopes." Ph.D. thesis, University of Nottingham, UK.
- Zacharopoulos, A. (2012). "Piles in unstable slopes." Mphil-PhD Transfer Report, University of Southampton, Southampton, U.K.
- Zacharopoulos, A. (2013). "Piles in unstable slopes." Ph.D. Thesis, University of Southampton, Southampton, U.K.
- Zeng, S., and Liang, R. (2002). "Stability analysis of drilled shafts reinforced slope." *Soils and Foundations*, Japanese Geotechnical Society, Vol. 42, No. 2, pp. 93-102.
- Zeng, S. (2001). "Elastodynamic solutions for multi-layer systems and analysis techniques for drilled shafts stabilized slopes." Ph.D. dissertation. The University of Akron; Akron, Ohio.

Zhang, J., Zhang, L.M., and Tang, W.H. (2011). “New methods for system reliability analysis of soil slopes.” *Canadian Geotechnical Journal*, Vol. 48, No. 7, 1138-1148.

Zienkiewicz, O. C., Humpheson, C., Lewis, R. W. (1975). “Associated and non-associated viscoplasticity and plasticity in soil mechanics.” *Geotechnique*, Vol. 25, No. 4, pp. 689-691.